NUCLEONICS

July 1952

Corrosion of aluminum jacket of fuel rod from Norwegian heavy-water reactor began in furrow in which copper had been deposited during forming of tube. For more information, see p. 19

A McGRAW-HILL PUBLICATION ★ SEVENTY-FIVE CENTS

THE VICTOREEN "THYAC"

Model 389

A *QUALITY*
GEIGER COUNTER

A GEIGER-TUBE TYPE BATTERY-OPERATED SURVEY RATEMETER FOR MONITORING LOW-INTENSITY BETA OR GAMMA RADIATION

THE "THYAC" FEATURES...

SPECIFICATIONS

Radiation: Beta, gamma, and cosmic

Indication: 3" meter and detachable headset

Sensitivity: 800, 8000, 80,000 counts per minute or 0.2, 2.0, 20.0 mr/hour on radium gamma rays using the 1885 Thyrode

Accuracy: 10%

Battery Life: 110 hours at 4 hours per day

Dimensions: 9½" long by 4½" wide by 6½" high

Weight: 5½ pounds

VIBRATOR POWER SUPPLY . . . The Victoreen low-drain, regulated high voltage vibrator power supply gives accurate and reliable operation using standard batteries.

LAMINATED PLASTIC CASE . . . The latest techniques in case design provide a waterproof, tough, lightweight laminated plastic case for the ruggedest service.

VERSATILITY . . . A wide selection of interchangeable counter tubes makes the instrument adaptable for many applications.

"FINGERTIP" CONTROL . . . "Fingertip" operation of the instrument is facilitated by proper placement of the one control knob.

BETA DISCRIMINATION . . . A sliding shield on the probe enables the operator to discriminate against beta radiation.

CATALOG SHEET AVAILABLE UPON REQUEST

The Victoreen Instrument Co.

5806 HOUGH AVE. CLEVELAND 3, OHIO

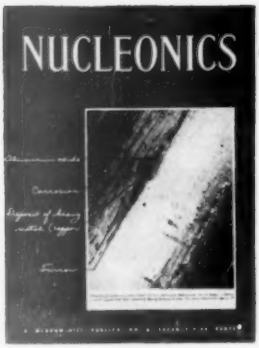

JULY • 1952
Vol. 10, No. 7

Methods of Producing Radioiron... 8
RAYBURN W. DUNN

The Luminescence of Organic Substances... 14
E. J. BOWEN

Pitting of Aluminum in a Heavy-Water Reactor... 19

Pulse-Amplitude Analysis in Nuclear Research—I... 20
A. B. VAN RENNES

Chemical Dosimetry Using Ferrous and Ceric Sulfates... 28
JEROME WEISS

Statistical Sampling of Nuclear Fuels... 32
F. PROSCHAN and S. B. ROBOFF

The Cosmotron—It Works... 34

Multichannel Collimators for Gamma-Ray Scanning with Scintillation Counters... 36
R. R. NEWELL, W. SAUNDERS, and EARL MILLER

Temperature Effects in Organic Fluors... 41
S. H. LIEBSON

Solid and Liquid Scintillation Counters... 46
GEORGE T. REYNOLDS

Gamma-Ray-Diffusion Experiments in Water... 54
M. A. VAN DILLA and G. J. HINE

AEC Work—Who's Doing It? What Does It Cost?... 59

Cross Sections

Automatic Data Recorder for Scintillation Spectrometer... 66
OTTO H. ZINKE and C. SHARP COOK

Remote Pipette Control for Radioactive Liquids... 67
ERVIN J. LILJEGREN and STEWART H. WEBSTER

Tools for Dismantling Contaminated Cells... 68
A. M. TRIPP and FRANK RING, Jr.

Departments

EDITORIAL..... 7
BOOKS..... 72
NUCLEONIC EVENTS..... 76
PRODUCTS AND MATERIALS..... 82

KEITH HENNEY, Editor
JEROME D. LUNTZ, Executive Editor
Ethel Pelzer, Associate Editor
C. J. Mosbacher, Jr., Associate Editor
Alan R. Liss, Assistant Editor
Thomas L. Cramer, Assistant Editor
Nancy E. Purves, Editorial Assistant
Harry Phillips, Art Director
Jack Gordon, Assistant Art Director
George B. Bryant, Jr., Washington Office
Gladys Montgomery, Washington Office
Russell F. Anderson, World News

H. W. MATEER, Publisher
WALLACE B. BLOOD, Manager
D. H. Miller, J. Girdwood, New York
Wm. S. Hodgkinson, New England
Warren W. Shew, Philadelphia
C. D. Wardner, Chicago
J. L. Phillips, Cleveland
T. H. Carmody, R. C. Alcorn, San Francisco
Carl W. Dysinger, Los Angeles
Ralph C. Maultsby, Atlanta
J. E. Blackburn, Jr., Director of Circulation

NUCLEONICS (with which is consolidated "Atomic Power" and "Atomic Engineering"), July, 1952, Vol. 10, No. 7. Publication Office: 212 East York St., York, Pa.; Editorial, Advertising, and Circulation Offices: 330 W. 42nd Street, New York 36, N. Y. Published monthly by McGraw-Hill Publishing Company, Inc. Entered as second class matter December 17, 1947, in the Post Office at York, Pa., under the act of March 3, 1879. Copyright 1952 by McGraw-Hill Publishing Company, Inc. All rights reserved. Curtis W. McGraw, President; Willard Chevalier, Executive Vice President; Joseph A. Gerardi, Vice President and Treasurer; John J. Cooke, Secretary; Paul Montgomery, Senior Vice President, Publications Division; Ralph B Smith, Vice President and Editorial Director; Nelson Bond, Vice President and Director of Advertising; J. E. Blackburn, Jr., Vice President and Director of Circulation. Allow at least three weeks for change of address. All communications about subscriptions should be addressed to Director of Circulation, 330 West 42nd Street, New York 36, N. Y. Price per copy $0.75. Subscription rates United States and U. S. Possessions $8 for 1 year, $12 for 2 years, $16 for 3 years. Canada, $10 for 1 year, $16 for 2 years, $20 for 3 years. Latin America, $15 for 1 year, $25 for 2 years, $30 for 3 years. All other countries, $20 for 1 year, $30 for 2 years, $40 for 3 years. Member of ABC. Member of ABP.

Tracerlab is very pleased, in this period of short supply of instruments, to be able to make immediate delivery on the widely-used SC-7 "100" Scaler. Because of fortunate purchases of component parts, a limited number of these scalers is now available for shipment. Orders, however, should be placed promptly.

The "100" Scaler is a direct reading "conventional" scaler which indicates the number of counts received during an arbitrary length of time. It utilizes two SC-11 Decasale plug-in units based on four cascaded scales of two with two feedback loops to provide a scale of ten. A Wizard Register capable of recording up to 600 evenly spaced counts per minute, makes it possible to count as many as 60,000 evenly spaced impulses per minute. The start-stop switch will also actuate a separate clock such as the SM-60A Electric Timing Clock.

The instrument has been designed to require a minimum of service, with all components overdesigned so that every part is rated for service in excess of that required for normal usage. *For further information, request bulletin XX-38.*

Tracerlab
130 HIGH ST., BOSTON, MASS.
BERKELEY, CAL. WASHINGTON, D. C.
NEW YORK, N. Y. CHICAGO, ILL.

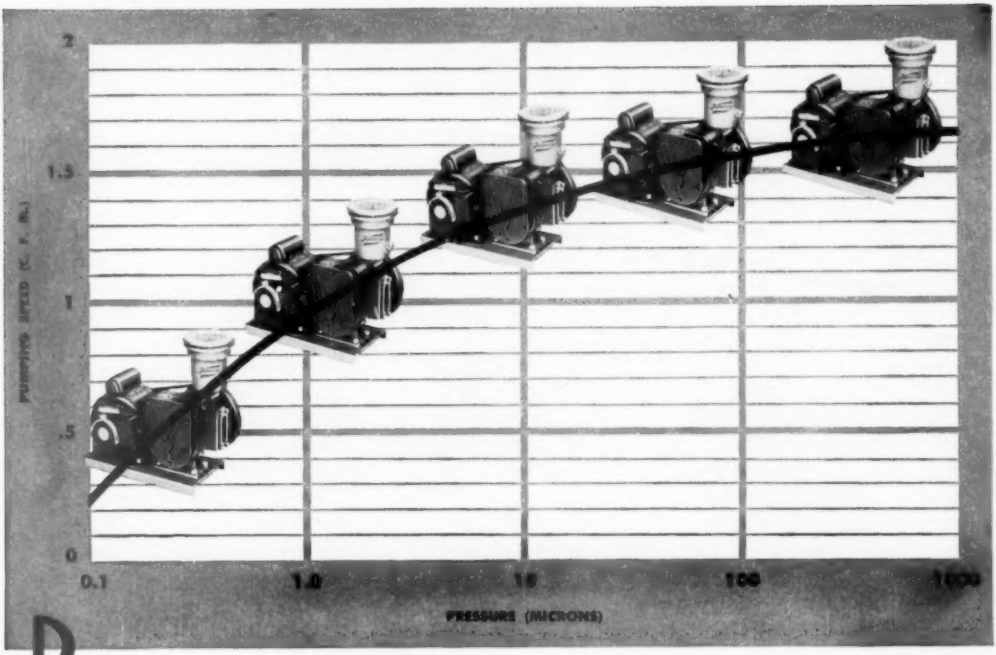

Pick this pump for full-range vacuum pulling power

Performance pays when you work with vacuum . . . the kind of smooth, steady pulling power that's yours with a Kinney Model CVM 3153 High Vacuum Pump!

It's small — only about a foot high — and weighs only 70 lbs. complete with its ¼ hp. motor. Kinney Model CVM 3153 gives you pumping efficiency of the highest order. Free air displacement is 2 cu. ft. per min. (57 liters per min.) and as shown on the graph, a very high percentage of this pulling power is retained right down to the less-than-one micron range. The rotating plunger mechanism of Kinney Model CVM 3153 is simple and long lasting . . . easy to take apart for inspection or servicing.

Whether you need a permanent vacuum pump for your laboratory or shop, or a portable unit for on-the-job service, test, or repair work, it will pay you to pick Kinney Model CVM 3153. Send coupon for complete details and price. Kinney Manufacturing Co., Boston 30, Mass. Representatives in New York, Chicago, Detroit, Cleveland, Atlanta, Philadelphia, Pittsburgh, Johnstown (Pa.), Los Angeles, Charleston (W. Va.), Houston, New Orleans, San Francisco, Seattle and foreign countries.

Kinney

KINNEY MANUFACTURING COMPANY
3614 Washington St., Boston 30, Mass.

Gentlemen:

☐ Please send me Bulletin V51-A describing the new Kinney CVM 3153 Midget Vacuum Pump and price information.

☐ Send name of nearest Kinney Distributor.

Name .....

Company .....

Address .....

City ..... *State* .....

SUBSIDIARY OF THE NEW YORK AIR BRAKE CO.

EKCO
VIBRATING REED ELECTROMETER

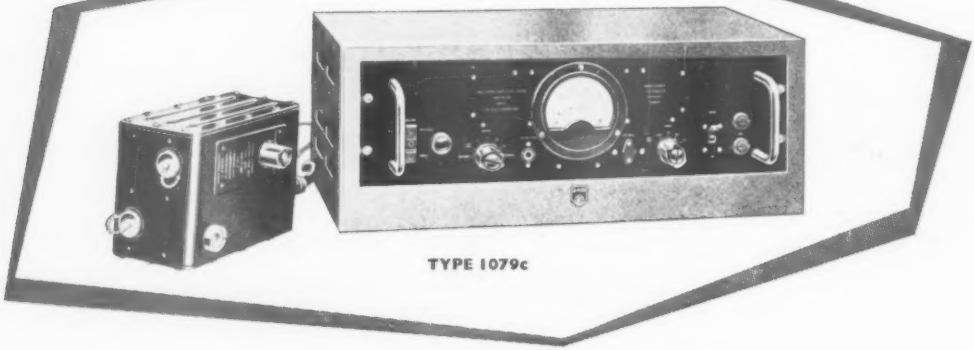

TYPE 1079c

THIS instrument has been designed in conjunction with the British Atomic Energy Establishment, expressly for measuring the small direct currents and voltages encountered in Nuclear research. It can be used as a replacement for most electrometers and has a zero drift of only 1 to 2 mV per day. Direct indication of the voltage or current being measured is given on the panel meter; simultaneously a 1 m.a. or 100 millivolt recorder may be operated.

Four voltage ranges are provided — 0–30, 0–100, 0–300 and 0–1000 millivolts. There are three switched input resistors, their value being 10^{9}, 10^{10} and 10^{12} ohms respectively. In its most sensitive conditions the Electrometer gives a full-scale deflection for a current of 0.03 micro-micro-amps.

For operation 110–115 and 200–250 volts A.C. 40–60 cycles.

Catalogue and further details can be forwarded on application.

EKCO *ELECTRONICS*

U.S. Sales & Service :—

AMERICAN TRADAIR CORPORATION, CHRYSLER BUILDING, 405 LEXINGTON AVE., NEW YORK 17, N.Y.

MANUFACTURERS : E. K. COLE LIMITED • ELECTRONICS DIVISION • 5 VIGO STREET, LONDON, W.1, ENGLAND

proton gun FOR THE COSMOTRON

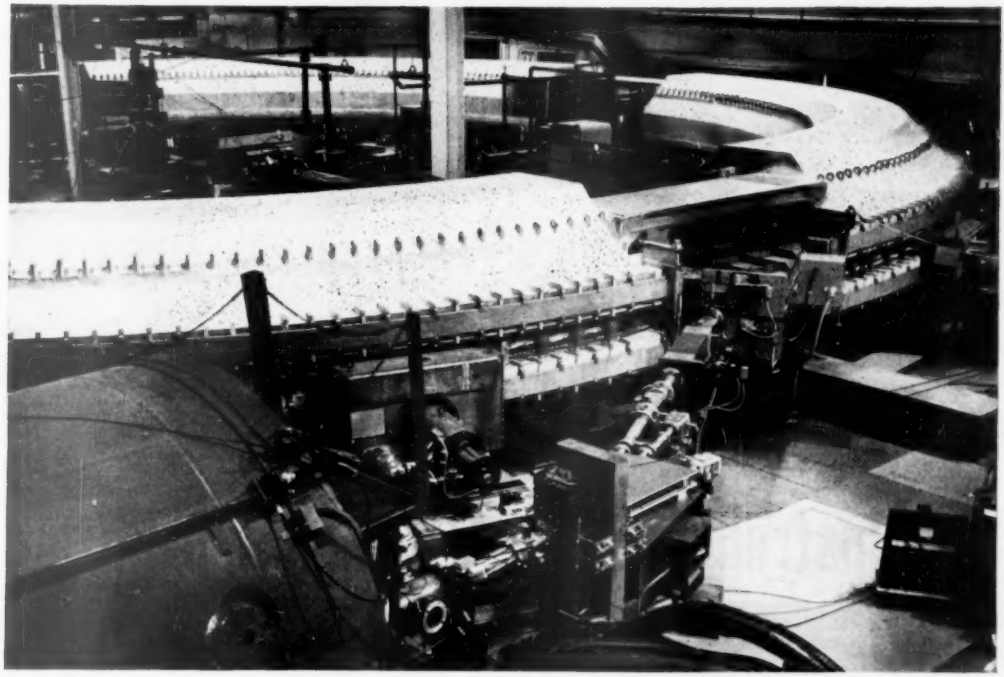

Photographs courtesy Brookhaven National Laboratory.

The homogeneous proton beam necessary for successful acceleration to more than two billion electron volts with the Brookhaven Cosmotron is furnished by a Van de Graaff positive-ion accelerator — one of the largest single components in this new research installation.

Chosen as the injector because of its very stable voltage, excellent beam-collimation, and precise control of the beam, the Van de Graaff accelerator has fulfilled all performance expectations.

This unit, designed and built by High Voltage Engineering Corporation to meet the special requirements of Brookhaven National Laboratory, is a modification of the Type D Model H Van de Graaff accelerator which has these characteristics:

Operating range — 1.0 to 4.0 MeV
Analyzed proton intensity (pulsed) — 1.0 ma.
Proton energy stability — ±1 part in 1000
Pulse length controllable from 1 to 100 μsec.

Our smaller Van de Graaff accelerators, in the 0.5—2.0 MeV range, are used in many of the world's largest laboratories as precisely controlled sources of electrons, x-rays, positive ions, and neutrons.

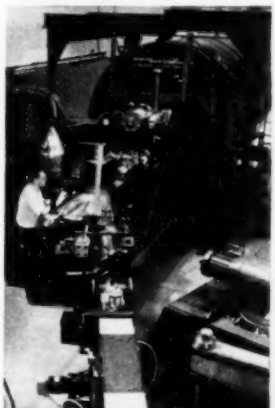

HIGH VOLTAGE ENGINEERING CORPORATION
7 UNIVERSITY ROAD CAMBRIDGE 38, MASSACHUSETTS

Research accelerators . . . Bulletins H and AK. ——— High-voltage electron-beam sterilization . . . Bulletin D.

Super-voltage x-ray equipment for radiation therapy, and industrial radiography . . . distributed exclusively by Keleket X-Ray Corporation.

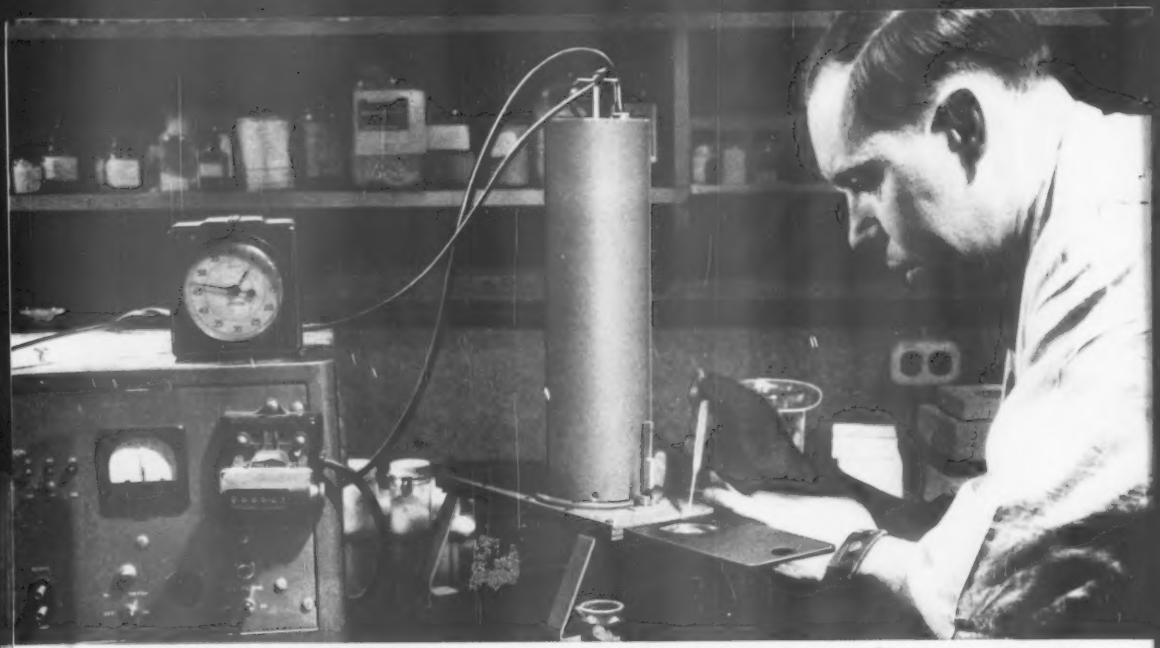

1 **G-E UNIVERSAL SCINTILLATION COUNTER** detects alpha, beta, gamma, and thermal neutron radiation on smears from contaminated surfaces. Phosphors can be rapidly interchanged. Any standard scaler can be used for counting.

New Instruments Detect Radiation Hazard

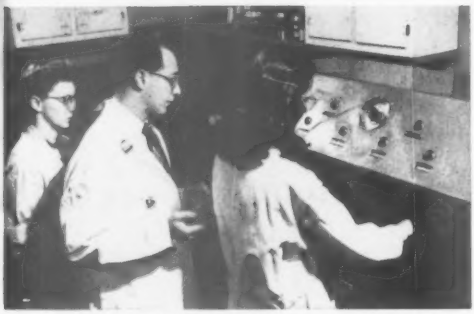

2 **G-E ALPHA HAND COUNTER,** a fast means of obtaining routine check on workers' hands for alpha contamination.

To help safeguard personnel encountering radioactive materials, the G-E Scintillation Counter (above) is also obtainable in portable form. Standard connector at rear of probe allows connecting cable of any length up to 50 feet. It is well adapted for contamination surveys of particle accelerators and nuclear reactors. A modified probe can be used for water monitoring.

The long-probe (below) is supplied in either four- or six-foot lengths. Range from 0.3 to 3000 roentgens per hour. Power is obtained from batteries in lightweight carrying case, permitting complete portability.

Write for catalog GEA-5735 to: General Electric Co., Sect. 687-93, Schenectady 5, N. Y.

GENERAL ELECTRIC

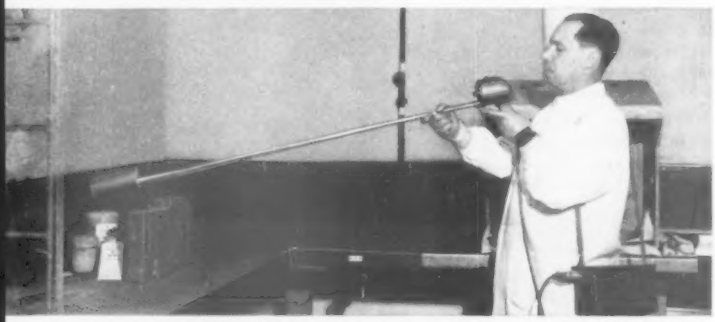

3 **G-E LONG PROBE GAMMA SURVEY METER** monitors areas of high-level gamma radiation. Helps locate beam of particle accelerators with minimum risk to user.

Write for new 8-page catalog of General Electric radiation detection instruments.

NUCLEONICS

JULY, 1952

Radiation and Common Sense

Fear of the unknown is the worst fear of all. When you have no idea who or what your adversary is, you magnify the facts tremendously. Nuclear radiation is an unknown in that the individual cannot personally sense it. Despite this, workers in the early Manhattan Project days were able to set up more than adequate defenses against the potential biological hazards. The successful experience of working safely with radiation has led to its matter-of-fact acceptance as being "part of the job."

Yet every now and then an incident shakes the confidence of those working with radiation or contemplating it. It's the same thing as if, when speeding along a highway in a car, you were to see the remains of a bad accident. The tendency is for you to slow down from 70 mph to 50 mph and to drive quite carefully. If you're a driver-to-be, you might even be more frightened.

But as in automobile driving where if you are fully aware of what is going on around you you are less likely to have an accident, so in the nucleonics field accidents can be held to a minimum. People working with radiation have come to appreciate the fact that if radiation is treated respectfully and experimental conditions analyzed, the radiation hazards can be controlled.

That this has been possible is attested to by the excellent safety record set by the Manhattan District and the Atomic Energy Commission. In a total of ten years of operation, there have been only nineteen cases involving significant radiation injuries, with two of these resulting in deaths. At least nine of the injuries could have been avoided by routine caution on the part of those involved.

Four of the nine injured were in an accident which took place at Argonne National Laboratory last month. They were making measurements on control rods using an exponential reactor. During the changing of rods, a slipup resulted in the safety rod not being replaced. As a consequence, four workers received an overdose of radiation—about 100 roentgens compared to the weekly tolerance of 0.3 roentgens.

Carelessness was also involved in five injuries in 1948. Four men at Eniwetok weapons tests burned their hands when they moved beta-contaminated material without using safety equipment which was provided. Later that year, another man burned his leg handling a beta-contaminated shipment.

However, in the only radiation accidents which have resulted in deaths, "calculated risks" rather than carelessness were involved. In 1945 and 1946 two temporarily uncontrolled nuclear chain reactions took place at Los Alamos. According to a report on these accidents, it was not then "technically possible to do critical assembly experiments by remote control in such a way that the operators would be adequately protected from the effects of a possible accidental nuclear reaction. Thus it was necessary, for about a year, to perform these experiments with operators in the immediate vicinity of the assembly, despite the dangers known to be inherent in such an operation." It was hoped that "stringent supervision of the experimental procedures" would be sufficient to "prevent the assemblies from inadvertently becoming supercritical."

We no longer need to set up experiments on such a basis. The means are within our hands to offer sufficient protection to all those who need it. As in all phases of our daily life, all that is required is common sense and an awareness of what is going on around us. —*J.D.L.*

Methods of Producing Radioiron

By RAYBURN W. DUNN*
Division of Medical Physics, Donner Laboratory, and the Radiation Laboratory
University of California, Berkeley, California

Of the four known radioisotopes of iron (*1*), only two are important from the standpoint of ease of production and length of half-life. They are 2.91-year Fe^{55} (*2*) and 46-day Fe^{59} (*3*).

These two isotopes can be produced simultaneously either by deuteron bombardment of iron in a cyclotron (*4–6*) or by neutron capture in a nuclear reactor (*7–9*). The only way to produce them free of each other is through a transmutation; that is, Fe^{55} is produced from manganese (*10, 11*), and Fe^{59} from cobalt (*10, 12–14*) or copper (*15*). Since a deuteron beam is needed for these three transformations, the reactions can be accomplished only in a cyclotron. However, fast neutrons from a bombardment of beryllium with deuterons will also yield Fe^{59} from cobalt (*10, 16*), and fast neutrons from a reactor will induce the same reaction (*17*).

Radioiron from Iron

With 14-Mev† and 12-Mev deuterons, reported cyclotron yields of Fe^{59} by the $Fe^{58}(d,p)Fe^{59}$ reaction are 0.03 and 0.05 $\mu c/\mu a$-hr, respectively, where the yield is given as a function of beam current and radiation time (*6, 14*). In the latter case, the specific activity was about 1.3 μc/mg of iron after long bombardment and when some 100 mg/cm^2 were milled from the surface of the target.

No recent quantitative information is available on radioiron production from iron targets by cyclotron bombardment, but, with higher energies, such as the 20-Mev beam of the 60-inch Berkeley cyclotron seen in the photo at the right, one might expect perhaps as high as 0.1 μc μa-hr. The stationary probe used in this cyclotron will take a beam of 200–250 μa, if the piece of target metal is 0.010–0.020 in. thick and is properly silver-soldered to water-cooled copper probe block.

By careful selection of the hottest area of the $1\frac{1}{2}$ in. by $2\frac{1}{2}$ in. surface, one might remove iron to a depth of 0.005 in. from, for instance, 10 of the total 24 cm^2, and obtain an estimated yield of some 20 μc of Fe^{59} for each hour bombardment per gram of iron, or 2 μc/mg after 100 hours. This compares favorably with the Oak Ridge Fe irradiation unit which has an Fe^{59} specific activity of only 0.06 μc/mg mixed with an Fe^{55} activity of 0.05 μc/mg (*9*). There are no data on Fe^{55} activity levels produced in cyclotron iron targets.

By increasing the time of Oak Ridge irradiation to 92 days, or two half-lives, one should be able to increase the specific activity to 0.15 μc/mg.

By either reactor or cyclotron production, the specific activity can be improved nearly 130-fold by using iron enriched in Fe^{58} (*18*). Because of the waste of the electromagnetically processed iron which would be left on the cyclotron probe, however, it seems impractical at present to use such material for other than reactor irradiations.

Oak Ridge Fe^{59} Unit 26-PX (*19*), prepared from iron enriched in Fe^{58}, is listed as having a specific activity of greater than 0.5 mc/mg (500 mc/gm of iron). Three such samples received at this laboratory, as assayed at Oak Ridge, had Fe^{59} activities of 1.2, 1.8, and 5 (estimated) mc/mg of iron, with accompanying Fe^{55} activities of 0.14, 0.22, and 0.2 (estimated) mc/mg of iron, respectively, at time of shipment. No report on total iron accompanied the third listed sample; the values were estimated from the reported total solids.

The Fe^{55} simultaneously produced in both cyclotron and reactor irradiations has, because of its decay characteristics, not been particularly useful in contributing to the over-all activity of the bombarded material. Whereas the short-lived isotope (Fe^{59}) decays with the production of betas of 0.26 and 0.46 Mev and gammas of 1.10 and 1.30 Mev (*3*), the longer-lived isotope (Fe^{55}) produces only manganese K-capture X-rays of 5.9 kev, with possibly a small percentage of weak gammas (*2*).‡

Detection of radiation from the Fe^{55}, therefore, is not so readily accomplished. The most useful instrument for radioassay of such weak emitters is the gas-flow proportional counter (*20, 21*). However, with recent improvements in gamma-sensitive scintil-

* Present Address: California Research and Development Co., P. O. Box 751, Livermore, Calif.

† Originally published as 16 Mev; this value was remeasured, at a later date, and found to be 14 Mev. The present 20-Mev energy of the 60-inch Berkeley cyclotron is a maximum; during operation it is known to vary between 19 and 20.

‡ Measurements of Fe^{55} X-ray activity, such as are reported in this paper, do not represent actual decay rates, as defined by the "curie," but are merely expressions of equivalent or apparent activities.

Quantitative data are given on the yields and specific activities of samples of Fe^{55} and Fe^{59} produced from iron and cobalt in reactor and cyclotron. Special attention is paid to the details of preparing high-specific-activity Fe^{59} by a (d,2p) reaction with cobalt

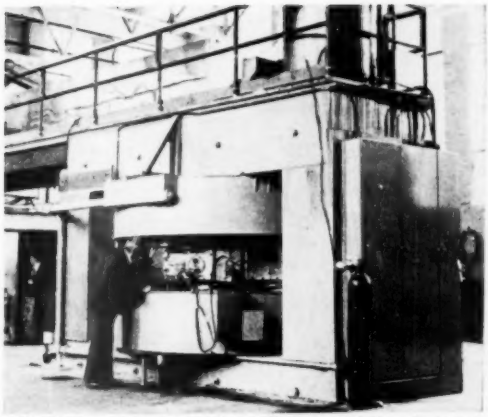

IRON-55 from manganese and iron-59 from cobalt have been produced in the University of California's 60-inch cyclotron seen above

lation counters (*22, 23*), an increase in X-ray counting efficiency may be achieved, making possible an increased counting efficiency for Fe^{55}. This would enhance the usefulness of this isotope for tracer applications, allowing full advantage to be taken of its longer half-life.

The presence of the long-lived isotope Fe^{55} in material to be used as a tracer in *in vivo* medical research is frequently undesirable because it remains as a source of ionizing radiation long after the Fe^{59} has decayed (*9*).

Carrier-free Samples

The term "carrier-free" is applied to the products of all or nearly all transmutation reactions.

For all practical purposes, a condition *approaching* carrier-free may be accomplished. It is in this less restrictive sense that the term is generally used; i.e., a very small but detectable amount of the stable isotope or isotopes of the element accompanies the radioisotope in the product.

To approach the carrier-free condition, it is essential (*a*) that the bombarded or activated material be highly purified insofar as the product isotope is concerned, (*b*) that precautions be taken to prevent external contamination of the sample with this element, (*c*) that all reagents employed in the radiochemical separation be purified before use, and (*d*) that glassware, etc., be thoroughly cleaned.

In tracer studies, particularly in biological and medical research, it is important to have samples that either are carrier-free or at least have very high specific activities. However, in practical applications, it is very difficult to purify the bombarded or activated sample in the complete absence of carrier, so that a balance that is compatible both with the chemistry involved and the end use of the product must be maintained.

Fe^{55} from Manganese

The $Mn^{55}(d,2n)Fe^{55}$ reaction, originally investigated by Hamilton (*11*), has been successfully applied also by Peacock *et al.* (*10*) for the production of useful amounts of Fe^{55}.

Bombardments in the 60-inch Berkeley cyclotron were estimated to produce 0.02 μc/μa-hr with 20-Mev deuterons (*24*). The activity level of the product was obtained by comparison with a radioactive standard, using a Lauritsen electroscope. The target material was manganese dioxide, packed under a thin tantalum foil; this chemical compound and bombardment arrangement are naturally not conducive to production of the best yields.

The cyclotron bombardments conducted at the Massachusetts Institute of Technology, were made with 14-Mev deuterons, using a 90% manganese alloy target and a beam of 100 μa (*10*). The yield was reported as approximately $\frac{2}{3}$ μc/μa-hr. The activity level of the purified product was estimated in this case by means of a beryllium-window counter tube. No specific activity data were given; however, the use of a ferric hydroxide precipitation step in the purification procedure and the addition of 1–10 mg of carrier, "if needed," would indicate that a 10-hour bombardment should produce a specific activity of not less than 0.07 mc/mg.

The use of a proton beam to produce Fe^{55} by the $Mn^{55}(p,n)Fe^{55}$ reaction has been investigated (*25*), but yield data are not available. In view of the higher energies of deuteron over proton beams, bombardments with the latter are unlikely to give greater yields.

Fe^{59} from Copper

Production of Fe^{59} from copper by 190-Mev deuterons in the 184-inch Berkeley cyclotron has been reported, and is listed as occurring, effectively, as a $Cu^{63}(A\text{-}6, Z\text{-}3)Fe^{59}$ reaction (*15*); i.e., the product isotope is six mass units and three nuclear charges less than the parent. Although of interest, such bombardments are not considered practical for production purposes because of the small beam currents obtainable at these high energies.

A test was made to find out if useful amounts of this radioisotope could be so obtained. The copper target was a current-testing probe that had received an unknown total amount of intermittent bombardment over an unknown period, followed by a cooling-off period of about one month. A reasonable estimate of the activity level at the time of assay would be about one-tenth of the maximum or saturation value. From this estimate and the assay data, it was determined that, at best, a recovery of 0.1 mc could be obtained from 10 to 20 gm of copper

target material, but that the specific activity would not be better than 10–15 $\mu c/mg$ of iron due to impurities in the copper. Thus no further work with these targets was done.

Fe^{59} From Cobalt

The use of fast neutrons for Fe^{59} production from cobalt by the (n,p) reaction as employed by Evans is reported to give yields of 0.023 $\mu c/\mu a$-hr (*10*). Although the specific activity is not given, it cannot have been very high, inasmuch as the cobalt which backed against the beryllium, and throughout which the radioiron was formed, weighed 40 gm. At best, this much metallic cobalt would contain not less than 10–15 mg of iron, unless previously purified.

This method is profitably employed if cobalt low in iron is used for the target. It is the only satisfactory method for cyclotrons with deuteron-beam energies of less than 18 Mev.

The exposure of highly purified cobalt to fast neutrons in reactors offers the possibility of producing Fe^{59} in good yield (*17*). So far as can be learned, quantitative data are not available. This source of production should be investigated further.

Cyclotron production by the Co^{59}-$(d,2p)Fe^{59}$ reaction, first investigated by Tobias, is the only convenient means of obtaining Fe^{59} free from Fe^{55}, and in an approximately carrier-free condition. The energy threshold for this reaction is somewhere in the neighborhood of 18 Mev (*13*).

In the 60-inch Berkeley cyclotron, the $(d,2p)$ reaction has produced about 0.07 $\mu c/\mu a$-hr of 20-Mev deuterons. The specific activity of the Fe^{59} so produced was of the order of 3–10 $\mu c/\mu g$. About 100 $\mu c/\mu g$, with a 100-hour bombardment at beam currents of 200 μa, is estimated as the maximum specific activity that could be achieved.

Some twelve samples have been prepared from cobalt in the 60-inch Berkeley cyclotron. The procedures used and described in what follows are satisfactory but still need improvement. Due to the expense involved in these bombardments, they were undertaken only at infrequent intervals, as dictated by the needs of the medical group.

Further experimental work on procedures was discontinued late in 1950 because of a transfer of personnel, and no further experimental work is contemplated at the present time.

The methods outlined are sufficiently reliable, however, to serve as a basis in meeting the growing needs for high-specific-activity Fe^{59}.

Preparation of cobalt chloride of low iron content. The iron content of all cobalt solutions was reduced by ether extraction, followed originally by conversion of the chloride to sulfate for electroplating. Later experiments, however, indicated that a better result could be obtained with a chloride electroplating solution, and it is this procedure that is given in detail here.

FIG. 1. Extraction apparatus for cobalt chloride purification

A saturated solution of $CoCl_2$ in 8*N* HCl contains slightly less than 1.2 moles/liter at room temperature by rough determination. To prevent the salt from crystallizing out if the laboratory temperature drops during the night, the solution should be prepared for extraction by dissolving not more than 1 mole of $CoCl_2 \cdot 6H_2O$ in sufficient 8*N* HCl to make 1 liter.

In view of the wider range of acid concentration, i.e., 6 to 8*N*, in which isopropyl ether will give almost quantitative extraction of iron (*26*), and for reasons of safety, this ether is recommended in preference to the ethyl. It is prepared for use by extracting two or three times each with equal volumes of 8*N* HCl and of water, ending with the water.

A batchwise or a continuous extraction of the cobaltous chloride solution may be employed, but the continuous process is preferable. It is the only method for which quantitative data were obtained in this work.

A convenient standard-taper joint extraction apparatus may be assembled using a flat-bottomed round flask, such as Ace No. 6895, into which is fitted adapter No. 5040. The side arm of this adapter is fitted into adapter No. 5075, and the latter into a round-bottomed distilling flask such as No. 6885. Between the top joint of No. 5040 and the bottom of the condenser, a straight adapter is needed that will fix the condenser drip-tip above the side arm at a distance equal to about $1\frac{1}{2}$ times the distance below this point.

The condenser itself is of the Liebig or Allihn type. Its length should be dictated by the rate of ether vaporization but should not be less than 250–300 mm. About 1 cm below the drip-tip and running all the way to the bottom of the acid chloride solution is a straight glass tube, 6 to 8 mm in diameter. It should be funneled at the top and have a Corning No. 39533 coarse porosity dispersion tube at the bottom.

To minimize the volume of isopropyl ether, the extraction flask size should be such that it will be about nine-tenths filled with the cobalt solution to be extracted. Also, the funneled top of the dispersion tube should be large enough to catch the condensed ether while still fitting through a $^{29}/_{42}$ joint, but not so large as to block the upward passage of vapor. All joints should be size $^{29}/_{42}$ or larger.

The boiling flask (1-liter size) should be provided with a hemispherical Glasscol mantle and glass beads.

The cobalt solution is introduced into the extraction flask and the complete apparatus is then assembled. The charge of washed ether is introduced through the top of the condenser until it overflows 200 to 300 ml into the boiling flask.

It is advisable to put an insulating layer of asbestos tape around these tubes, because of the distance which the vapor travels before reaching the condenser. Otherwise, a large portion of the ether would merely reflux without passing through the aqueous solution.

No determinations of minimum extraction time were made, nor was the liquid ether flow rate measured. However, satisfactory results were obtained

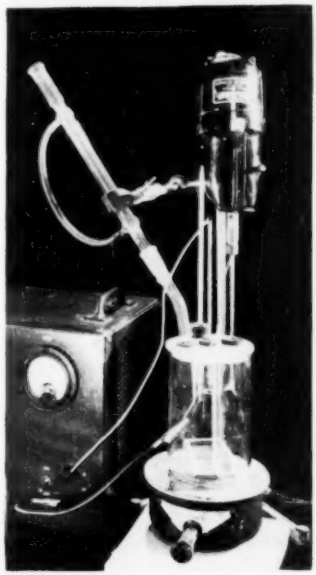

FIG. 2. Power supply, assembled electroplating apparatus, and details of electroplating cell

The electroplating cell consists of a heavy-walled Pyrex jar about 93 mm in inside diameter and 150 mm high. The beaded lip is ground flat to make a seal for the $\frac{1}{2}$ in. Lucite flange top, the lower face of which is 92 mm in diameter, and machined to fit about 8 mm down into the beaker.

The top is drilled with three 1-in. holes in line, one of which is in the center, and the other two with centers $1\frac{1}{8}$ in. on each side. Teflon stoppers are recommended for these holes.

The stopper for the center hole is drilled to take a 5-mm-dia. glass tube. Sealed into the lower end of this tube, with connecting wireleading up through the center, is a flat spiral of 0.051-in.-dia. platinum wire, 5 in. long. Two $\frac{9}{32}$-in.-dia. holes are also drilled $1\frac{1}{2}$ in. from the center on a line at right angles from the line of the larger holes. A thermometer is inserted in one of these holes, and the other serves for the introduction, through a stopper, of a vertical 15-mm glass tube bent to about 45 degrees from the vertical 5 or 6 cm above the stopper. This tube has an outer $\frac{19}{38}$ standard-taper joint at the top, to which a 350-mm condenser is attached to prevent excessive evaporation losses during plating.

A small glass propeller fixed in a variable-speed electric stirrer is introduced through a silicone-lubricated stopper in the remaining large hole. A 7-mm glass tube is inserted through the other small hole to bring out the cathode connection wire.

by extracting for four hours with the ether boiling at a maximum rate obtainable with a 380-watt Glascol heating mantle. This is followed by a further two-hour period after adding 1–5 ml of 30% hydrogen peroxide to oxidize any ferrous iron remaining.

Upon completion of extraction, the condenser, extension, and dispersion tubes are disconnected. By tipping, as much ether is poured through the extraction flask side arm to the boiling flask as is convenient. The remaining ether is almost completely removed with a pipette.

The extracted solution should be washed by shaking with several small volumes of the purified ether to free it of any small amounts of organic decomposition products that may have been formed during the six hours of extraction.

Following these operations, the sample is *at all times* carefully protected from contamination with iron. It is evaporated initially under a hood, and finally in an oven, at 70° C, until dry and free from HCl.

Determination of iron extraction efficiency. One batch of 3.5 moles of reagent grade $CoCl_2 \cdot 6H_2O$ was processed by a modification of the procedure just outlined which permitted obtaining data on the completeness of iron extraction. Instead of a separate adapter with side arm, the apparatus was actually prepared by joining a side arm to a long-necked 3-liter flat-bottomed flask having an outer $\frac{29}{42}$ standard-taper joint at the top and an inner $\frac{35}{20}$ spherical joint at the side. The assembly is illustrated in Fig. 1.

The solution volume was 3.3 liters, which filled the extraction flask up to the neck. As noted previously, a smaller volume should have been used to permit a better separation of ether and aqueous droplets between the top of the cobalt solution and the side arm. As it was, a small amount of cobalt chloride solution was carried over with the ether but this did not effect the results, and might, indeed, have happened anyway.

After a five-hour extraction period, the apparatus was disassembled, the ether charge removed, and the boiling flask cleaned for reuse. A second four-hour extraction was then made with fresh ether after adding H_2O_2, and this charge was also removed as described.

The iron was quantitatively recovered from each of the two batches of ether by extraction into several small portions of water, and iron analyses were run on the combined aqueous extracts from each batch. The results indicated that 59 mg of iron were removed in the first extraction period, less than 0.1 in the second.

Two pieces of reagent grade iron wire of approximately the same mass as the iron extracted were cut off and weighed. Each was dissolved in HCl. The first solution, containing 61.2 mg of iron, was added to the cobalt solution, together with 2.0 ml of a tracer Fe^{59} solution, and thoroughly mixed.

The tracer solution assayed 18,160 counts per minute, neglecting coincidence correction. This counting rate was determined in a scintillation counter having reproducible geometry; the 2 ml of solution were contained in a sample vial which was placed above the sodium iodide crystal. After counting, the contents of the container were transferred quantitatively to the cobalt solution.

The added normal and radioactive iron were then extracted for four hours, plus two more after adding 1 ml of H_2O_2. The ether charge was again removed and the boiling flask cleaned for reuse.

The second iron solution, containing 60.0 mg of iron was then added to the cobalt solution and thoroughly mixed. The same extraction procedure was again followed. The ether was removed and the iron recovered by extraction with water, as before. The

aqueous iron solution was evaporated to small volume, transferred quantitatively to a sample vial, diluted to 2.0 ml and counted. Likewise, the used ether was evaporated and counted.

The iron solution assayed 572 counts per minute; the ether residue activity was essentially at background. The original activity, corrected for decay, would have been 17,100 counts per minute at the time the second assay was made. As a first approximation, therefore, the unextracted iron was $61.2 \times 572/17{,}100$, or close to 2 mg. This amount in 3.5 moles of cobalt solution is equivalent to some 10 μg of iron per gram of cobalt.

Electroplating apparatus. Figure 2 shows a setup that has been used for this work. The apparatus illustrated and later described needs to be improved insofar as the stirring and anode-cathode arrangements are concerned to eliminate completely the collection of precipitated material on the surface of the cathode. The simple expedient of mounting the cathode vertically does not solve this problem, since, in this position, the evolved hydrogen prevents a smooth plate.

A $1\frac{1}{2}$ by $2\frac{1}{2}$ in. cathode is used. It is made of copper $\frac{1}{4}$ in. thick. Although thinner copper probably would also be satisfactory, too thin a piece is warped during plating, producing a concave deposit. The preparation of the copper surface for electroplating is quite important. The smoother it is, the less chance there is for production of pinholes due to continuing evolution of hydrogen at fixed locations; if too smooth, the deposit will break loose after several hours and will be useless. The best results are obtained by polishing one side with successively finer pieces of emery paper, ending with wet polishing using number 400. Before plating, the copper is washed with detergent, rinsed, and dried.

To prevent electroplating of cobalt on the sides and bottom, and to minimize the "edge effect," the copper block is fitted into a square glass holder, $\frac{1}{2}$ in. deep, having an all-around clearance of about 0.010 in. between the sides and metal. The bottom of this holder is drilled through with two holes $\frac{5}{8}$ in. in diameter centered about $1\frac{1}{2}$ in. apart. They serve to ease the block out of the holder after plating, and one hole is used to bring out the cathode connection.

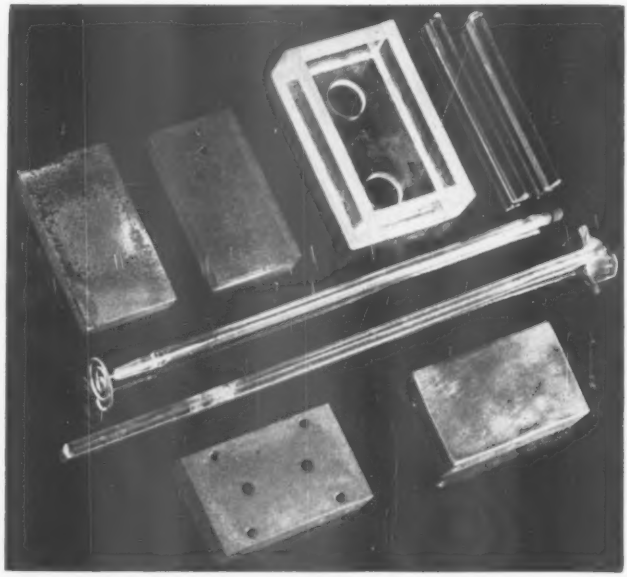

FIG. 3. Electroplated cobalt, electroplating parts, probe block, and finished cobalt target. See text for details

The copper block is drilled and tapped $\frac{1}{8}$ in. deep for a small brass screw at a position corresponding to the center of one of the holes in the holder. A thin glass-insulated copper wire is attached to this screw, and a length of small diameter polyethylene or Tygon tubing is slipped over the wire ending against the block.

Before placing the block in the holder, a small hole is punched on the centerline, about $1\frac{1}{4}$ in. from the short side, of a 3 by 4-in. piece of thin polyethylene sheet. The enclosed cathode wire is then pulled through the hole, and the sheet is held against the back of the block while the latter is dropped into the holder. The excess polyethylene is then trimmed off close to the surface of the copper, using a scalpel, but without touching the block, so as not to introduce iron in excess of that already present as an impurity in the copper.

The plastic sheet serves as a gasket, preventing, in some measure, attack of the copper by the hot solution during plating, with consequent increase in the iron content.

Two 4–5 cm lengths of 7 or 8-mm diameter glass rod are placed in the bottom of the electroplating beaker, and the copper and glass cathode assembly is placed upon them. This arrangement provides a quiescent area under the block where precipitated solids can collect during plating.

When the condenser, stirrer, anode, and the cathode lead have been fitted through the cover plate and the assembly has been placed on a hot plate, the unit is ready for introduction of the cobalt solution. The electrolysis current may be obtained from a 6-volt storage battery or two batteries connected in parallel, with a variable resistance in series for controlling the current. The preferable means is from a 5-amp, 10-volt rectifier unit with a Variac input such as seen in Fig. 2.

Fig. 3 illustrates several of the parts described. In the upper row, starting at the left, are: (1) a cathode block with electroplated cobalt, the uneven surface of which has been partly smoothed on a belt sander; (2) a copper cathode block with reverse side up to show tapped hole for electrical connection; (3) the glass holder; (4) glass rods on which the holder is placed; (5) the platinum anode; (6) glass stirrer. Also illustrated is the reverse side of a cyclotron copper probe block, showing four tapped holes for mounting on the probe, and two center holes for water cooling. To the right of this block is

a finished target, with cobalt soldered on, ready for use.

Electroplating solution and procedure. The standard electroplate procedure for cobalt uses a cobalt sulfate and boric acid bath, and employs, preferably, a cobalt anode (*27–29*). Since no cobalt anode that is sufficiently low in iron is available, electroplating was originally performed using spectroscopically pure aluminum anodes. Fairly satisfactory pieces of cobalt of sufficient thickness were thus obtained, but the difficulty and uncertainty of overcoming the passivity of the aluminum surface made this an unreliable procedure.

The latest electroplating procedure employs the flat spiral platinum anode in a solution of cobalt chloride, sodium chloride, and boric acid. This procedure needs considerable improvement, since consistently satisfactory results are not obtainable. The reasons for this were not determined, because the work was discontinued.

An approximately 4% solution of reagent grade boric acid (about 80% of saturation) is prepared and freed of iron by passing it through a column (3-cm inside diameter, 40 cm long) of hydrogen-form 50–100 mesh Dowex-50 at a rate of about 0.3 liter/hour.* The dimensions of the column are not critical, but the flow rate should be adjusted in accordance with the size adopted. A more saturated solution may just as well be used, provided that its temperature does not decrease, thus crystallizing out some solid acid which would clog the resin bed.

(The reagent grade sodium chloride was not repurified before use, since the amount of iron impurity in this salt was deemed to be sufficiently low that it would not be greater than the amount introduced with the cobalt. However, it is probably safer to use a batch ether extraction of a nearly saturated solution of the salt in 8*N* HCl, and to prepare the purified dry salt in the same manner as with the cobalt.)

Between 0.2 and 0.3 mole each of the purified cobaltous chloride and of reagent grade sodium chloride are dissolved in 500 ml of the purified 4–5% boric acid solution, and the *p*H is adjusted to around 3.

The solution is placed in the electroplating beaker, the hot plate turned on, and the stirrer set to slow speed. This speed adjustment is more or less a matter of trial and error. The rate should be such that precipitated material will not remain on the cathode surface, but will collect under the cathode assembly. With fast stirring, an uneven deposit is obtained.

The anode should be fixed at a maximum distance from the cathode, but sufficiently below the surface so that it will remain in the solution if the volume of the latter decreases due to electrolysis and evaporation. When the temperature reaches 60° C, the current is turned on and set to about 0.5 amp at 4 to 5 volts. The current must not be interrupted until plating is completed, and the temperature should be maintained at 60°–70° C.

Under the conditions outlined, plating efficiency is low. Deposition may or may not be complete after 24 hours, but if incomplete, the solution *p*H and salt concentration will have changed sufficiently so that no further deposition will be obtained and the cathode should therefore be removed. No more plating occurs, apparently, after the *p*H has dropped to or below 2.5.

A precipitate of what is presumably cobaltic oxide usually occurs shortly after the start of electroplating, which may or may not clear up at a later time. The conditions necessary to prevent formation of this precipitate were not determined. Although additions of hydroxylamine and of hydrogen peroxide will redissolve the precipitate, they will not prevent its formation. Furthermore, if these reagents are initially present they have a deleterious effect on the deposit.

The most satisfactory conditions of temperature, salt concentration, *p*H, stirring rate, anode-cathode distance, etc., have not been ascertained. Even though consistently good results were not obtained, however, several excellent plates weighing between 7.5 and 9 gm were produced in this manner. Spectrographic analysis showed less than 20 ppm of iron in these pieces of cobalt. Further experimental work on this procedure is definitely indicated.

Related techniques. In a companion article entitled "Techniques Related to Production of Fe^{59}," to be published in NUCLEONICS next month, preparation of the probe target, removal of the radioactive material from the target after bombardment, radiochemical separation of the iron from the cobalt, and preparation of the purified material for medical use are described. Additional details on Fe^{59} yield and specific activity are included.

* * *

This work was supported by the U. S. Atomic Energy Commission.

* This manner of purification was tested by ascertaining that a tracer amount of radioactive iron, placed at the top of a similar column was completely retained at the top after passage of several liters of boric acid solution.

BIBLIOGRAPHY

1. G. T. Seaborg, I. Perlman. Table of isotopes, *Revs. Mod. Phys.* **20,** 594–5 (1948)
2. K. Way *et al.* Nuclear data, Circular 499, p. 51 (National Bureau of Standards, U. S. Department of Commerce, Washington, D. C., 1950)
3. Page 52 of ref. *2*
4. J. J. Livingood, G. T. Seaborg. Radioactive isotopes of iron, *Phys. Rev.* **54,** 51 (1938)
5. J. J. Livingood, G. T. Seaborg. Long-lived radioactive Fe^{55}, *Phys. Rev.* **55,** 1268 (1939)
6. M. Deutsch, J. R. Downing, L. G. Elliott, J. W. Irvine, Jr., A. Roberts. Fe^{59} by deuteron bombardment of iron, *Phys. Rev.* **62,** 3 (1942)
7. A. H. Snell *et al.*, as reported in Plutonium Project Report CP-257 (1942)
8. R. Wilkinson, J. Levinger, as reported in Plutonium Project Report CP-641 (1943)
9. Isotopes Catalog and Price List No. 4, (U. S. Atomic Energy Commission, Oak Ridge, Tenn., 1951)
10. W. C. Peacock, R. D. Evans, J. W. Irvine, Jr., W. M. Good, A. F. Kip, S. Weiss, J. G. Gilson, 2d. The use of two radioisotopes of iron in tracer studies of erythrocytes, *J. Clin. Invest.* **25,** 605 (1946)
11. J. G. Hamilton, item H127 in ref. *1* above; also personal communication to the author
12. Page 32 of ref. *9*
13. C. A. Tobias, item T46 in ref. *1* above; also personal communications to the author
14. J. G. Hamilton. The applications of radioactive tracers to biology and medicine, *J. Applied Phys.* **12,** 440 (1941)
15. D. R. Miller, R. C. Thompson, B. B. Cunningham. Products of high-energy deuteron and helium-ion bombardments of copper, *Phys. Rev.* **74,** 347 (1948)
16. J. J. Livingood, F. Fairbrother, G. T. Seaborg. Radioactive isotopes of manganese, iron, and cobalt, *Phys. Rev.* **52,** 135 (1937)
17. J. W. Irvine, Jr., Plutonium Project Report MonC-142 (1946)
18. Page 39 of ref. *9*
19. Page 13 of ref. *9*
20. Annual Buyers' Guide, 1951–52, NUCLEONICS **9,** No. 5, D-20 (1951)
21. W. L. Graf, C. L. Comar, I. B. Whitney, Relative sensitivities of windowless and end-window counters, NUCLEONICS **9,** No. 4, 22 (1951)
22. Page D-22 of ref. *20*
23. H. O. Anger. Scintillation counters for the measurement of radioactive samples, UCRL-886 Rev. (1951)
24. W. M. Garrison, J. G. Hamilton. Production and isolation of carrier-free radioisotopes, UCRL-1067 Rev. (1951)
25. S. N. Van Voorhis, item V4 in ref. *1* above
26. E. H. Swift, "A System of Chemical Analysis," p. 293 (Prentice-Hall, Inc., New York, 1939)
27. W. Blum, G. B. Hogaboom, "Principles of Electroplating and Electroforming," p. 360 (McGraw-Hill Book Co., Inc., New York, 1949)
28. F. K. Shelton, J. C. Stahl, R. E. Churchward, Electrowinning of cobalt from cobaltite concentrates, Report of Investigations 4172 (U. S. Bureau of Mines, Washington, D. C., 1948)
29. C. W. Davis, U. S. Bureau of Mines, Boulder City, Nev., personal communication

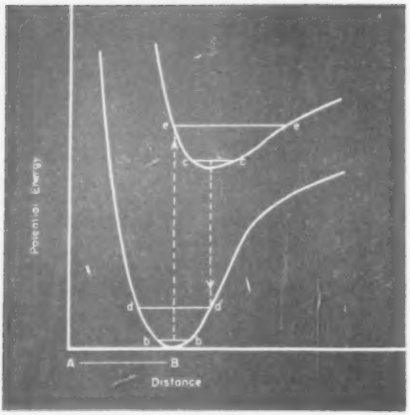

FIG. 1. Potential-energy curves of a diatomic molecule

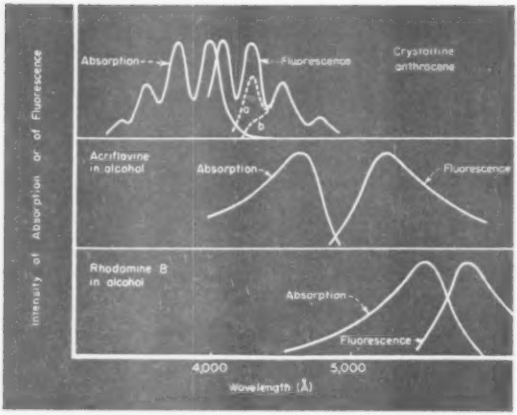

FIG. 2. Fluorescence and absorption bands showing overlap

The Luminescence of Organic Substances

Re-radiation of the radiant energy incident on a material is a complex process. The mechanism of the process is discussed here for the case of ultraviolet light, with extension to the case of nuclear radiations

By E. J. BOWEN
University College
Oxford, England

IT WAS NOTICED very early in the history of radioactivity that nuclear radiations produce luminescence in some materials, and this effect was used by Rutherford and Geiger to count α-particles by visual observation. The development of photomultipliers as exceedingly sensitive detectors of light has greatly extended the convenience and accuracy of this method of measurement. Inorganic and organic substances have been used as luminescent targets, and similar substances, particularly inorganic, have been used in other fields as fluorescent screens for X-ray and cathode-ray tubes, for fluorescent lamps, and for rendering infrared radiation visible.

There are many difficulties in the way of understanding the mechanism of the luminescence process. These difficulties are fewer for organic substances, where the light emitter is a characterizable molecule whose energy levels are much the same in the gaseous, liquid, or crystalline states. The study of fluorescence excited by ultraviolet light instead of by nuclear radiations greatly simplifies the matter, and from it a coherent picture of energy absorption and light emission can be built up and applied to more complicated situations.

Absorption and Emission

The absorption of a quantum of visible or ultraviolet light, and the emission of a quantum of fluorescent light is best understood by the use of a diagram such as shown in Fig. 1. The horizontal axis represents the internuclear distance in a diatomic

molecule AB, and the vertical axis represents the internal energy of the molecule. The atom A is imagined as attached to the vertical axis, so that vibrations due to heat energy are measured by the movements to and fro of the atom B. The lower curve gives the amplitudes of oscillation of B for different energies; it is not truly continuous since vibrational energy is quantized and the curve merely joins the ends of a number of horizontal lines representing the discrete vibrational levels, of which two are shown as bb' and dd'. At ordinary temperatures practically all the molecules will be on the lowest vibrational level, bb'.

The upper curve represents the molecule AB in an electronically excited energy level. The molecule may be induced to jump from the lower to the upper curve by the absorption of visible or ultraviolet light. The electron shift occurs too rapidly for the atomic nuclei to change their distance apart, and therefore corresponds to the vertical line to cc' (Franck-Condon principle). Since the bond length of the excited molecule is usually greater than that of the normal molecule, the former finds itself in a compressed state and vibrates along cc' at a rate of about 10^{12} times per second. This excess vibrational energy is quickly lost to neighboring molecules, and the electronically excited molecule comes into temperature equilibrium with its surroundings by dropping to level cc'.

There is now the possibility that the molecule may drop to the ground level by radiating. This occurs after a mean life in the excited level of 10^{-8} sec, or more. Radiation corresponds to passage down the vertical line from cc' to d', giving a molecule with a stretched ground level with excess vibrational energy of level dd' above the normal bb'. Because of the two losses of vibrational energy, the emitted quantum has less energy and a longer wavelength than that of the absorbed quantum (Stoke's law). This is the phenomenon of fluorescence excited by light; it is essentially the reverse of light absorption, modified by operation of the Franck-Condon principle which leads to some energy loss as heat.

Overlap

The vertical dotted lines of Fig. 1 represent the transitions of maximum probability, and since energy = $h\nu$ they also correspond to the positions, on a frequency scale, of the maxima of the absorption and fluorescence bands. Since these bands have considerable width, however, the long-wave end of the absorption band overlaps the short-wave end of the fluorescence band. The degree of overlapping depends on a number of factors, and usually diminishes in going from gaseous to crystalline state (*1*).

Figure 2 shows the overlap effect for three fluorescent materials. Alcohol solutions of the two dyes, acriflavine and rhodamine B, have a considerable difference in their absorption-fluorescence maxima. Overlap means that when fluorescent light generated in a substance escapes to the surface, especially if it has to pass through a thick layer, more or less of its short-wave part is removed by re-absorption. This part is lost as heat if the substance has a quantum yield of less than unity. How serious this effect can be in losing light is shown in the upper part of Fig. 2. The solid line of the fluorescence curve is the ideal one for no re-absorption; the dotted curve, a, is what is observed for small crystals about 1×0.1 mm, and curve b is for crystals about 10×1 mm in size.

Where the exciting light is strongly absorbed, it makes a great difference whether the fluorescence is observed from the front or the back of a thick layer of a fluorescent block. Directional emission by molecules in flat crystals, and internal reflection effects at surfaces, may increase the length of path of the fluorescent light before emergence and so enhance the re-absorption loss (*2*). Excitation by α-particles, where the penetration is small, makes front-surface observation desirable; γ-ray excitation, with deep penetration, means that re-absorption effects are bound to be large even if diffusion losses are avoided by the use of large clear crystals or fluorescent blocks.

Quenching

In view of the reciprocal relation between light absorption and emission, it is surprising that so few chemical substances are fluorescent. Ideally, each absorbed quantum would re-appear as an emitted quantum, and the fluorescence yield would be unity. In the majority of instances, light absorbed is not re-emitted, but is degraded to heat by a variety of processes. The anticipated fluorescence may then be said to be "quenched."

When the absorbed light brings about a photochemical change, fluorescence is of course prevented, but this is not the usual reason for quenching. Much commoner are processes, either intramolecular or dependent on collisions with other molecules, whereby an excited molecule has its electronic energy degraded to heat by a radiationless path.

In a polyatomic molecule, the curves of Fig. 1 are replaced by complicated surfaces in space of many dimensions, owing to the numerous ways in which the molecule can vibrate. If the upper and lower surfaces approach one another closely at some point, the excited molecule can change over, without emitting light, into a highly vibrating form of the ground level. This excess vibrational energy is then quickly dissipated as heat. Intramolecular energy conversion of this type is the chief reason why so few molecules show fluorescence. The effect is often associated with the existence of a triplet electronic level lying between the upper state and the ground state.

The electronic levels of ordinary molecules, ground levels and those reached in light absorption, are classed by spectroscopists as singlets, which implies that all the electrons are spin-paired. Levels where one electron has its spin reversed are classified as triplets, because spin-orbital interaction gives rise to three closely spaced levels which here are treated as one.

Singlet-Triplet Transitions

Singlet-triplet transitions do not occur freely unless the electron can pass near an atomic nucleus, preferably a heavy one, where the strong magnetic field causes spin reversal. Light absorption takes the molecule from the singlet ground level to a singlet excited level. This is shown as AB in Fig. 3, where the effects of superposed vibrations are neglected for simplicity. Fluorescence is represented by CD, but it may happen that the path EF is preferred, so that a triplet level is formed. Because of the operation of the selection rules of spectroscopy, the molecule cannot readily leave this level by radiation, and is usually degraded to the ground level by collisions and intramolecular conversion processes.

The reality of these triplet levels

has been shown by the work of Lewis and Kasha (3). At low temperatures, when dissolved in a liquid which sets to a "glass," many substances show new luminescent phenomena. The usual effect is a long-duration glow after excitation, sometimes lasting a second or more. This differs from true fluorescence in two ways: the emitted light has a longer wavelength and the mean life is as much as a hundred million times longer. The triplet-singlet transition JK of Fig. 3 explains both these features, quenching during the long life of the triplet level being inhibited by the low temperature.

In certain materials this effect is accompanied by another, the emission of the ordinary fluorescence band but with a greatly lengthened lifetime. This happens when the triplet and upper singlet levels are not far apart, so that the transition EF can be reversed via GH a number of times by thermal energy, with a final delayed return down CD. The mean life of this process depends on the temperature, while that of the transition JK does not. In the general case there are, therefore, three forms of emission: short-period fluorescence, CD; long-period luminescence, CD, after EF,GH transitions; and long-period luminescence, JK, of longer wavelength.

The term phosphorescence for these long-life effects is avoided here because of the lack of general agreement on the definition. If length of mean life is used to distinguish fluorescence from phosphorescence, there would be two phosphorescences and one fluorescence. If Perrin's original definition is used, only the second would be true phosphorescence (4), while if the criterion is difference of spectra, only the third would be. Occasionally, as with hexabromobenzene or tetraphenylmethane excited by 3,650-Å radiation, or dehydrated oxalic acid excited by 2,537 Å, emissions of the JK type can be observed with the solid material at ordinary temperatures.

Substances prone to singlet-triplet transitions are obviously of no use for crystal counters, being either slow or inefficient. Aromatic hydrocarbons often show strong true fluorescence, and have therefore been extensively studied as counters, but nitro-, azo-, keto-, and many heterocyclic substances such as phenazine, together with molecules containing heavy atoms such as halogens or sulfur, are usually nonfluorescent at ordinary temperatures and show triplet-singlet luminescence when cooled in liquid nitrogen.

Resonance Energy Transfer

A phenomenon of particular importance is known as photosensitized fluorescence or resonance transfer of excitation energy. A well-known example is provided by anthracene crystals containing a minute proportion (1 part in 10^4) of naphthacene (5). Pure anthracene fluoresces blue-violet, and the presence of a small amount of naphthacene in solid solution changes the fluorescence to green, characteristic of the latter molecule. Naphthacene has an absorption band in the blue region, and the effect at first sight might be attributed to emission followed by re-absorption and re-emission. At such low concentrations, however, this cannot account for the facts. It is necessary to assume that the electronic energy of excited anthracene molecules can pass rapidly, before fluorescence occurs, into the naphthacene molecules, which then by Stokes' law emit a longer-wave fluorescence of their own. The efficiency of the transfer, which may approach 100%, must be ascribed to a resonance effect due to near coincidence of energy levels.

Many descriptions in the literature on the fluorescence of supposedly pure crystalline materials are vitiated by energy transfers to minute amounts of impurity as described. The fluorescence band of naphthalene, for example, lies wholly in the ultraviolet, but small quantities of anthracene usually present give the blue-violet fluorescence of anthracene itself.

Photosensitized fluorescence has proved of great practical importance in matching the emitted fluorescence band to the spectral-sensitivity curve of the photomultiplier. The latter, in its commonest form, has a sensitivity maximum in the blue region, while the fluorescence emission from organic substances with high efficiency for γ-ray measurement, such as naphthalene or stilbene, is in the near ultraviolet. The presence of a small quantity of anthracene in these substances gives the blue fluorescence of the latter which is easily measurable with the photomultiplier.

Resonance-transfer effects may also be harmful. If a nonfluorescent impurity whose absorption band overlaps the primary fluorescence band is present, even in small amount, the fluorescence process is quenched. An example is anthracene containing a trace of phenazine or similar nonfluorescent substance. Care in purification may therefore be an important matter in securing a high over-all efficiency.

Concentration Quenching

The use of a solid organic substance for γ-ray measurement has necessitated the preparation of large, clear crystals. This is by no means easy, and the difficulty varies in an unpredictable manner among different materials. The use of a liquid would obviate this difficulty and enable thick layers of optically clear, nondiffusing detectors to be obtained easily. Unfortunately, there is no known example of a single, pure substance which is strongly fluorescent in its liquid state. This effect is called concentration quenching, and is observed in strong solutions of fluorescent substances. For example, crystalline anthracene is highly fluorescent, and so is its dilute solution in benzene, but both its saturated solution and molten anthracene are nonfluorescent. Though the average distance apart and the rates of collision of molecules in the crystal and the pure liquid are nearly the same there is this difference: in the crystal, the thermal motion is a fairly regular vibration about mean lattice positions, whereas in the liquid, distances can vary from close approaches to rather wide separations. It is during the close approaches between molecules that quenching occurs, possibly due to distortion of potential-energy curves, bringing upper and lower curves into juxtaposition and allowing a radiationless disappearance of electronic into vibrational energy.

The use of dilute solutions of fluorescent substances for radioactivity measurements was originally thought to be impracticable since the rays act at random and only a small proportion of their effects would reach the solute. It was found by trial, however, that benzene solutions of terphenyl gave quite high yields of fluorescent light. This effect must be ascribed to a resonance-energy transfer between solvent and solute molecules (6). For the requisite condition of resonance to be fulfilled, since the solvent absorbs at much shorter wavelengths than the

solute, one must assume that the transfer takes place between high energy levels, about 6–7 ev above the ground state, during the step-wise energy conversion described below. The low level of the fluorescent excited molecules acts as an efficient collector, or trap, of energy quanta. That resonance-energy transfer can occur in liquid systems is shown by the recent work of Förster (7) with dye solutions; under some conditions it seems that energy can be transferred over distances up to 50 Å, or more, with high efficiency. Anthracene or diphenyl butadiene dissolved in a polystyrene plastic afford good examples of energy transfer because of favorable band overlaps (8).

A Typical Substance

As a typical fluorescent organic substance, crystalline anthracene may be chosen to illustrate the physical principles involved when it is caused to luminesce by ultraviolet light or by radioactivity rays. The molecules composing the crystal have excited electronic energy levels at about 3.25 and 5 ev above the ground level, and others at higher energies. Above an excitation of about 6.5 ev, the crystals show photoconductivity, i.e., mobile electrons are liberated within the crystal lattice and some molecules are ionized. (The isolated gaseous molecule of anthracene, while showing energy levels very similar to those of the crystal, requires about 10 ev for ionization.)

When molecules in the crystal are excited by light absorption to the 3.25-ev level, a blue-violet fluorescence (4,000–4,500 Å) is emitted. This emission occurs with a very high efficiency, the ratio of absorbed to re-emitted quanta being near 100% at −190° C and about 90% at ordinary temperatures.

If the molecules are excited to the next higher electronic level at 5 ev, fluorescence of high efficiency is again observed, the emission being the same blue-violet band and not a new one of shorter wavelength. A similar behavior occurs with still higher energy excitation. This phenomenon appears to be a general one with fluorescent substances. The fluorescence band corresponds to radiation from the lowest singlet-excited level above the ground level, irrespective of the actual level to which the molecule is excited.

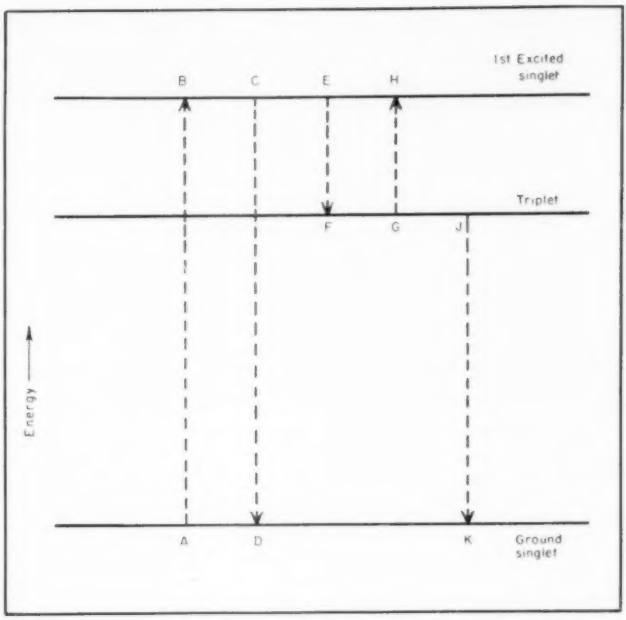

FIG. 3. Energy levels of a molecule showing emission and absorption paths

A rapid process of internal degradation of portions of the electronic energy to vibrational energy must occur with the higher excited molecules, so that they drop back step-wise to the lowest excited level and then radiate the remainder of the energy. This somewhat unexpected fact means that differences in the states of polarization of the electronic levels offer no hindrance to rapid interconversion, and that each fluorescent substance has one characteristic fluorescence band which is independent of how the molecule is excited up to its ionization limit.

Effects of Different Rays

Radioactivity rays have energies of thousands of electron volts, and their effects on matter are complex. As they are stopped by molecules they produce excitation and ionization, as well as chemical decomposition. The earlier stages are very little understood in detail. The energy of the rays is converted into heat and low-energy excitation of molecules by a complicated series of successive steps, until finally in a fluorescent substance each radioactivity ray leads to the emission of a number (generally a few hundred) of quanta of fluorescent light. The efficiency must depend on the material and on the rays.

Alpha rays produce very short straight tracks of dense ionization and excitation; beta rays give longer and more erratic tracks in which the effects are less concentrated; and gamma rays act at widely separated points distributed at random. Powders may therefore be efficient for α-rays, but β- and particularly γ-rays require large, optically clear materials to enable fluorescence generated at some depth to escape.

Chemical decomposition may be an important factor controlling the practical efficiency of the energy conversion, particularly for α-rays with their intense localized action. In the absence of systematic knowledge of the stages between the stopping of radioactivity rays and the production of electronically excited molecules capable of fluorescence, the selection of suitable materials must be made largely on an empirical basis, assisted by the principles mentioned above.

Recent work by Birks (9) on the relations between the specific fluores-

cence and the specific energy loss for different types of radiation that cause scintillations in a given crystal, is interpreted by means of a combination of the hypotheses of resonance transfer of energy and of chemical decomposition. As the nuclear particle passes through the crystal it creates in its track both excited molecules and decomposition products. Before radiation occurs, the former engage in the process of resonance transfer to other molecules, and the decomposition products can act in competition for the energy, which they quench. The more densely spaced in the tracks are the effects of the nuclear particles, the greater will be the quenching arising from newly-formed decomposition products. With a fresh crystal, each nuclear particle takes a track along unchanged material which it then contaminates; after long exposure to intense radiation, the accumulation of decomposition products must be expected to render the crystal useless.

Mean Life

An important matter for high-speed counting is the mean life of the fluorescence radiation, since this determines the time width of the particle scintillation peaks. The mean life is connected theoretically with the degree to which the electronic transition is quantum-mechanically permitted. This depends on symmetries of electron orbitals and on electron spins, and is measurable from the intensity of the absorption band of the transition.

If we define the molar extinction coefficient, ϵ, by the relation that the fraction of the incident light absorbed from a monochromatic parallel beam by a thickness of 1 cm is $1 - 10^{-\epsilon c}$, where c = number of moles of absorbing substance per liter, and plot measured values of ϵ against ω, the wave number of the light in cm^{-1}, we obtain an absorption curve (see Fig. 2) whose area is inversely proportional to the mean life of the electronic transition. If the molecules are arranged at random, and absorb only when the electric vector of the light lies along one direction, it can be shown that the mean life, in seconds, is the reciprocal of the quantity

$$87 \times 10^{-10} n^2 \omega_0^2 \int \epsilon \, d\omega$$

where n = refractive index of the material, ω_0 = wave number of the maximum of the absorption band, and the integral is the band area (*10*).

Values of mean life so obtained range from about 10^{-9} sec for fully permitted transitions, to 1 sec or more for largely forbidden ones. Rough values of the mean life can be judged from the maximum value, ϵ_{max}, of the extinction coefficient of an absorption band. For $\epsilon_{max} = 10^5$, 10^3, and 10^{-1}, the mean lives are of the order of 10^{-9}, 10^{-7}, and 10^{-3}, respectively. Substances must have values near the first of these figures to be useful for counters.

The theory on which the calculation of these mean lives is based, assumes that all the excited molecules regain the ground state by emission of light. If collisional quenching is present, reducing the fluorescence efficiency to some fractional value, then the actual mean life of the residual fluorescence is reduced by the same fraction. It is, however, obviously not practical to use quenching for artificially producing short mean lives, since the amount of available light is seriously reduced.

The mean life of a normal fluorescence process, in the absence of quenching effects, should be substantially independent of temperature. The actual mean life in a counter will depend on other factors, including the effects of resonance transfer of energy, which may be temperature dependent. More work is required on the direct determination of mean lives of radiation, which is a difficult problem because of the short time intervals involved.

The effect of temperature on mean life must be carefully distinguished from its influence on emission intensity. Rise of temperature practically always facilitates quenching processes, collisional or intramolecular, and therefore luminescence phenomena are commonest at low temperatures. Cooling of a material to increase its emission is useful, however, only if it is not already almost fully efficient at ordinary temperatures, as is the case for anthracene as mentioned before.

BIBLIOGRAPHY

1. S. L. Altmann. *Proc. Phys. Soc. (London)* **A63,** 1234 (1950); S. Sambursky, G. Wolfson, *Phys. Rev.* **62,** 357 (1942)
2. E. J. Bowen, P. Lawley, *Nature* **164,** 572 (1949)
3. M. Kasha, *Chem. Revs.* **41,** 401 (1947)
4. F. Perrin, *Ann. Phys.* **12,** 169 (1929)
5. E. J. Bowen, E. Mikiewicz, F. W. Smith, *Proc. Phys. Soc. (London)* **A62,** 26 (1949)
6. H. Kallmann, M. Furst, *Phys. Rev.* **79,** 857 (1950); **81,** 853 (1951)
7. T. Forster, *Z. Elektrochem.* **53,** 93 (1949)
8. W. S. Koski, *Phys. Rev.* **82,** 230 (1951)
9. J. B. Birks, *Proc. Phys. Soc. (London)* **A63,** 1044 (1950)
10. G. N. Lewis, M. Kasha, *J. Am. Chem. Soc.* **67,** 994 (1945); E. J. Bowen, W. S. Metcalf, *Proc. Roy. Soc. (London)* **A206,** 437 (1951)

Recovery of Radioiodine from Urine

A METHOD for recovering radioiodine from the urine of patients has been developed by H. D. Purves of the New Zealand Medical Research Council. Such recovery is necessary in New Zealand because the air-freight rates and the loss of activity during transit increase the cost of the radioiodine to about four times its cost in Great Britain.

The method depends on the filtration of the urine through a filter bed which contains silver chloride on a support of Gooch asbestos. Iodide is collected in the filter, and is recovered as iodic acid by passing 50 ml of chlorine water containing 0.1*N* sulfuric acid through the filter. Most of the radioiodine appears in the first 25 ml passed through the filter.

After reduction of the iodic acid the solution is free of odor and unpleasant taste and can be given to a patient without further treatment.

Some of the iodine is in organic compounds and is not removed by the method. Removal of I^{131} as iodide is 99% complete. Recovery of the I^{131} from the filter leaves 2–8% of the activity in the filter.

A recovery experiment with 1 liter of urine containing 11.46 mc of I^{131} gave a recovery of 11.06 mc, or 96.47%. The average recovery for three experiments was 91%.

Recovery and standardization of the recovered radioiodine was completed within 2 hours.

The complete technique is described in *Nature* **169,** 111 (1952).

Pitting of Aluminum in a Heavy-Water Reactor

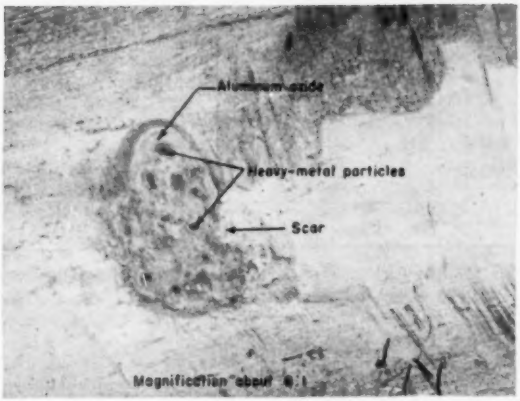

ONE OF LARGEST corrosion scars has typical heavy-metal particles surrounded by hydrated aluminum. Largest particle was 0.3 × 0.1 mm

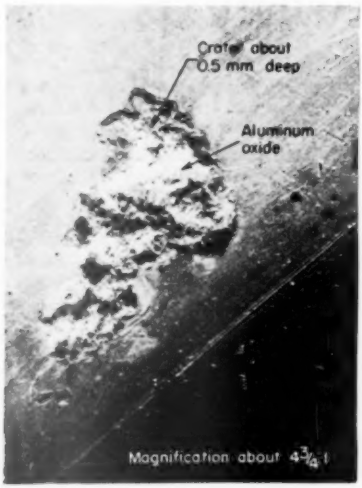

DEEPEST SCAR, shown here, was nearly 0.5 mm deep. Deposits of hydrated aluminum were noticed first, leading to discovery of the pitting

THE FUEL RODS in the heavy-water reactor at Kjeller, Norway, (NU, Nov. 51, p. 5) consist of uranium slugs stacked inside aluminum tubes with 2-mm walls. As shown in these photographs from Dr. G. Randers, pitting and corrosion have affected the outer surface of these tubes where they were immersed in the heavy-water moderator. The cover picture shows corrosion in a furrow in which copper had been deposited in microscopic amounts during drawing or pressing of the tube.

These fuel rods had been in the reactor for about four or five months when the pictures were taken. During this period, only test runs at low energy were made, the flux near the rods being about 10^{10} to 10^{11} neutrons/cm²/sec. The temperature of the heavy water very seldom rose above that of the air in the room.

No corrosion was observed above the level of the heavy water. The depth of the pitting below the water level was so small (usually 0.1–0.2 mm) that the pitting would not have been discovered except for the hydrated aluminum that was deposited. The interior walls of the aluminum reactor tank, however, were not affected by similar corrosion phenomena.

The purity of the heavy water did not change during the period when the pitting occurred; its specific conductivity remained constant at about 10^{-6} ohm^{-1} cm^{-1}.

MICROSCOPIC examination showed that pittings were shaped like craters with particle peak in center. Analysis of particle shown here proved that it was copper. In one case, center particle was iron

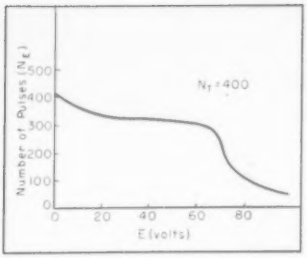

FIG. 1. Typical integral-bias curve

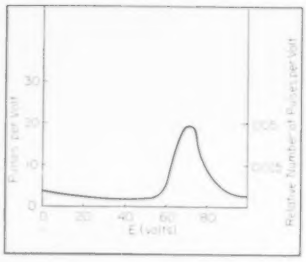

FIG. 2. Pulse-amplitude distribution

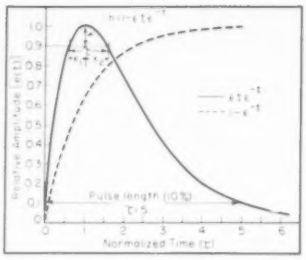

FIG. 3. Typical pulse shape

Pulse-Amplitude Analysis in Nuclear Research

PART I

VOLTAGE DISCRIMINATORS

This article introduces the analysis problem and discusses the requirements of voltage-selection devices. A number of different voltage-discrimination techniques are treated in detail

By A. B. VAN RENNES
Electrical Engineering Department
Massachusetts Institute of Technology
Cambridge, Massachusetts

WITH CURRENT DEVELOPMENTS in nuclear science and the allied field of electronic nuclear instrumentation, the need has arisen in many laboratories for equipment capable of determining the pulse-amplitude spectrum of a series of voltage pulses developed by a nuclear-radiation detector. These pulses, which usually arrive at random intervals (*1*), may have durations as short as 0.5 μsec, and separations between leading edges occasionally less than 1 μsec.

An early method of determining approximately a pulse-amplitude distribution, one still in considerable use, consists of photographing, on a stationary piece of film, the face of a cathode-ray tube in which the electron beam is deflected vertically a distance proportional to the value of the incoming pulses, while being swept across the screen horizontally during the pulse interval (*2*). On the resulting film record the density of exposure at a given height depends upon the relative number of pulses having a corresponding amplitude. The pulse-amplitude distribution is then obtained by plotting the density, measured with a densitometer, as a function of pulse height.

The distribution function can also be observed in diffuse outline by viewing or exposing the film through an optical wedge in which the density decreases linearly along the horizontal axis. Maeder (*3*) has described how

the diffuse outline can be sharpened by re-photographing the function with high-contrast film. This method is deficient in that film is not linear; i.e., the density of exposure is not linearly proportional to the amplitude distribution. By suitable calibration or comparison techniques, these nonlinearities may be nullified.

Integral-bias curve. Two general methods are widely used at present for obtaining a pulse-amplitude distribution spectrum (also called a differential-bias curve). The first (and indirect) method consists of measuring, during a given time interval, the number of pulses, N_E, whose amplitudes are greater than a particular level, E. A plot of this number as a function of level is called an integral-bias curve. An example is shown in Fig. 1.

By taking the derivative of the integral-bias curve one gets the desired pulse-amplitude distribution. The ordinate, dN_E/dE, represents the pulse-amplitude density, or number of pulses whose amplitudes lie within a unit channel width as a function of E.

The distribution curve corresponding to the integral-bias curve of Fig. 1 is plotted in Fig. 2. A normalized scale, $(1/N_T)dN_E/dE$, is also shown, from which can be determined the fraction of pulses having amplitudes lying within a unit channel width at level E. The total number of pulses, N_T, is the value of N_E when $E = 0$. It can be read from the integral-bias curve directly, or by determining the area beneath the pulse-amplitude distribution. Data for differential-bias curves are usually presented in quantized—discrete, not continuous—form; the curves so plotted are really histograms and are subject to the statistical uncertainties inherent in the process of counting random events.

Clearly, an integral-bias curve can be obtained by using an amplitude discriminator and performing repeated counts over a given time interval with the discriminator set at different levels. The results obtained are valid only if the pulse-amplitude distribution does not change between successive measurements and if the time for each count is sufficiently long to reduce statistical errors to a negligible value.

Direct measurement. A second method for obtaining a pulse-amplitude distribution spectrum entails the direct measurement of the pulse-amplitude spectrum with a differential pulse-amplitude discriminator, which counts, during a time interval, the number of pulses whose amplitudes lie between two nearly equal levels separated by a "window" or "channel" width. The spectrum is obtained, therefore, by plotting directly the differential count as a function of the window level.

The validity of these data is subject to the same limitations as above, with one exception. In a given time interval, the statistical counting errors present in a differential count are considerably lower than those in the derivative of an integral-bias count, as has been shown quantitatively by Westcott and Hanna (*4*) and others (*5*). As a brief intuitive explanation for the high error in the latter method, it is noted that the differentiation of an integral-bias curve involves taking the difference between two almost equal independent numbers, each of which is subject to a statistical uncertainty. The uncertainty in the difference is proportionally much greater than that in the original data.

Both the integral-bias and the differential-measurement methods are time-consuming procedures in that as many counting intervals are required as are desired numbers of data. Furthermore, as mentioned above, the data obtained are valid only if the pulse-amplitude spectrum does not change during the period of measurement.

Multichannel analyzer. An alternative method, which shortens the measurement time by virtue of a greater information-handling capacity, utilizes a multichannel pulse-analyzer system in which each pulse triggers only the channel corresponding to the amplitude of that particular pulse. Pulse counts are recorded in each channel, and a plot of these quantized data as a function of channel level constitutes a pulse-amplitude spectrum. In this case, only one time interval is required to collect all the data—an obvious advantage. The greater the desired resolution of the distribution curve, the greater must be the number of channels.

The major characteristics required of an acceptable pulse-analyzer system are stability and speed of response. The need for speed arises because the analyzer may be asked to sort with unchanged sensitivity a pulse which arrives very shortly after the occurrence of a previous pulse. This time, which for high speeds of analysis should preferably be as low as 2 μsec, is called the resolving time.

So that no significant histogram error is introduced by variations in window width, the window boundaries must be as stable as possible. If the count registered within a window whose width is ΔE volts is to be accurate within p per cent (neglecting statistical considerations), the boundary levels may not drift more than $p\Delta E/100$ volts relative to each other. The boundaries of a 3-volt channel, for example, if 1% stability is desired, may not vary by more than 30 mv, regardless of contact-potential drifts, supply-voltage variations, etc. Drifts common to all levels simultaneously are not as serious, however, and can be tolerated to a greater extent.

Voltage Discrimination

A voltage discriminator is a nonlinear device, usually an electron-tube circuit, which has the characteristic of delivering an output signal if, and only if, it receives an input pulse having an amplitude exceeding a preset critical level. Such a discriminator is simply constructed, for example, by coupling the input pulse to a following amplifier or counter stage through an RC coupling circuit and series diode, as will be discussed subsequently in conjunction with Fig. 4. If the diode is biased to the desired critical level, only that portion of a pulse exceeding this level will appear beyond the diode.

It appears that for best discriminator resolution, the discriminator element should have an input-output characteristic as highly nonlinear as possible; i.e., the ideal characteristic would have a step discontinuity in output voltage. This suggests the use of regenerative amplifiers or trigger circuits to indicate whether or not the input pulse has exceeded a critical level.

It is of interest to consider the interval of time during which a short pulse remains above a critical level, i.e., to consider the duration of the portion of the pulse actually observed by a discriminator. Assume that the pulse is one received from an amplifier designed for a maximum signal-to-noise ratio (*6*). In such an amplifier, the high-frequency and low-frequency responses are governed, respectively, by single RC circuits, the time constants of which are made equal. The response of such an amplifier to a unit step excitation, or to a relatively long

Symbols Used

E = pulse amplitude, volts
N_E = number of pulses with amplitude $> E$
N_T = total number of pulses
dN_E/dE = number of pulses having amplitudes within a unit channel at level E
$\frac{1}{N_T}\frac{dN_E}{dE}$ = fraction of pulses having amplitudes within a unit channel at level E
ΔE = window width, volts
p = window width stability, %
$e(t)$ = instantaneous pulse value as function of time, t
ϵ = Naperian logarithm base
h = amount normalized pulse exceeds critical level
t_1, t_2 = times at which pulse, normalized in amplitude and time, crosse h in positive and negative direction, respectively
x = $t - 1$, when t is in normalized units
x_1, x_2 = values of x corresponding to t_1, t_2
τ = normalized time during which pulse remains above $1 - h$
τ' = real time during which pulse remains above $1 - h$
i_b = instantaneous plate current
e_b = instantaneous plate potential with respect to cathode
E_{bc} = plate-cathode contact potential difference
i_b = total emission current
e_c = instantaneous grid potential with respect to cathode
e_{cn} = instantaneous grid potential with respect to ground
e_{bn} = instantaneous plate potential with respect to ground
e_k = instantaneous cathode potential with respect to ground
e_s = threshold of Schmitt circuit with preamplifier
e_2 = threshold of Schmitt circuit
e_1 = threshold of preamplifier
K = amplifier gain
Δe_s = drift in e_s
Δe_2 = drift in e_2
Δe_1 = drift in e_1
ΔK = change in amplifier gain

and steep input pulse, is a standard curve, represented in normalized form

$$e(t) = \epsilon t \epsilon^{-t} \quad (1)$$

The magnitude and time values of this pulse have been so normalized that the peak value, unity, occurs when $t = 1$. In these articles, the symbol ϵ will be used for the natural logarithm base, to avoid confusion with the symbols for voltage.

Let h equal the distance by which the pulse amplitude exceeds a stated critical level. Then the points of normalized time, t_1 and t_2, at which the pulse crosses the critical level are those values of time satisfying the equation (see Fig. 3)

$$h = 1 - \epsilon t \epsilon^{-t} \quad (2)$$

For convenience, define a new variable, x, such that $x = t - 1$. Then x_1 and x_2 are the time intervals separating the intersections of the critical level with the leading and trailing edges of the pulse from the instant $t = 1$. The relative (normalized) time, τ, during which the pulse remains above a stated level h units below peak is, therefore, $\tau = x_2 - x_1$. It is desired to find this time as a function of the height, h. By expanding the function

$$h = 1 - \epsilon(1 + x)\epsilon^{-(1+x)} = 1 - (1 + x)\epsilon^{-x} \quad (3)$$

in a power series, one obtains

$$h(x) = \frac{x^2}{2} - \frac{x^3}{3} + \frac{x^4}{4} - \cdots \quad (4)$$

It is of interest to determine the time, τ, when h is a very small fraction of unity. In this case, x is so small that the cubic and quartic terms may be neglected. Hence

$$\tau \approx 2x \quad (5)$$

and

$$h \approx x^2/2 \approx \tau^2/8 \quad (6)$$

For values of h lower than 0.01, the error in this approximation is less than 10%.

To convert this normalized function into units of real time, τ', note that the duration of the pulse of Fig. 3 between 10% points is five units of normalized time. For a 0.5-μsec pulse, for example, (measured between 10% points) one unit of normalized time represents 0.1 μsec. Since

$$\tau = \sqrt{8h} = 2.83\sqrt{h} \quad (7)$$

$$\tau' = 0.283\sqrt{h} \ \mu\text{sec} \quad (8)$$

A 100-volt, 0.5-μsec pulse thus exceeds a 99-volt level for only 0.028 μsec, and a 99.9-volt level for only 0.009 μsec. To respond properly to the short top of a pulse which barely exceeds the threshold, and accurately to determine the amplitude, an electronic discriminator must operate rapidly indeed. To alleviate the resulting requirement for unusually high operating speed, many experimenters prefer to shape the input voltage pulse with a delay line—artificial transmission line (7)—instead of RC circuits. A more nearly rectangular pulse can be so generated. The duration of the top of such a pulse does not vary so rapidly with discriminator bias.

Biased Diode

Perhaps the most basic method of discrimination, a biased diode followed by an amplifier, is illustrated in the circuit of Fig. 4 (4). Here the diode will not conduct unless a signal pulse of sufficient magnitude is received. That portion of a pulse which exceeds the discriminator bias is amplified and triggers (via an amplifier) a counter circuit. Note that the diode circuit alone does not entirely control the discrimination level; an output count is not obtained until the amplified pulse top is sufficiently large to actuate the counter. The discontinuous counter characteristic then shares in the discrimination process.

A serious disadvantage of the biased-diode discriminator is the forward coupling that exists by virtue of the diode plate-cathode capacitance. A pulse having a short rise time and an amplitude lower than the discriminator bias can still produce an output signal because of the capacitive coupling. To neutralize this diode self-capacity effect, a paraphase signal may be supplied to the diode plate through an auxiliary coupling condenser (4, 5).

Any threshold drift in the counter circuit that follows may introduce an uncertainty in net discrimination level due to the finite curvature of the diode volt-ampere characteristic at the conduction point. This uncertainty can be minimized by choosing a diode having as sharp a cutoff characteristic as possible. A diode-connected 6AC7 has an unusually steep semilogarithmic behavior (8). In fact, a comparison of the volt-ampere characteristics of various diodes with the transfer characteristics of some multi-electrode tubes, including the gated-beam tube, type

6BN6 (*9*), indicates that a diode-connected tube has the sharpest discrimination characteristic.

A measure of the sharpness of cutoff in a diode can be obtained by noting that at low currents, the plate current of a plane-parallel or cylindrical diode is an exponential function of net plate voltage and cathode temperature, T (in degrees Kelvin), (*5, 8*)

$$i_b = i_0 \varepsilon^{\frac{11{,}600(e_b + E_w)}{T}} \qquad (9)$$

$$\ln i_b = \ln i_0 + 11{,}600E_w/T + 11{,}600e_b/T \qquad (10)$$

A plot of $\ln i_b$ as a function of e_b is a straight line of slope $11{,}600/T$ and zero logarithm intercept at $e_b = -(T/11{,}600)\ln i_0 - E_w$. The slope of this logarithmic curve is a measure of the sharpness of cutoff. Inspection of the above equation reveals that this slope may be increased by reducing the cathode temperature. A 20% increase in slope without impairing emission current is practical. Since the zero intercept is a function of temperature (i_0 also is temperature-dependent), the need for stabilizing the cathode temperature is evident.

Westcott and Hanna (*4*), whose diode discriminator is shown in Fig. 4, report a long-term drift in discrimination level of only 0.05 volt. Negative pulses from a pulse-shaping circuit are supplied to the diode, V_1, the output of which is fed to the amplifier V_2. Positive pulses from a phase inverter in the pulse-shaping circuit are connected to the paraphase input to neutralize capacitive coupling across the diode. Small residual pulses resulting from imperfect neutralization are suppressed by purposely introducing "back-lash" in the amplifier consisting of V_2 and V_3. The second 6SH7, V_3, is normally cut off. No output is produced at the plate of V_3 unless a signal of at least 0.25 volt appears at the grid of V_2.

Crystal diodes have been suggested for use in diode discriminators (*2*). Because of its relatively high back resistance and self-healing power after being subjected to overloads, germanium has found wide application in crystal-rectifier construction (*10*). The use of these devices in pulse-amplitude discriminators would have several advantages; namely, the elimination of heater-power requirements, compactness, low capacitance (usually

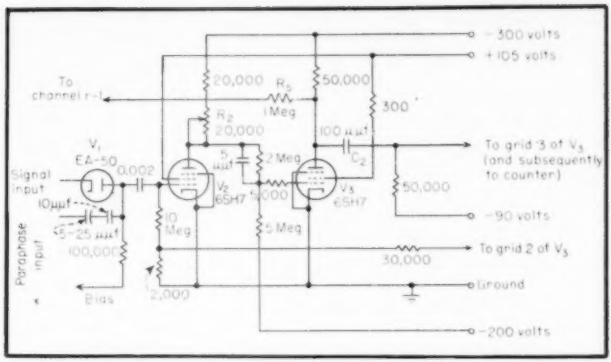

FIG. 4. Biased-diode discriminator (*4*) which is followed by an amplifier

from 0.2 to 1.0 μμf), and a "break" in the volt-ampere characteristic which may be five times as sharp as that of a thermionic diode and is located at zero voltage (rather than at a negative temperature-dependent voltage as is true for a thermionic diode) (*8*).

However, the back resistance of a crystal diode is not infinite and is, furthermore, highly temperature dependent (*5, 8*). Even the type 1N63, a unit selected for high inverse-voltage capability and high back resistance, conducts 400 μa at 50° C when 100 volts are applied in the non-conducting direction (*10*). This back current flowing through even a low diode load resistance would disturb the discriminator bias by an amount unacceptable for precision applications.

Parsons (*2*) has described a differential discriminator using three 1N38 crystal diodes connected in series. The 1N38 crystal has nearly the same inverse-voltage and back-resistance rating as the 1N63. The series combination of three units does not increase these capabilities fully three-fold, however, since the back resistance of crystal diodes is not uniform.

Biased Amplifier

A logical variation of the diode discriminator consists of a triode or pentode connected as an amplifier or cathode follower with its grid biased beyond cutoff. An output from such a circuit results only when an input pulse drives the grid to plate conduction. One advantage is the substantial voltage gain which can be incorporated in the discriminator. However, a discrimination uncertainty arises because the slope of the logarithmic current characteristic for any multi-electrode tube is lower when the tube is connected as a triode or pentode than when connected as a diode (*8*). Because of the larger number of variables, a multi-electrode tube is naturally subject to greater drift in its cutoff characteristic than is a diode. Such causes as changing tubes, varying plate- or heater-supply voltages, and drift in contact potentials are significant (*8*). The effects of such variations can be substantially reduced, however, by operating the discriminator tube in parallel with a second tube of the same type so that the drifts in the two tubes balance. Such a difference-amplifier connection tends to make the output signal depend only upon the difference in potential between the grids of the two tubes (*7*).

The gated-beam tube, type 6BN6, has a transfer characteristic whose discontinuity at the conduction point is nearly as sharp as a good diode (*9*). It has, therefore, found application as a biased amplifier (*11*). Moreover, the availability of a second high-transconductance control grid permits the use of this tube for coincidence and gating applications. An additional feature of the tube is the low control-grid current—less than 0.5 ma for grid voltages under +50 volts.

As with the diode, the output from a biased amplifier is not independent of the amount by which the input pulse exceeds the threshold. The over-all characteristic thus depends upon the circuitry that follows the discriminator, for an output will not be obtained from the subsequent counter circuit unless

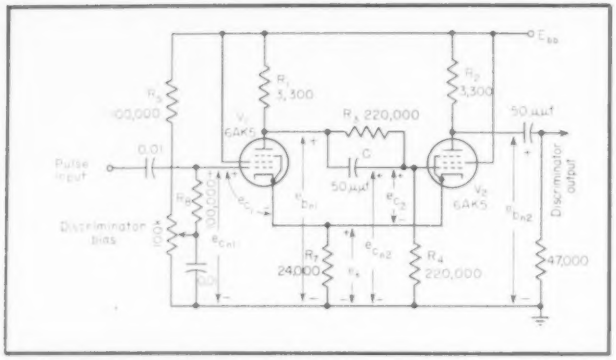

FIG. 5. Circuit of Schmitt discriminator (7)

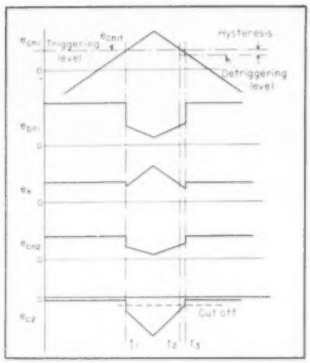

FIG. 6. Idealized waveforms in a Schmitt circuit for a triangular input pulse

the pulse received from the discriminator exceeds a minimum value. An application of this principle is used in the Model A-1 amplifier and will be discussed more completely as a variation of the Schmitt circuit.

As implied above, the beginning of the output pulse from a biased amplifier is somewhat indeterminate because of the logarithmic nature near cutoff of a tube's transfer characteristic. Furthermore, the initial rise of the output pulse is slow, because the transconductance of a tube is low near cutoff, and increases with plate current.

A "breakaway" diode, with its plate connected to the plate of the amplifier tube and its cathode to a point of potential several volts below the plate supply, is sometimes used to make the leading edge of an output pulse more abrupt (*12*). In this arrangement, a quiescent current flows through the plate load resistance and diode. When an input pulse drives the tube to conduction, no output signal appears until the tube has "robbed" all the quiescent current from the diode and then is operating in a high-transconductance region. The discrimination uncertainty (referred to the input) now depends on the diode characteristic divided by the gain of the amplifier. In effect, two discriminators are cascaded. The apparent diode resistance must be made low compared to the plate load resistance so that prior to breakaway the load resistance is effectively short-circuited. This precaution is especially necessary in a feedback-amplifier circuit where a high loop gain tends to remove any nonlinear characteristics, be they deliberate or accidental.

The breakaway diode is also used by connecting it between the plates of a difference amplifier or between the plates of two cascaded amplifier tubes. The latter configuration is of interest academically because, for increments, the diode is connected effectively between plate and grid of the second tube. The net effect upon the apparent grid-ground volt-ampere characteristic is similar to the Miller effect involving grid-plate capacitance (*8*). This diode connection is, therefore, termed an "amplified diode" (*13*). Frequent use of breakaway diodes in various configurations will be observed in the single and multichannel analyzers to be described (*11, 12*).

Schmitt Circuit

A desirable feature of a discriminator circuit is that the output signal is essentially independent of the amount by which the input pulse exceeds the discriminator bias. Such a characteristic can be obtained by the use of a trigger circuit having two stable states.

A popular circuit, called the Schmitt circuit, is diagramed in Fig. 5 (*6, 7*). It consists of a two-tube, direct-coupled, common-cathode circuit, which because of its balanced nature has a stability comparable to that of a difference amplifier. Usually the control grid of the left tube is biased below cutoff by the desired discriminator bias. This tube is nonconducting and the right tube is conducting.

When a pulse arrives that has an amplitude sufficiently large to drive the left tube to conduction, a switching action occurs, with conduction shifting from the right tube to the left. This triggered state continues until the input pulse falls below the approximate triggering level. For very short input pulses, insufficient time may be available for the output voltage to reach its final value (*7*).

Triggering of the input tube in a Schmitt circuit from nonconduction to conduction occurs at a higher input voltage than when triggering from conduction to nonconduction occurs. This backlash, or hysteresis, may range from a fraction of one volt to as many as 50 volts, and sets a lower limit to the size of a pulse that can be analyzed.

The basic reason for the hysteresis is that the potential e_{c2} which exists when e_{cn1} is at triggering level e_{cn1T}, depends upon the state of the circuit. In Fig. 6 are shown idealized waveforms of e_{cn1}, e_x, and e_{c2} for a triangular input pulse, subject to the assumption that the tubes are linear in the conducting region. Tube V_1 delivers two out-of-phase signals, e_{cn1} and e_x, to V_2. Since

$$e_{cn2} = R_4/(R_3 + R_4)\, e_{bn1} \qquad (11)$$

and

$$e_{c2} = e_{cn2} - e_x \qquad (12)$$

e_{c2} depends upon both signals.

Prior to t_1, V_1 is cut off, and e_{c2} is only slightly negative. At t_1, $e_{cn1} \geq e_{cn1T}$, and V_1 triggers on. If now e_{cn1} crosses e_{cn1T} from above (as at t_2), e_{c2} is very negative, and reverse triggering is delayed until e_{c2} reaches cutoff (at t_3). The additional drop in e_{cn1} needed to so raise e_{c2} is the hysteresis.

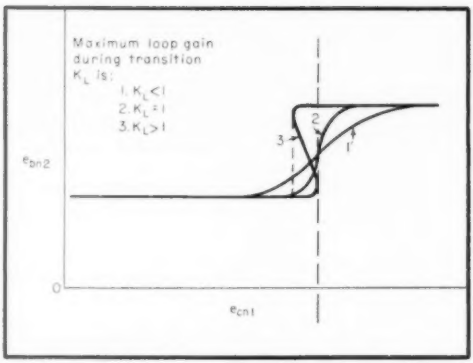

FIG. 7. Change in input-output characteristic of a Schmitt circuit

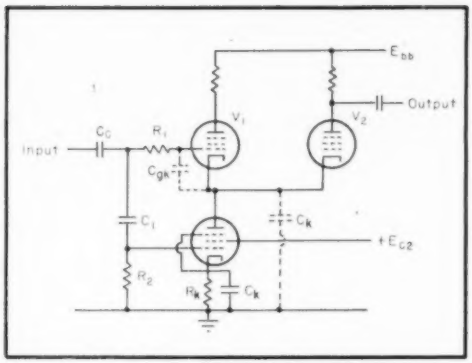

FIG. 8. Circuit for compensating against effects of grid-cathode capacitance

For rapid response to very short pulses, conventional techniques, such as inductive compensation of plate-load resistors and frequency compensation of the coupling network between the tubes are used to increase bandwidth (7). This voltage divider may not be over-compensated, however, or univibrator behavior near threshold may result.

The triggering process in any trigger circuit requires a maximum loop gain exceeding unity. Fig. 7 illustrates the change in input-output characteristic of a Schmitt circuit when the maximum loop gain is increased through unity. The rounded corners of characteristic 3, present because the transconductance of the tube driven to conduction is initially insufficient to permit triggering, can be eliminated by use of a breakaway diode. A more abrupt response can also be obtained by triggering V_1 off instead of on. Initially, V_1 then has a high transconductance, and the grid of V_2 is driven rapidly into conduction. Use of this technique has been made in the discriminator circuit of the A-1 amplifier (*14*).

The ability of the Schmitt circuit to accept positive voltage pulses greatly exceeding threshold without drawing grid current (by virtue of the cathode-follower action of V_1) is useful in preventing bias shifts which would otherwise occur. Replacing the large common-cathode resistor with a "constant-current" tube may enhance this ability. A constant-current tube is a tube (and associated circuit) which displays a high dynamic resistance.

Input pulses of short rise and fall times place severe demands on a Schmitt circuit because of the large currents needed for rapid charge and discharge of the unavoidable cathode-heater capacitance. The rapid fall of a pulse may prematurely cut off V_1 so that the cathode voltage relaxes slowly and cannot follow the input waveform faithfully.

In addition, the grid-cathode capacitance of V_1 can introduce an undesired signal. The rapid rise and fall of an input pulse insufficiently large to cause triggering, coupled through this capacitance, disturbs the cathode potential (hence, the threshold) and generates spurious signals at the plate of V_2. A similar difficulty frequently arises in a biased amplifier, particularly a difference amplifier.

An interesting technique by which a constant-current tube in the common-cathode-return circuit compensates against the effect of grid-cathode capacitance (*12*) is illustrated in Fig. 8. The compensating elements R_2 and C_1 deliver to constant-current tube V_2 a signal which increases its plate current instantaneously by an amount equal to the displacement current through C_{gk}. Any disturbing accumulation of charge across C_k is thereby prevented.

Uncertainty in the triggering level of a Schmitt circuit may be due to variations in bias voltage, to variations in cutoff characteristics of the left tube, to changes in values of R_1, R_2, R_k, R_3, and R_6, or to a shift in quiescent-cathode potential, which, in turn, results from changing characteristics of the normally conducting tube. The effects of a change in plate-supply or filament-supply voltages are not serious because of the balanced nature of the circuit. Except for short-term measurements, the triggering level is subject to an uncertainty of about 0.1 volt (*7*), a value sufficiently high to influence the usefulness of a Schmitt circuit for high amplitude-resolution applications.

Schmitt Circuit; Preamplifier

A system used in the A-1 amplifier (*14*) which retains the attributes of the Schmitt circuit, but increases the effective amplitude resolution, is shown in Fig. 9. The discriminator itself, a modified Schmitt circuit, has been preceded by a gain-of-10 difference amplifier biased to the desired discrimination level. An output from the discriminator occurs when the amplified pulse top is sufficiently large to trigger the Schmitt circuit. The relatively nonsharp amplifier conduction characteristic is here of no disadvantage, for whether or not an output appears is determined primarily by the on-off characteristics of the trigger circuit. The apparent threshold, e_s, at the input of this system consists of the necessary input signal for the Schmitt circuit, e_2, divided by the gain, K, of the amplifier, plus the amplifier conduction threshold, e_1,

$$e_s = e_2/K + e_1 \qquad (13)$$

By total differentiation of e_s

$$\Delta e_s = \frac{1}{K}\Delta e_2 - \frac{\Delta K}{K}\frac{e_2}{K} + \Delta e_1 \qquad (14)$$

one observes that drift of input threshold may arise from drift in amplifier

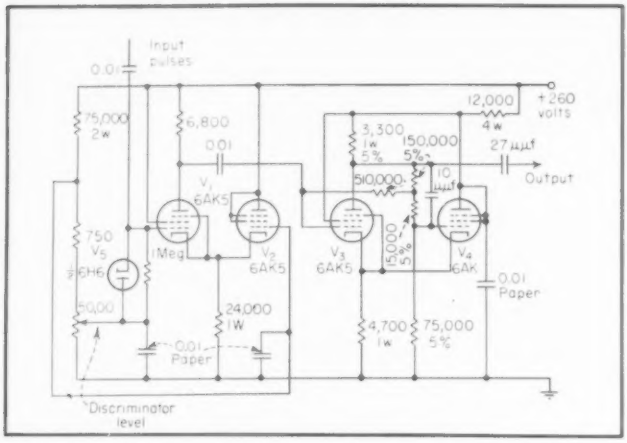

FIG. 9. Pulse-height selector which increases effective amplitude resolution (*14*)

bias potential, drift in Schmitt circuit characteristics, or from a change in amplifier gain. Since the level instability, Δe_1 of a difference amplifier should normally be no smaller than that of a Schmitt circuit, Δe_2, this system offers no stability improvement. (Note that in both the difference amplifier and Schmitt circuit, potentials for the two grids are obtained from the same voltage divider.) It does, however, permit the analysis of smaller-sized pulses, because the apparent hysteresis, that of the Schmitt circuit divided by the gain of the amplifier, is very small. A wider dynamic range of usefulness results. Preamplification also reduces the slight uncertainty in threshold caused by pulses too short to permit the output signal to reach full size.

The input difference amplifier exhibits the same anti-overload characteristics as those mentioned earlier for the Schmitt circuit. A large input pulse cuts off V_2 so that the cathode of V_1 may freely follow the grid positive nearly 100 volts before grid conduction occurs. A rapid response by the Schmitt circuit to exceedingly short pulses is obtained by triggering off V_3 (conducting quiescently), instead of the usual reversed process. Tube V_3 is made to conduct quiescently by returning its control grid to a higher bias potential than that for V_4. When properly adjusted, the Schmitt-circuit threshold should exceed the hysteresis by a reasonable margin, or the circuit can never return to its original state.

The difference-amplifier in this system is well suited to the use of techniques for compensating against effects of grid-cathode capacitance. This technique, described earlier, may be required where the input pulses have a short rise and fall time. No such compensation is needed in this particular Schmitt circuit, however, because prior to triggering, its grid never swings over a wide voltage range.

Usually a discriminator is used to measure the height of input pulses above the zero baseline. At high counting rates, the coupling capacitor shifts the baseline by the average value of the input waveform. To avoid this error, diode V_5 is provided to clamp the baseline to the discriminator bias. Actually, the noise and "contact potentials" generated within the diode disturb the apparent baseline and cause a smearing of measured data, so that the diode is usually removed except when counting at high rates.

Schmitt Circuit; Known Deadtime

Frequently one desires to determine accurately the statistical counting losses which result from the resolving time of a discriminator circuit. Usually the resolving time depends partly upon the duration and amplitude of a pulse just received. However, in a circuit proposed by Cooke-Yarborough (*15*), a known deadtime is deliberately introduced to enable accurate calculation of the statistical counting losses.

In Fig. 10, tube V_1 and its associated circuit form a Schmitt circuit in which the cathode resistor is replaced by a constant-current tube V_{2A}. The two halves of V_2 are connected, however, in a univibrator circuit in such a manner that the appearance of a positive output pulse at the plate of V_{1B} triggers the univibrator, V_2, thereby cutting off plate current in V_1 and disabling the discriminator. This negative gate lasts for an interval which depends upon the time constant of the RC differentiating circuit connected between the plate of V_{1B} and the grid of V_{2B}. Thereafter, the circuit returns to its original quiescent condition to await another input pulse. By means of switch S_2, deadtimes ranging from 5 μsec to 10 msec can be provided. With switch S_2 in position 12, univibrator action is prevented, and the only deadtime resulting is that due to the Schmitt circuit alone, approximately 1 μsec. If in one second, n' counts are recorded by the discriminator, the actual number of pulses per second, n, applied to the discriminator is

$$n = n'[1 + nt + (1/2)n^2w^2] \quad (15)$$

where t is the deadtime of the discriminator and w is the average interval during which an input pulse exceeds the discriminator threshold.

High-Speed Discriminator

A recent design by Wells (*16*) for a high-speed discriminator circuit is shown in Fig. 11. This unit has a fixed dead-time of 0.2 μsec; precise determination of the counting loss at high rates is thereby possible. In this circuit, a biased difference amplifier, V_1, is followed by a nonoverloading regenerative-feedback amplifier. An input pulse at the grid of V_{1A} excites V_{1B} via the common-cathode coupling. Two feedback loops exist. The first, which provides fast trigger action, consists of V_{1B}, V_4, and V_6. The second holds the circuit over for an accurately determined period, and consists of V_{1B}, V_4, V_6, V_7, and V_2. Diodes V_{5A} and V_{5B} are d-c restorers which establish the quiescent potentials at the grids of V_4 and V_6. An output pulse from the plate of V_3 feeds an accurately determined charge into a fast scaler each time a pulse occurs.

Operation is as follows. Input pulses (preferably shorter than 0.1 μsec) are supplied to V_{1A}. Those exceeding the bias cause a signal at the common cathode which begins to cut off V_{1B}. Aided by the 6-volt negative

pulse which arrives at the grid of V_{1B} from amplifier V_4 via cathode follower V_6, V_{1B} shuts off regeneratively. The plate load of V_7, a part of the second feedback loop, consists of a shorted, 0.05-μsec artificial delay line. The fast negative step which appears at the cathode of V_7 generates, therefore, a negative 0.1-μsec, 10-volt pulse at the plate. This signal produces a 10-ma, 0.1-μsec current pulse from V_3 to drive the scaler; moreover, it cuts off V_2, the constant-current tube in series with V_1, thereby isolating the level-selector circuit from the input. The pulse at the plate of V_7 ceases 0.1 μsec later. If the input signal has meanwhile disappeared, current is restored in V_{1B}; otherwise, it restores when the input pulse ends.

Restoration of current in V_{1B} cuts off current in V_7, thereby generating a 0.1-μsec positive pulse at the plate. This 10-volt positive pulse, applied to the grid of V_2, insures that V_3, which is shut off quiescently, will stay off for 0.1 μsec after V_{1B} turns back on. An input pulse arriving during this interval cannot deliver an adequate charge pulse to the scaler. For input pulses shorter than 0.1 μsec, a deadtime of approximately 0.2 μsec results.

Other Types

A number of additional techniques exist for discriminating against voltage pulses smaller than a preset amplitude. Trigger circuits other than the Schmitt circuit, such as blocking-grid oscillators, univibrators, or multiars (*8*) have been suggested for this purpose, but have never received wide use.

Beam-deflection tubes are of interest as discrimination devices because a pulse amplitude can be measured in terms of the position of an electron beam or a spot of light. A recently explored technique converts the height of each pulse to a proportional time duration which can then be measured with high accuracy. Multichannel analyzers based on these methods of measurement will be described in subsequent articles.

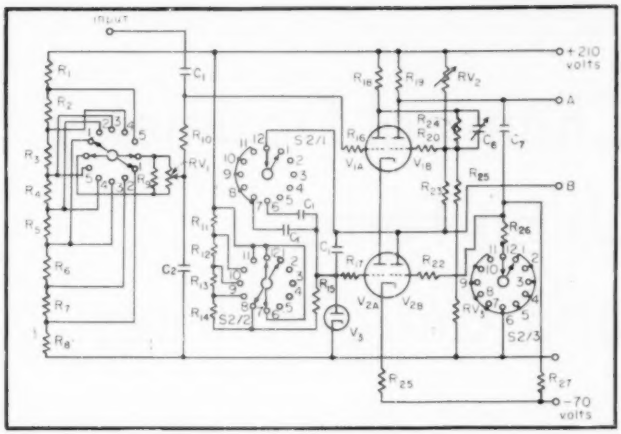

FIG. 10. Discriminator circuit that has known deadtime (*15*)

NEXT IN THIS SERIES . . .
will be articles on
Single-channel differential analyzers
Multichannel analyzers—I
Multichannel analyzers—II
in August, September, and October, respectively

BIBLIOGRAPHY

1. H. Bateman, *Phil. Mag.* **20,** 704 (1910)
2. J. H. Parsons, *Proc. I.R.E.* **37,** 564 (1949)
3. D. Maeder, *Helv. Phys. Acta* **20,** 139 (1947)
4. C. H. Westcott, G. C. Hanna, *Rev. Sci. Instr.* **20,** 181 (1949)
5. N. F. Moody, W. J. Battell, W. D. Howell, R. H. Taplin, *Rev. Sci. Instr.* **22,** 551 (1951)
6. W. C. Elmore, NUCLEONICS **2,** No. 2, 14; No. 3, 16; No. 4, 43; No. 5, 50 (1948)
7. W. C. Elmore, M. Sands, "Electronics—Experimental Techniques," National Nuclear Energy Series, V-1 (McGraw-Hill Book Co., Inc., New York, 1949)
8. B. Chance, *et al.* "Waveforms," pp. 58, 163, 174, 179, 325 (McGraw-Hill Book Co., Inc., New York, 1949)
9. R. Adler, *Electronics* **23,** No. 2, 82 (1950)
10. "Germanium Diodes" (General Electric Co., Syracuse, New York, 1950)
11. G. G. Kelley, P. R. Bell, W. J. Gerhard, L. A. Meaks, private communication
12. J. E. Francis, P. R. Bell, J. C. Gundlach, *Rev. Sci. Instr.* **22,** 133 (1951)
13. F. I. Magee, P. R. Bell, W. H. Jordan, *Rev. Sci. Instr.* **23,** 30 (1952)
14. W. H. Jordan, P. R. Bell, *Rev. Sci. Instr.* **18,** 703 (1947)
15. E. H. Cooke-Yarborough, *J. Sci. Instr.* **26,** 96 (1949)
16. F. H. Wells, *J. Sci. Instr.* **29,** 111 (1952)

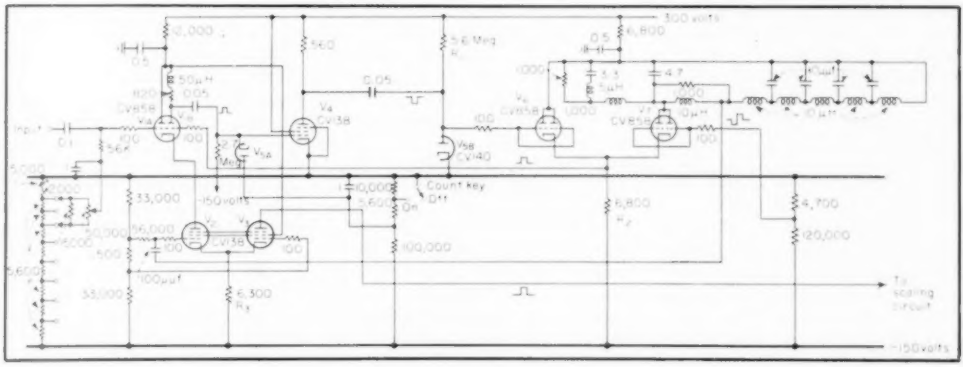

FIG. 11. High-speed amplitude discriminator that has known deadtime (*16*)

Chemical Dosimetry Using Ferrous and Ceric Sulfates

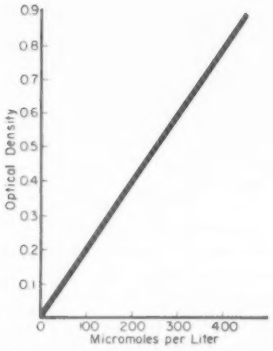

FIG. 1. Optical density versus concentration of Fe^{++} in 0.8N H_2SO_4

High-level dosimeters are a major need for fission-product research. Results with aqueous $FeSO_4$, for use under 50,000 rep, and $Ce(SO_4)_2$, for use up to 12,000,000 rep, are reproducible and independent of dose rate and intensity over wide ranges

By JEROME WEISS
Brookhaven National Laboratory
Upton, New York

AT PRESENT several universities have at their disposal kilocurie radiation sources which are being used for research in the fission-product utilization program. To correlate the chemical and physical changes of substances exposed to these sources with the radiation received, it is necessary to know how large a dose has been delivered to the sample.

There are several methods of dosimetry in use. Some investigators are using ion chambers, of one sort or another, which measure the amount of ionization caused in air. This method is good if the sample to be irradiated is air or some other gas. However, if the sample to be exposed is a liquid or a solid, the ion chamber reading usually will not indicate how much energy the sample has received from the source.

To obtain a reliable dose measurement, it is convenient for the dosimeter and sample to have the same, or nearly the same, stopping power for the radiation being used. In addition to having an equivalent stopping power, the dosimeter and sample should be geometrically alike, in order to eliminate any geometry effect. This would require, in the case of ion chambers, the construction of a chamber of the same material and dimensions as the sample container. This necessity makes the ion chamber rather inconvenient to use, especially when the size of the sample container is frequently changed. One could make a small ion chamber to be immersed in the liquid or solid, but this would be difficult or impossible in many cases. A knowledge of relative stopping powers would also be required, but even then the reading obtained would not average the dose over the volume of interest.

To eliminate these complications, the tendency has been to develop dose-measuring devices which would take these factors into account. Several types of dosimeters have been proposed, and are in use at the present time. The majority of these methods rely upon a chemical or physical change which is easily measured, and which is some function of the dose received.

Since there are several methods of dosimetry in use, it would be advantageous either to intercalibrate all the methods or adopt one method as a standard to be used by everyone. If one of these alternatives is accepted, the terms "sterilization dose" and "killing dose" could be established as a definite number of rep to take the place of different values obtained by different methods. At present, this is not the case, since a dose of 2 million rep as measured with a methylene blue dosimeter has not been shown to be equal to 2 million rep as measured with ferrous sulfate solution or polyvinyl chloride films.

The purpose of this report is to outline the procedures to be followed

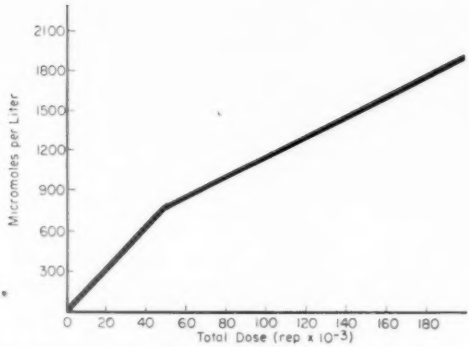

FIG. 2. Micromoles of Fe^{2+} oxidized as a function of the total irradiation

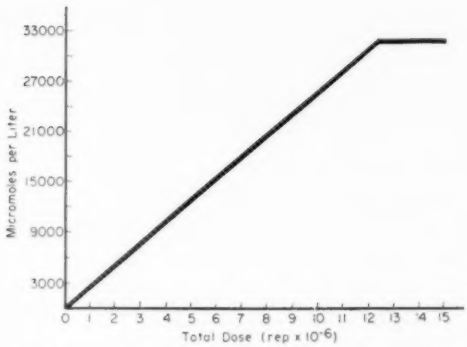

FIG. 3. Micromoles of Ce^{4+} reduced as a function of the total irradiation

in the use of ferrous sulfate or ceric sulfate solution as a dosimeter. Some of the experimental findings are also included to give the reader an indication of the range of usefulness of these methods.

Ferrous Sulfate Dosimetry

It has been known for some time that an aqueous solution of ferrous ions will be oxidized to ferric ions when subjected to ionizing radiation (*1, 2*). The oxidation yield has been shown to be independent of original ferrous ion concentration from 10^{-2} to $4 \times 10^{-3}M$ (*2, 3, 4, 5*). The yield has also been shown to be independent of quantum energy for 100-kv X-rays to 2-Mev γ-rays (*2, 6*). Dose rates from $\frac{1}{50}$ r/sec to approximately 200 r/sec seem to have no effect on the yield (*6, 7*).

The sensitivity to pH is overcome by specifying that the solution be made $0.8N$ in sulfuric acid. The initial yield of iron oxidized decreases with decreasing acid concentration. This decrease is greatest between $10^{-2}N$ and $10^{-3}N$ H_2SO_4. From $0.1N$ to $1.0N$ H_2SO_4 no change in yield is observed (*8*).

Reagent solutions. Ferrous ammonium sulfate (reagent grade) is recrystallized several times from triply-distilled water containing a sufficient amount of sulfuric acid (reagent grade) to prevent hydrolysis of the iron. Recrystallization is not necessary if the grade of reagent is good.

The desired amount of salt is added to $0.8N$ H_2SO_4, made up with the pure water, to make up the ferrous sulfate solution. The exact concentration of ferrous ion need not be known since only the ferric concentration will be determined.

Method of analysis. Ferric ion has an absorption maximum at approximately 304 mμ. It is therefore possible to determine the amount of iron oxidized by using the non-irradiated sample as a blank and reading the optical density of the irradiated sample with respect to it. The peak of the absorption maximum is at 304 mμ; however, it is quite a broad peak and therefore not very sensitive to wavelength setting. All the results which have been listed were obtained at 305 mμ with a slit width of 0.5 mm. Quartz cells and a hydrogen lamp were used for all determinations.

The preliminary work involves the construction of an optical-density vs ferric-ion-concentration curve. For convenience, the concentration of ferric ion is expressed in micromoles per liter (see Fig. 1). It would be best if this calibration were made for the spectrophotometer to be used since there are slight variations between instruments. Since all answers are based upon the accuracy of the curve, it is extremely important that it be constructed with great care. It was found that the best way to make up standard ferric ion solutions was to make up an approximate concentration of ferric ion 0.001 $-$ 0.005M. This solution was quantitatively reduced in a Jones reductor and aliquots titrated with standard permanganate. A known amount of the reduced solution was then quantitatively oxidized with peroxide and diluted to a known total volume. Various concentrations were made by dilution of this standard ferric ion solution.

Yield. Since there is still some discrepancy among experimental results for the oxidation yield for this reaction, the individual operator can decide on which number to use. The two most popular yields are 15.4 μm/l/1,000 rep (*9*) and 20.2 μm/l/1,000 rep (*7*). (These values are based on 93 ergs/gm for the energy absorbed in water for 1 r of radiation.)

The lower value is being used at Brookhaven, since the calorimetric method used in determining it is felt to be more direct and less subject to geometrical errors.

Once a yield is decided upon, it is then possible to rescale the calibration curve so that a plot of optical density vs dose is obtained.

Limitations. The iron oxidation is dependent upon oxygen concentration and therefore the yield is different for aerated and deaerated solutions.

Since it is most convenient to use aerated solutions, a word of caution is necessary. The reaction in aerated solutions consumes oxygen and, since there is only a limited amount of oxygen present, it will eventually be entirely consumed. The total dose at which all the original oxygen is consumed is approximately 50,000 rep. This value is based upon the solubility of oxygen in the solution and the yield of four ferrous ions oxidized per O_2 molecule consumed (*10*). Therefore, in using the ferrous dosimeter, it is best to maintain a total exposure of less than 50,000 rep, since the oxidation

yield drops by a factor of two when the oxygen is consumed.

However, if the curve is determined up to high total doses, one can use this dosimeter above 50,000 rep. Figure 2 is such a plot up to 200,000 rep.

Ceric Sulfate Dosimetry

Aqueous solutions of ceric sulfate are relatively new in the field of dosimetry. As a consequence, less is known about the limitations of this solution as a dosimeter. There have been some reports that it is not as reproducible as the ferrous sulfate reaction.

The reaction which takes place is a reduction of ceric to cerous ion. The yield is independent of concentration from 3.2×10^{-2} to approximately $10^{-4}M$. The yield has also been shown to be independent of energy from about 100-kv X-rays to 2-Mev γ-rays. Dose rates seem to have no effect on the yield from approximately $\frac{1}{2}$ r/sec to approximately 500 r/sec (*9*).

There is no dependence on oxygen concentration as was found in the ferrous sulfate system. Therefore, a plot of cerous ion concentration vs dose does not exhibit a change in slope. Figure 3 is a plot of cerous ion concentration vs dose (the dose was determined with a ferrous sulfate actinometer using 15.4 μm/l 1,000 rep for the oxidation yield).

Solutions. A weighed quantity of ceric sulfate (reagent grade) was added to 0.8*N* sulfuric acid and then diluted to volume with 0.8*N* H_2SO_4. The exact concentration to be used depends upon the total dose to be measured.

Since the cerous ion concentration is determined by difference, it is advantageous to start with a low initial ceric ion concentration. Experience has shown that a concentration change of 30% or more gives excellent results. The concentration was determined volumetrically against sodium oxalate.

Method of Analysis. Ceric ion has an absorption maximum at 320 mμ in H_2SO_4 solution. The absorption maximum is not a broad one and is therefore sensitive to wavelength setting. This maximum should be determined for the instrument to be used. The slit width used was 0.5 mm. Quartz cells and a hydrogen lamp were used for all determinations. In this case the ceric ion concentration is determined before and after irradiation and the cerous ion concentration is obtained by difference.

As in the ferrous sulfate method, one must construct a curve of optical density vs ceric ion concentration. The concentration should be expressed in micromoles per liter (see Fig. 4). The careful construction of this calibration curve is the key to the successful use of ceric sulfate as a dosimeter.

Yield. The ceric sulfate reduction yield is based upon the ferrous sulfate oxidation yield. If ceric sulfate and ferrous sulfate are subjected to the same irradiation (same energy, dose rate and total dose) and the amount of iron oxidized is compared to amount of cerium reduced, one finds that approximately six times as much iron has reacted as cerium. The table lists the results of several determinations of this ratio. If the iron yield one chooses is 15.4, the cerium yield will be 2.58; if one uses 20.2, the cerium yield will be 3.39.

Ratio of Ferric to Cerous Yields

Dose (kilorep)	*Ce^{3+} yield (μ-moles)*	*Fe^{3+} yield (μ-moles)*	*Yield ratios (Fe^{3+}/Ce^{3+})*
7.50(a)	19.2	115	5.98
10.0 (b)	26.0	154	5.93
15.0 (a)	38.7	231	5.97
20.0 (b)	51.5	308	5.98
25.0 (a)	65.0	385	5.93
30.0 (b)	77.5	462	5.97
45.0 (c)	116.0	693	5.96
		Average	5.96 ± 0.03

Dose rates: (a), *3 rep/sec;* (b), *28 rep/sec;* (c), *100 rep/sec.*

Limitations. The only limitation in this method of dosimetry is the possibility of an energy dependence at very low energy. This fact has been reported but not as yet confirmed.

A large error may be introduced if one has a high initial ceric ion concentration and the change in concentration is small. For example, if the initial concentration is 30,000 μm/l and the change is 100 μm/l (approx. 35,000 rep), it may not be detected since it is only a 0.33% concentration change, which is of the same order of magnitude as the sensitivity of the instrument. However, if the initial concentration were 300 μm/l, the same amount of reaction is a 33% concentration change and easily measurable with great accuracy.

Advantages of Fe^{2+} and Ce^{4+}

Experiments have been performed at this laboratory in which it was desirable to have a dosimeter in the radiation field with the samples during the entire irradiation. The total dose was of the order of 6 million rep. Ferrous and ceric dosimeters were used for this experiment. The ferrous system proved to be unsatisfactory for this high total dose. Its failure was due to the high original concentration of ferrous ion which was required. There are some reports of a back-reaction taking place after approximately 90% of the original iron is oxidized. In order to avoid reaching this per cent conversion, the original ferrous ion concentration would have to be slightly over 0.1*M*. It was found that on long standing this solution auto-oxidized and complicated the blank determination.

The ceric system, however, was quite stable and gave no indication of a back-reaction. This fact is clearly shown in Fig. 3. For subsequent work of this nature the ceric dosimeter was used exclusively.

Another advantage of the ceric system is the excellent sensitivity of the concentration determination. A comparison of Fig. 1 with Fig. 4 shows that

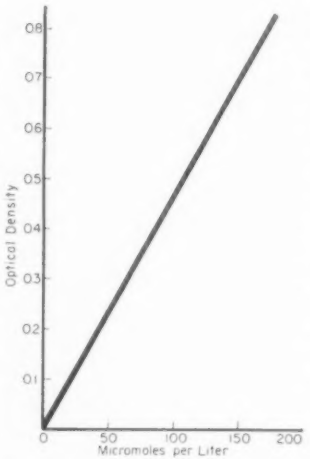

FIG. 4. Optical density as a function of the concentration of Ce^{4+} in 0.8*N* H_2SO_4

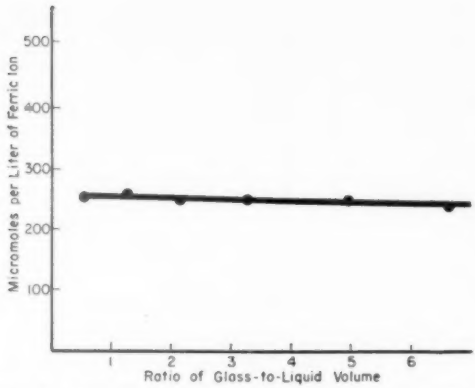

FIG. 5. Micromoles of Fe^{3+} produced as a function of glass-to-liquid-volume

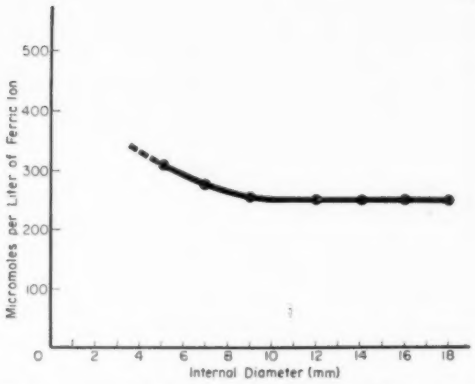

FIG. 6. Micromoles of Fe^{3+} produced as a function of the internal diameter of the sample vial

the cerium determination has a greater change in optical density per unit change in concentration. Therefore, as long as the total change is appreciable, the accuracy of the determination will be better than one can achieve with the iron system.

The advantage of the ferrous dosimeter is the large oxidation yield per 1,000 rep. This fact should enable lower dose measurements to be made quite accurately. The policy at this laboratory is to use the ceric dosimeter for very intense sources and the ferrous dosimeter for weaker sources.

Effect of Reaction Vessel

During the course of the experimental work which was carried out, it was noticed that the amount of reaction which took place per unit time was altered when the sample vessel was changed from a 6-cm^3 to a 0.6-cm^3 vial. A series of experiments, designed to determine the reason for this change in reaction rate, was then undertaken. It was felt that the ratio of glass to liquid volume might have had some significance.

A series of reaction vessels was constructed having identical internal diameters and glass walls of varying thickness. These vessels gave a series of glass-to-liquid-volume ratios from 0.5 to 6.6. Samples were irradiated for 10 minutes in the same field, and the amount of iron oxidized was determined. It is obvious from the results plotted in Fig. 5 that there is no significant change in reaction rate other than that due to shielding by the thick glass walls.

The next possibility was that the change in reaction rate was associated with the internal diameter of the sample vessel. A series of vials were made with different internal diameters and approximately the same wall thickness. The internal diameters ranged from 5 mm to 18 mm. Figure 6 is a plot of the results obtained when samples were irradiated in these vials for 10 minutes. It is obvious, from the experimental data, that the internal diameter of the sample container is significant. The values in Fig. 6 were obtained from irradiation carried on inside a cylindrical source.

One can conclude from these results that the increase in reaction rate for a small-diameter vial is due to an increased importance of the secondary electrons from the glass walls. With a large enough diameter one approaches a situation characteristic of the liquid, with the effect of secondaries from the wall still present but having a negligible effect on the total volume. The liquid near the walls receives more secondaries than the liquid away from the walls. The value of dose measured is an average for the entire volume. If one uses the same vial for dosimetry as for a reaction being studied, a correct average dose can be obtained.

* * *

This research was supported by the U. S. Atomic Energy Commission.

BIBLIOGRAPHY

1. D. E. Lea, "Actions of Radiations on Living Cells" (The Macmillan Company, New York, 1947)
2. H. Fricke, S. Morse, *Am. J. Roentgenol. Radium Therapy* **18,** 426, 430 (1927)
3. H. Fricke, *Phys. Rev.* **31,** 117 (1928)
4. N. A. Skishachow, *Phil. Mag.* **14,** 198 (1932)
5. H. Fricke, E. J. Hart, *J. Chem. Phys.* **3,** 60 (1935)
6. N. Miller, *Nature* **162,** 448 (1948); *J. Chem. Phys.* **18,** 79 (1950)
7. T. J. Hardwick, *Can. J. Chem.* **30,** 17 (1952)
8. H. A. Dewhurst, CRC-419 (1949)
9. C. J. Hochanadel, ORNL-870 (1950)
10. H. Fricke, S. Morse, *Phil. Mag.* **7,** 129 (1929)

Reprints are available of

"Industry's Role in Atomic Energy"

The distribution of atomic energy monies through American industry was graphically analyzed in the June issue of NUCLEONICS. Now, reprints of that special section are available at the following prices:

Single copies, 30 cents; in multiples of 100 copies, 25 cents each; over 500 copies, 20 cents each.

Please enclose remittance with your order addressed to NUCLEONICS, Reprint Department, 330 West 42nd St., New York 36, N. Y.

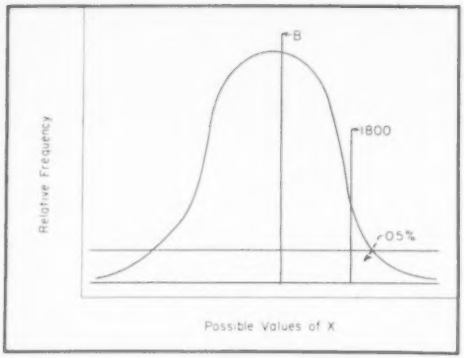

FIG. 1. Relative frequencies of different possible values of X

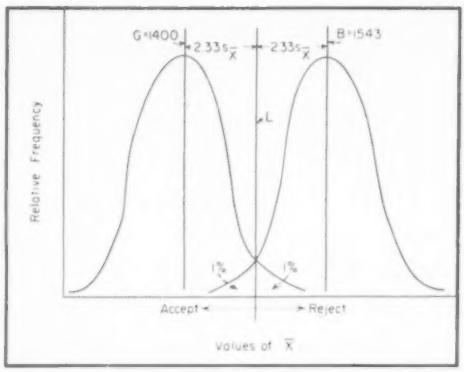

FIG. 2. Frequency distribution of means of samples of N ingots

Statistical Sampling of Fuels

An acceptable quality can be maintained—and 90% of the chemical analyses involved in inspection of individual reactor fuel elements avoided—with statistical sampling

By F. PROSCHAN* and S. B. ROBOFF†
Production Division
New York Operations Office
U. S. Atomic Energy Commission
New York, N. Y.

As NUCLEAR REACTORS become more numerous and their use in industry widespread, the producers of nuclear fuels will be confronted by the problem of furnishing fuels of a quality acceptable for reactor use.

Naturally, a reactor installation is interested in the freedom of the fuel metal from certain chemical impurities. However, since the operation of a reactor is dependent in large measure on the over-all purity of the fuel, reactor engineers are concerned with the *average* quality of large numbers of fuel elements, rather than with the quality of individual elements. What is needed, therefore, is a random sampling plan mathematically calculated to distinguish low-average quality lots from high-average quality lots.

To illustrate the design and operation of such a plan, let us consider an actual situation in a certain fuel metal processing plant. On the basis of a weighted average of chemical impurities, a specification was already in operation for each metal ingot produced. Let us suppose that this weighted average spec, X, for all chemical impurities was 1,800 (all figures given are fictitious). Under this plan, if for an individual ingot $X \leq 1{,}800$, the ingot was accepted; but if $X > 1{,}800$, the ingot was rejected. As a result, a great many chemical analyses were required, since, to obtain the weighted average for any one ingot, a number of separate chemical analyses had to be performed. It became apparent that some sort of sampling plan would have to be set up if the inspection costs were not to be overwhelming.

Sampling Plan

1. Designate 200 ingots as an inspection lot. The lot size is chosen on the basis of engineering and operational considerations.

From each lot a random sample of N ingots is selected. To insure random selection, a table of random numbers is used (*1*). N is so determined mathematically (as shown later) as to give the desired degree of assurance that low quality lots are rejected and high quality lots are accepted.

2. Determine a value G such that a lot of average value G is considered a "good" lot, and a value B such that a lot of average value B is considered a "bad" lot.

B and G are best determined by a study of the engineering economics involved. However, because of the

* PRESENT ADDRESS: C/O Statistical Engineering Laboratory, National Bureau of Standards, Washington, D. C.
† PRESENT ADDRESS: Sylvania Electric Products, Inc., P. O. B. 6, Bayside, N. Y.

complexity of the factors involved, the difficulty of determining certain of the unknowns, and the limited time available, the value of G is set at 1,400, the average value occurring during the latest three-month period. This is justified because the product during this period was satisfactory.

B is so determined that if a lot has an average value of B, then 0.5% of the ingots of the lot, or one ingot out of the lot of 200, will be outside of the spec, 1,800 (on the average). This is tolerable to the reactor installation.

Specifically, B is determined in this manner: Using a large mass of past data, the standard deviation of X, s (a good measure of "scatter"), is calculated to be 100. Now, if past data show that the normal curve approximates the relative frequencies of the different possible values of X (which it did in this case), we may draw a diagram as in Fig. 1.

A table of normal curve areas (*2*) will show that 0.5% of the area of the normal curve lies beyond $2.57s$ to the right of the mean. Thus

$$1{,}800 - B = 2.57s = 257$$

$$B = 1{,}800 - 257 = 1{,}543$$

3. Under a statistical sampling plan there is some small risk that a "good" lot will be rejected. Let us designate this risk as α. Similarly, there is some small risk that a "bad" lot will be accepted. Let us designate this risk β. The values of α and β must be set in advance on the basis of practical engineering and cost considerations. In our problem, α and β are both set equal to 1%. In other words, there is one chance in 100 that a lot of average quality G (a "good" lot) will be rejected; and, similarly, there is one chance in 100 that a lot of average quality B will be accepted.

4. Next calculate N, the number of ingots that must be randomly selected from the lot to constitute the sample. Each ingot of the sample is then measured, the mean of the sample, $\overline{X}$, calculated, and finally $\overline{X}$ is compared with an acceptance limit, L, to determine whether to accept or reject.

N and L are calculated as follows: First we use the mathematical theorem that if X is described by the normal curve, then the mean of a random sample of N observations, $\overline{X}$, is also described by a normal curve having $1/\sqrt{N}$ the "scatter" of the normal curve for X. In other words, the standard deviation of $\overline{X}$, $s_{\overline{X}}$, equals $(1/\sqrt{N}) \times s$.

We may now calculate N and L using Fig. 2. The 2.33 shown in Fig. 2 represents the number of standard deviations from the mean such that 1% of the area under the normal curve lies beyond L in one of the "tails." This expresses mathematically the fact that only 1% of the "good" lots will be rejected, and only 1% of the "bad" lots will be accepted. Hence

$$L - 1{,}400 = 2.33s_{\overline{X}} = 233/\sqrt{N}$$
$$1{,}543 - L = 2.33s_{\overline{X}}$$

Adding and solving for N, $N = 10.6$. N is rounded up to 11 to make it a whole number. L is evidently halfway between 1,400 and 1,543 so that $L = 1{,}471$.

Lots of intermediate quality will be accepted less often than "good" lots and more often than "bad" lots. Figure 3 gives the probability of acceptance versus the average quality of the submitted lot.

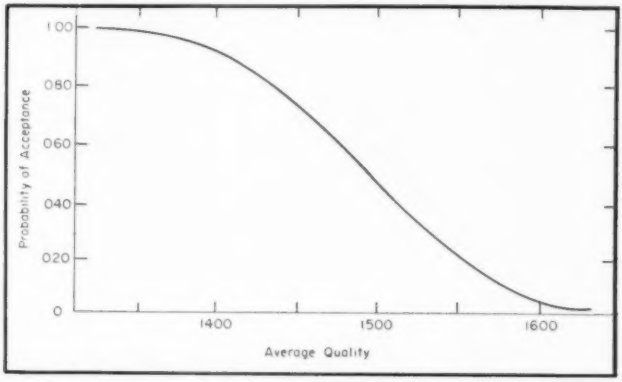

FIG. 3. Probability of acceptance versus the average quality of the submitted lot

General Solution

The following are general formulas for sampling plans intended to segregate good lots of nuclear fuels from bad lots.

Let G be the average value of a "good" lot; B ($>G$), the average value of a "bad" lot; α, the producer's risk (the probability of rejecting a good lot); β, the consumer's risk (the probability of accepting a bad lot); s, the standard deviation of an individual item; N, the size of the sample; L, the acceptance limit for the sample mean; t_α, the number of standard deviations from the mean such that a proportion, α, of the area of the normal curve lies in the tail; and similarly for t_β. Find

$$N = \frac{(t_\alpha + t_\beta)^2 s^2}{(B - G)^2}$$

If N is not an integer, round it up to the next higher integer. Then

$$L = B - t_\beta s/\sqrt{N}$$

(The fact that N was rounded up will make L come out slightly larger than it should. This tends to make α slightly smaller than specified.)

If the plan is to be set up for items for which $B < G$, obvious modifications must be made.

One limitation to this plan must be noted. In the case of certain physical specifications, the physical characteristics of individual elements become an important consideration. For such specifications, an acceptance plan should be designed to give a high degree of assurance that *individual* fuel elements are of good quality.

BIBLIOGRAPHY

1. R. A. Fisher, F. Yates, "Statistical Tables," p. 104 (Hafner Publishing Co., New York, 1949)
2. R. A. Fisher, F. Yates, "Statistical Tables," p. 31 (Hafner Publishing Co., New York, 1949)
3. L. H. C. Tippett, "Technological Applications of Statistics," ch. 7 (John Wiley and Sons, Inc., New York, 1950)
4. J. H. Curtiss, Acceptance sampling by variables, with special reference to the case in which quality is measured by average or dispersion, *J. Research Natl. Bur. Standards* **39** (1947)

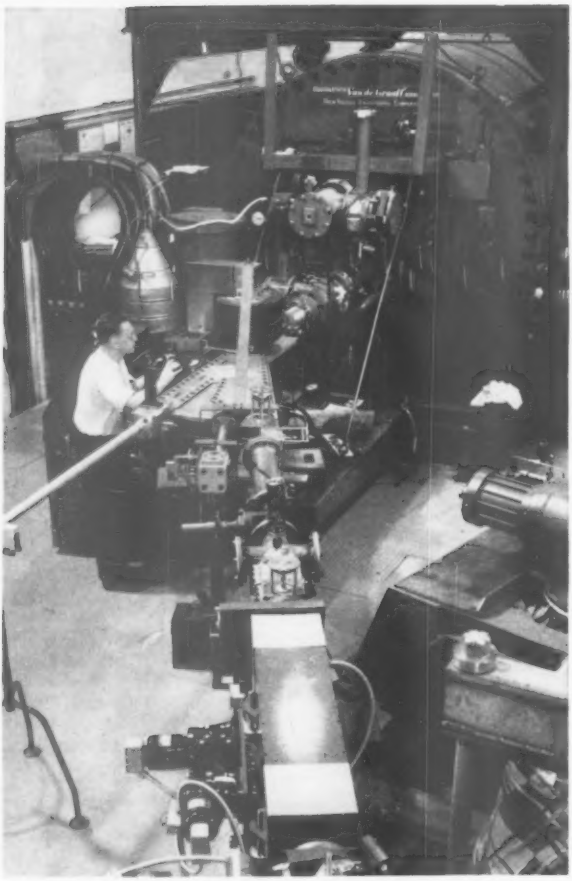

VAN DE GRAAFF injects 4-Mev protons into cosmotron. Magnet in front of generator analyzes beam. One component is protons; other is singly ionized hydrogen molecules which regulate generator energy

THE COSMOTRON –IT WORKS

A proton energy of 2.25 Bev was reached when the cosmotron at Brookhaven National Laboratory, Upton, N. Y., was operated on June 10. Three weeks previously, at the first operation of the machine, an energy of 1.3 Bev was attained.

The next step in the progress of the cosmotron will be to reach 3 Bev. To do this it will be necessary to make some changes in the pole faces and the magnetic field. The energy of 2.25 Bev is the design energy for the present magnetic field.

The machine is now shut down and will not be started up again until the beginning of August. When it does get into operation again, the first task will be to examine the operating characteristics, such things as the effects of accelerating voltage and of gas pressure in the chamber.

The idea of building a machine to generate particles in the billion-volt range came up in 1946 when the Atomic Energy Commission set up a policy to double the number of accelerators. After a meeting of leading people in the accelerator field, it was decided to build a 2–3-Bev machine at Brookhaven and a 4–6-Bev machine at Berkeley.

In the spring of 1947, AEC approved the Brookhaven design and assigned 83-million to the project. The design group was headed by M. Stanley Livingston (on leave from Massachusetts Institute of Technology). Other members of the group were Leland J. Haworth, G. K. Green, and John P. Blewett. Milton G. White (on leave from Princeton) succeeded Livingston, and, in 1950, George B. Collins succeeded White.

The original 83-million budget has been subject to rising costs. To May 1952, the cost of the cosmotron has been 86.5-million, of which 85-million is direct construction cost.

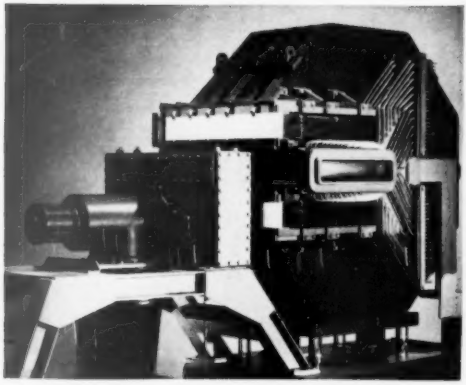

SCALE MODEL of cosmotron cross section. Hollow center section is racetrack. At left is one of 12 vacuum pumps. Magnet has 288 flat steel blocks, 8 x 8-ft each

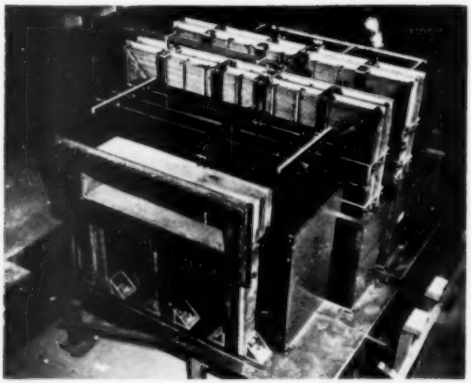

RADIOFREQUENCY transformer, whose core is shown, delivers 1,000 volts to protons in each of their trips around chamber Three million trips are completed in a second

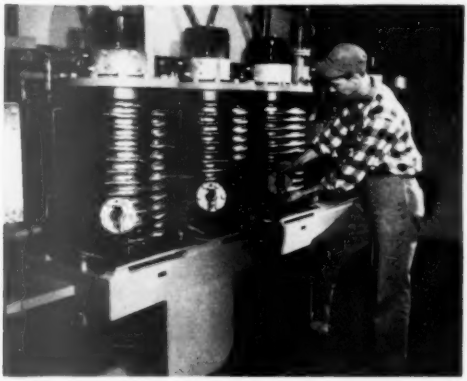

IGNITRONS act as rectifiers to supply d-c to magnet, and as inverters so most of magnetic energy can be stored in flywheel. Motor generator feeds 24 ignitrons and delivers 40 megawatts

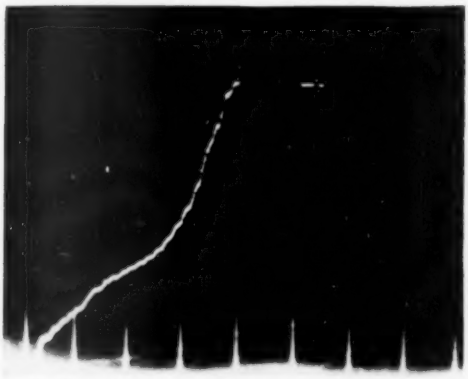

OSCILLOSCOPE SCREEN shows that protons were accelerated to 1.3 Bev. Markers at bottom show proton energy. Trace height is number of protons; a few had energies over 1.3 Bev

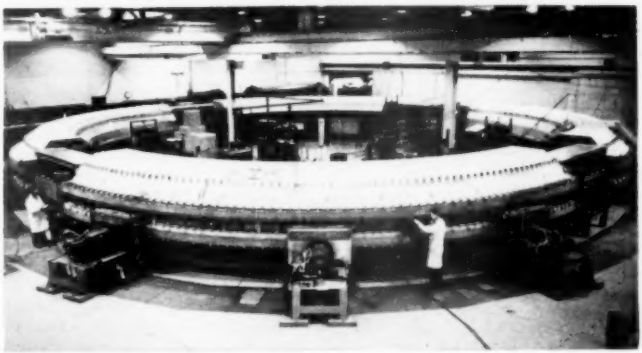

COSMOTRON gets protons once every 5 sec. Magnet, 75 ft across, gets 1-sec pulses

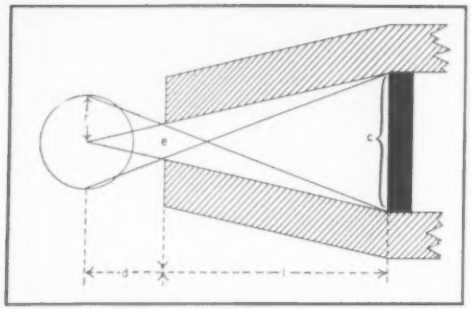

FIG. 1. Conical collimator that produces a scanning beam equal in diameter to a tumor at its focus

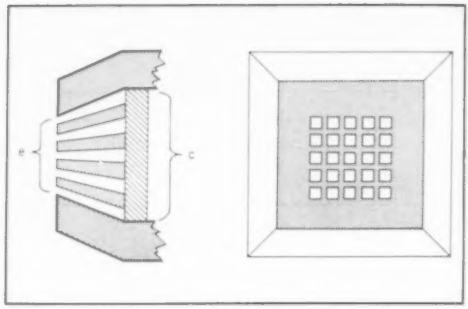

FIG. 2. Cross section and front view of a multichannel collimator used for gamma-ray scanning

Multichannel Collimators for Gamma-Ray Scanning with Scintillation Counters

To locate a tumor that has taken up radioiodine, the counter must look through a narrow collimator if the tumor is at the center of the brain. A multichannel collimator gives both a narrow scanning beam and a high counting rate

By R. R. NEWELL*
WILLIAM SAUNDERS†
and EARL MILLER‡

A BRAIN TUMOR that has taken up I^{131}-enriched diiodofluorescein can be detected with a counter by finding the point on the surface of the head where the counting rate is largest. This method, called the normal method by Moore (*1*), fails when the tumor lies at the center. Scanning must then be done with a counter which looks through a narrow collimator. Moore (*2*) thinks a conical collimator and a grid are both to be avoided. We believe this point needs further discussion.

Corbett and Honour (*3*) have designed a collimator for use with I^{131} gammas and a small cylindrical G-M tube. They mentioned the interesting possibilities of scintillation counters, but did not pursue this further and so had no call to study the adaptation of a collimator to a large frontal area of detector. They were interested in mapping the margins of the thyroid and were preoccupied with avoiding subsidiary peaks of response on the wings. They were little concerned with attaining a maximum signal, and readily accepted a very small aperture. Their analysis has, therefore, many differences from ours here.

To get a sufficient number of counts for statistical significance the counting rate must be high if the time available is limited. For example, the relatively high concentration of diiodofluorescein in a brain tumor persists for only an hour or two. The advantage of scintillation counters with their high efficiency for gamma rays becomes obvious. As much of the tumor radiation as possible should be caught by exposing a large area of crystal. The frontal area of the crystal is limited by

* Radiobiology Department, Stanford University School of Medicine, San Francisco, California.
† U. S. Veterans Hospital, San Francisco, California.
‡ University of California Medical School, San Francisco, California.

the ability of the light flashes to escape into the window of the photomultiplier.

The advantages of a collimator for these purposes are great. The problem is to design an optimum collimator. For a cylindrical collimator, however long, the crystal cannot be larger than the scanning beam (we call this a beam, although it is a limited bundle of rays coming in instead of going out). A conical collimator can be made to cover a large crystal.

Figure 1 shows a conical collimator that produces, at its focus, a scanning beam equal in diameter to the tumor. The collimator length, l, equals the tumor distance, d, multiplied by the ratio of crystal diameter, c, to tumor radius, r,

$$l = d\frac{c}{r}$$

The size of the entrance throat, e, equals the tumor radius multiplied by the ratio of collimator length to the sum of collimator length and tumor distance

$$e = r\frac{l}{l+d}$$

Thus, if the tumor is small and lies deep, the collimator has to be long, unless the crystal is small.

The larger the crystal, however, the longer the collimator, and the smaller the throat in relation to the crystal for a given narrow scanning beam. The ratio of throat area to crystal area is a measure of the efficiency of use of the crystal. It can be shown that

$$\text{efficiency} = \frac{d^2}{(d+l)^2}$$

The collimator should, therefore, be short. Since this means a narrow channel to get a narrow scanning beam, it uses only a small crystal.

To get a high counting rate, many of these narrow collimators are mounted abreast, all aimed at the same point. Such a multichannel collimator is shown in Fig. 2. The counting rate depends on how big the crystal is. The efficiency is measured by the ratio of areas of entrance throat and crystal, $(e/c)^2$, corrected for the area covered by the septa.

The optimum design of the multichannel collimator is not the same for all situations. Since large tumors close to the surface are easy diagnostic problems, they do not require optimum design. The optimum design pays off on the small deep-seated tumor.

As an example, take a 2-cm globular tumor (volume about 4 cm^3) in the middle of a 16-cm head (volume about 2,000 cm^3). Suppose that the specific uptake in the tumor is 4 times that in the brain generally. Let the total signal from the brain at a distance of 10 cm (2 cm from the surface) be 2,000 cps; this amounts to 1 cps/cm^2. Each cubic centimeter of tumor gives 4 cps, a total of 16 cps. The tumor displaces a volume of brain which would have given 4 cps. The effective tumor signal is the difference, 12 cps.

Noise-to-Signal Ratio

Without a collimator, the ratio of n, the total background including the brain, to s, the tumor signal, is 2,000/12 for the example above. But detection is hardly possible unless the tumor signal is at least three times the standard error of the measurement. To detect this tumor in the presence of such an overwhelming background without a collimator, even at the high counting rate of 2,000 cps, would require 10 min for each station, or setting, even if one had a dependable "normal" head for comparison.

In 300 sec the normal control head would give 600,000 counts. In another 300 sec one measures the patient's head and gets 603,600 counts. The difference, 3,600 counts, is due to the tumor. The standard error of the difference is $(600{,}000 + 603{,}600)^{1/2}$, which is about 1,100 counts. The difference, being more than three times the standard error, is taken as statistically significant.

The columnar signal. No matter how perfectly the scanning beam is adapted to the size of the tumor, the radiations from a column of brain in front of the tumor and behind it are accepted by the collimator and can't be stopped.

Figure 3 shows how a radioactive tumor is detected by scanning. The volume of brain enclosed in the scanning beam is a truncated pyramid. Its radiatively effective volume, for comparison with tumor volume, is equivalent to a prism with the cross section of the tumor. When the scanning beam moves "off tumor" a distance equal to $\frac{1}{8}$ the diameter of the head, the length of path through the head is shortened by about 4%.

It will be shown later that the optimum scanning beam for a 2-cm tumor is about 3 cm square. For a beam of this size in a 16-cm head, the effective columnar volume of this beam that passes completely through the head is 144 cm^3. (The beam does actually expand toward the far side of the head, but the expansion is almost perfectly balanced by the reduction in effectiveness due to the distance.) This is 36 times the volume of the tumor, and even though the tumor has 4 times the concentration, the augmentation of the total column signal by the presence of the tumor is only 1 part in 9. About 1,500 counts are required for significant detection.

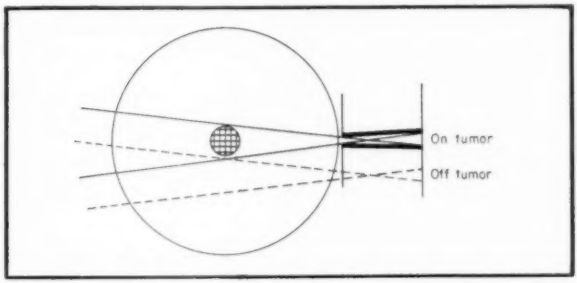

FIG. 3. Detection of a radioactive tumor in the center of the head

It is not apparent how this columnar radiation can be avoided, although some small amelioration becomes evident when the collimator's efficiencies for column and tumor are considered.

Length of Collimator

The mass of lead (or other material) in the collimator must be great enough to reduce to an acceptable level the radiation that comes from outside the

scanning beam. Most of this radiation comes from the head.

One finds that one should not attempt to attenuate this to much less than $\frac{1}{4}$ of what comes (inescapably) from the column of brain lying along the scanning beam. The reason is that a longer collimator puts the crystal further away, and so reduces the counting rate, which results in an increase in the statistical error.

The collimator rejects most of the radiation coming from the lateral portions of the scanning beam. The average acceptance of the radiation coming from that portion of the brain enclosed within the scanning beam is $\frac{1}{4}$. When the tumor is at the focus of

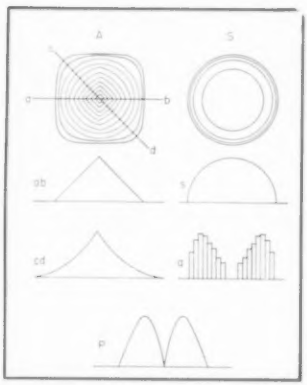

FIG. 4. Collimator acceptance contours (*A*), and tumor thickness contours (*S*)

a collimator channel (Fig. 1) only the center of it sends radiation to the entire exposed crystal face. The radiation from all other source points is partly shielded, or occulted, by the collimator wall.

Figure 4 illustrates the acceptance of the collimator. Diagram *A* shows, for a square scanning beam, the contours of equal percentage occultation over the face of the source of radiation, or what amounts to the inverse of the occultation, the acceptance, of the collimator for the radiation coming from the source. The contour lines are at intervals of 10%, from 100% at the center to essentially zero at the margins of the scanning beam. Section *ab* shows the profile square across, and *cd* shows the diagonal profile.

From a spherical tumor, more radiation per unit projected area comes from the thick center than from the edges. Diagram *S* in Fig. 4 shows contours of tumor thickness at intervals of 25%; *s* is the profile, and *q* is a histogram of the volumes in successive rings. The product of ring volume and percentage acceptance, when the tumor is exactly the size of the scanning beam, is shown at *P*. The area under *P* is a measure of the quantity of radiation that reaches the crystal. The shape of *P* changes when the ratio of scanning beam to tumor size changes.

In addition to reducing the beam to $\frac{1}{4}$ because of the average acceptance of the collimator, the septa of a multichannel collimator block off about half of the radiation within the beam (Fig. 2). This makes a total reduction to $\frac{1}{8}$. Consequently, the 144 cm³ of a 3-cm-square beam column gives a signal only as large as 18 cm³ would give without a collimator.

To reduce the radiation from the whole 2,000 cm³ of head down to $\frac{1}{4}$ of what would come from 18 cm³ means attenuation to $\frac{1}{440}$, which takes about 3.1 cm of lead, if the tracer is I^{131} (from our own absorption curve). If the collimator is half channels and half septa, its average density will be half as great as a block of solid metal, and its length will have to be twice as great, 6.2 cm, for the same attenuation.

Figure 5 summarizes the balance of effects between single and multichannel collimators. The curve labeled "inverse square" is calculated on the supposition that the channel of the collimator must limit the scanning beam to a 3-cm square at 8 cm from the face of the collimator. As the collimator is made longer, the crystal may be larger (Fig. 1), but the entrance aperture has a smaller ratio to the crystal size, cutting down the efficiency as shown. The points marked are where the exit aperture is large enough to expose crystals that are 0.5, 1.0, 1.55, 2.0, and 2.2 cm square.

When the channel is short and the efficiency high, a reduplication of the collimator multiplies the usable area of the crystal. If the sheaf of collimators is backed up by a single large crystal, the septa between channels shade part of the crystal face. The shorter the collimator the thicker these septa have to be to provide the necessary 3.1-cm lead-equivalent shielding.

The two "occultation by septa" curves show how this goes in terms of efficiency, which is the ratio of crystal face exposed to total crystal face. Obviously the efficiency goes to zero when a lead collimator is only 3.1 cm long, because then it has to be solid lead. But tungsten, being $\frac{3}{2}$ as dense, can be $\frac{1}{3}$ open channels and still give the necessary 3.1-cm lead-equivalent shielding when it is only 3.1 cm long.

The product of these two efficiency factors gives the resultant relative efficiency for every length of collimator. The highest efficiency for a multichannel tungsten collimator is the same as that of a single-channel collimator with a 1.55-cm-square exit aperture. To make use of a crystal larger than this, the multichannel collimator is better. For lead, the multichannel construction is better for crystals larger than 2.2-cm square. These critical sizes are shown by the horizontal dotted lines.

The vertical dotted lines in Fig. 5 show the required length of collimator for the optimum design in tungsten and lead. The optimum design for a 3-cm-square scanning beam focused at 8 cm from the face of the collimator gives an efficiency of 24% for gold or tungsten, and 16% for lead. For lead, a multichannel collimator is better than a single-channel one if the crystal is more than 5 cm² (2.2-cm square). For gold or tungsten, the balance tips at 2.4 cm². If one can use a 40-cm² crystal (a 6.3-cm square, or a 7-cm circle) we calculate that a multichannel collimator made of tungsten will prove 6.5 times as good as a single channel one. Made of lead, it would be only 4.3 times as good.

Optimum Size of Beam

For any single channel, either a pyramid or a truncated cone (Fig. 1), the rays from the center of the tumor reach, at the focus, the whole surface of the exposed crystal. They are 100% accepted. Rays from lateral portions are partly cut off, so that the acceptance gradually falls away to zero at the edges of the beam. Figure 4 shows the way the acceptance falls away from center to edge of the scanning beam. By arithmetic integration of the product of area and acceptance, we find that the acceptance for the total cross section of the beam (round or square) is about $\frac{1}{4}$.

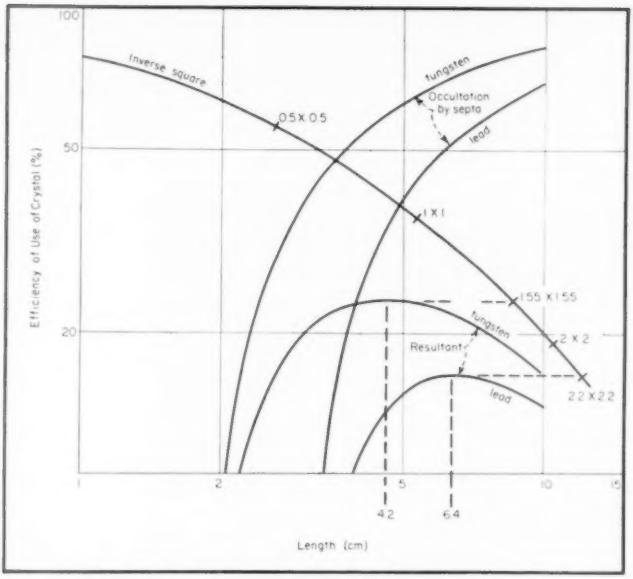

FIG. 5. Balance of effects between single and multichannel collimators

But the radiation from the tumor comes mostly from the middle, where the tumor is thickest. A similar arithmetic integration for a tumor of exactly the diameter of a round scanning beam focused at its center, results in an acceptance value of 0.38. If the beam is smaller than the tumor, the acceptance falls off markedly because the outer tumor rays are cut off completely. If the beam is larger than the tumor, the acceptance increases because the tumor is better limited to the center of the beam where collimator acceptance is high.

Figure 6 is a graph of collimator acceptance for various relative diameters of scanning beam. It is calculated for a 2-cm spherical tumor, at the focus of a conical collimator which is focused at a distance of 8 cm (Fig. 1).

Figure 7 shows the optimum size of the scanning beam for a 2-cm tumor. As the scanning beam is made larger, the background increases because a larger column of brain is included. Tumor signal increases because more of it lies in the center of the larger beam, where collimator acceptance is higher, but this goes on more slowly.

The tumor signal keeps up with the background for a while because collimator acceptance is increasing for the tumor but remains constant at $\frac{1}{4}$ for the column through the head. With still larger beam, this effect can no longer overcome the fact that the volume of the tumor remains constant while the volume in the column increases with the beam cross section. As the tumor signal falls away, the ratio of background to signal grows larger, and the counts required increases as the square of this ratio.

The upper curve shows the time required (at that counting rate) to attain a tumor signal three times its standard error. The time can obviously be shortened by giving a larger dose of tracer isotope.

The necessary total number of counts to reduce the statistical error to the required degree goes up as the square of the ratio of background to tumor signal. But the increase in counting rate shortens the time required for a given number of counts. The result is that time is best conserved, not by choosing a maximum ratio of signal to noise (minimum ratio of background to tumor signal), but by choosing a somewhat larger beam.

The difference between a square beam and a round one is negligible (less than 10% in required time). The optimum is fairly broad, and any beam size between 0.9 and 2 times the diameter of the tumor will be within 20% of the optimum.

Detecting a Small Tumor

There might be hope of detecting a 2-cm tumor (4 cm³) in a 16-cm head (2,000 cm³). A multichannel lead collimator built for a 3-cm-square scanning beam at a distance of 8 cm, is 6.5 cm long, which puts the crystal 14.5 cm from the center of the head. The septa shade 48% of the surface of the crystal. The collimator blocks off radiation coming from all parts of the head that are not within the scanning beam. The equivalent volume of head within the scanning beam is that of a square prism $3 \times 3 \times 16$ cm, which is about 7% of the volume of the head. The average acceptance for radiation from this column is 25%. The product of these factors is 0.0091.

If the patient has received a dose of I^{131}-enriched diiodofluorescein that makes the average activity in the head high enough to give 10,000 cps on a large crystal 14.5 cm from the center of the head, then the interposition of a perfect collimator of the above dimensions would reduce the columnar signal to 91 cps. But the collimator is not perfect. Its thickness is equivalent to only 3.1 cm of lead, and it attenuates the gamma rays by a factor of $\frac{1}{440}$. Thus the radiation from the whole head adds only 23 cps to the signal, and the total signal is, 114 cps.

On this total background is superimposed the extra radiation from the tumor. We suppose the tumor to have a volume of 4 cm³ and a specific activity four times that of its surroundings. It displaces 4 cm³ of brain and substitutes 300% more radiation for this fraction ($\frac{4}{144}$) of the beam column. However, the acceptance of

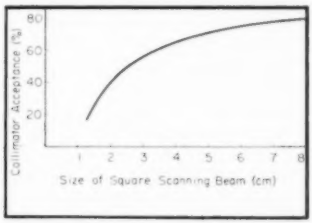

FIG. 6. Acceptance of collimator for radiations from tumors of different sizes

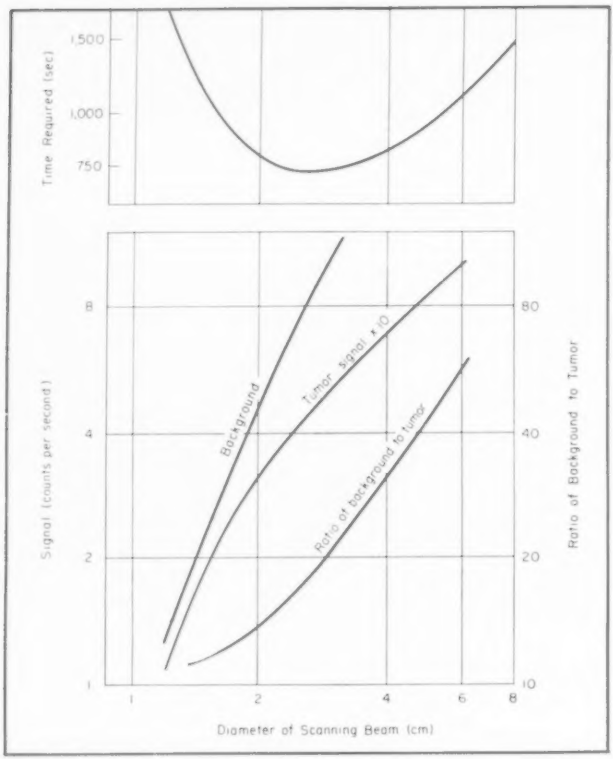

FIG. 7. Optimum size of scanning beam for a 2-cm tumor

this radiation is 56% instead of 25% (Figs. 5 and 6), so that the actual increment of signal is 18% of the column signal, or 16 cps. The background plus tumor is 130 cps.

Now displace the scanning beam laterally 2 cm (Fig. 3). The edge of the beam still cuts through 0.5 cm of the side of the tumor (15% of its volume), but collimator acceptance is so low at the edge of the beam that the tumor signal is reduced to about 5%, or 0.8 cps. The beam column is shortened about 6 mm, which reduces the column signal to 87.4 cps. The 23 cps from the whole head remains the same. The counting rate "off tumor" is the sum of all these, or 111.2 cps. The difference between this and 130 cps, the counting rate "on tumor," is 18.8 cps, of which 3.6 cps is attributable to the change in length of column path through the head, and only 15.2 cps is significant of the presence of tumor, i.e., a change of 11.7% from the "on tumor" signal.

Statistical error. If the "on tumor" and "off tumor" positions are each run to 2,000 counts, the standard error of each run is 2.5%. The standard error of the difference is $2.5\% \times \sqrt{2}$, which is 3.5%. The change in signal is more than three times its standard error, and can be taken as statistically significant.

Each station should be run to 2,000 counts, which takes about 18 sec. It should be possible to make enough such readings to survey the whole head in a reasonable total time.

If the isotope dose is smaller, so as to diminish the hazard to the patient, the time required for the measurements is correspondingly lengthened.

If the tumor is smaller it will be much more difficult to detect, unless its specific uptake is greater. If a 1-cm tumor is to be detected, it seems likely that it will require a collimator designed especially for it. Such a collimator made of lead would be 10 cm long, the time required would be increased 8 times, and the job of surveying the head would take half a day. It might be worth while to make a collimator for a 1-cm tumor, and hope for a higher specific uptake. For a tumor so very small, if a 25-cm² crystal is used, the multichannel collimator is 10 times as good as a single-channel collimator.

Collimator Construction

Our first collimators were made by casting lead around a number of smooth rods and driving out the rods.

We also made a collimator of sheet lead cut in the shape of a circular skirt. Several layers of masking tape were cemented along the greater and lesser curved edges, the greater being thicker. When rolled on itself, this sheet made a truncated cone. When the small end was pressed onto a spherical surface of proper size, this structure took a nearly perfect form, with the slit well focused on a point.

Since the parameters for good efficiency are moderately critical, it pays to calculate and make the collimator with more precision. We found that an easy way to do this is to make saw cuts in a block of light wood and cast a heavy alloy into this form. Wood's metal is convenient because it does not char the wood, although it is less dense than lead. The wood core is left in place. We hope to incorporate tungsten sheet, or tungsten powder to increase density and efficiency.

The saw cuts have parallel sides, instead of the theoretically correct wedge shape. This makes the bundle of channels point to a focus further away than the focus of the individual channel. The effect is a small one, and unimportant. With simple saw cuts, the density of the collimator is a little less than it ought to be for the chosen ratio of channel area. The collimator should, therefore, be a little longer, but this is also a small effect.

* * *

The opinions expressed here are those of the authors, and are not to be taken as reflecting any official views of the Veterans Administration.

BIBLIOGRAPHY

1. G. E. Moore, D. A. Kohl, J. F. Marvin, J. C. Wang, C. M. Caudill, *Radiology* **55**, 344 (1950)
2. G. Boyack, G. E. Moore, D. F. Clausen, NUCLEONICS **3**, No. 4, 62 (1948)
3. B. D. Corbett, A. J. Honour, NUCLEONICS **9**, No. 5, 43 (1951)

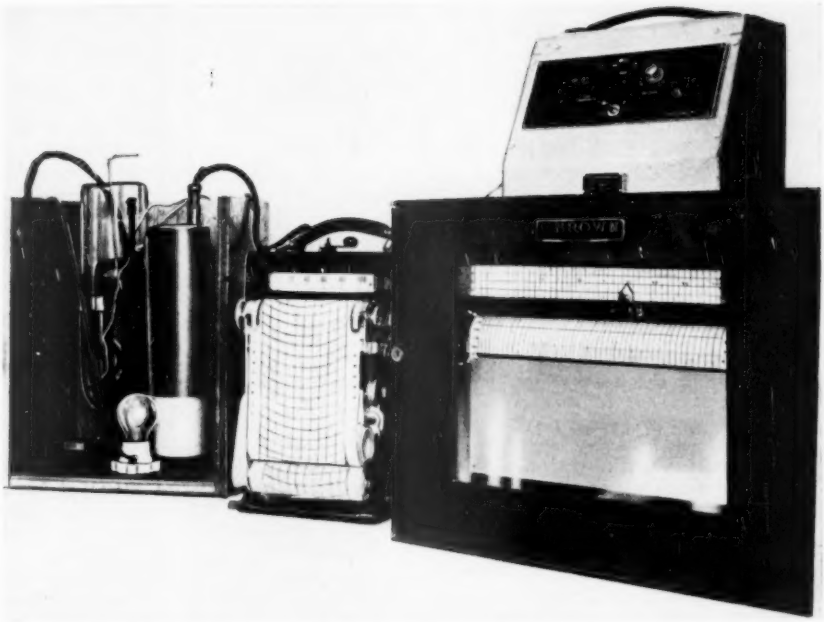

FIG. 1. Equipment used for measurement of temperature variation of light output

Temperature Effects in Organic Fluors

Little is yet known about the energy transfer mechanism or energy states of organic fluors. Their decay times have been found to decrease or remain constant with decrease in temperature. The author's observations are presented and related to research done since the first organic scintillators were used in 1947

By S. H. LIEBSON

Electricity Division
Naval Research Laboratory
Washington, D. C.

THE MOST important advantage of organic crystals over most other forms of radiation detectors is their speed of response, involving times of the order of magnitude of mean lifetimes for electronic transitions. However, because inorganic phosphors and gaseous detectors were more suitable for measurements of radioactivity with available equipment, it was not until 1947 (*1*) that organic crystals were successfully used for the detection of single gamma quanta.

In contrast to the simpler problems faced in investigations of inorganic phosphors, comparatively complex problems are presented in the study of organic fluors. Little is known about their energy transfer mechanisms. Their speed of response is relatively fast, and their energy states involve the quantum-mechanical solution of many-body problems.

The literature has indicated that there are three relatively independent

physical processes involved in the production of scintillations in organic crystals under gamma excitation: the transfer of energy to the crystal from the electron produced by the interaction of the gamma ray and the molecules, the migration of energy through the crystal, and the emission of light from excited centers.

Very little is known about the transfer of energy from particles to the lattice, other than the experimental observations that, contrary to measurements on inorganic phosphors, the resultant light scintillations are smaller for heavy particles than for lighter particles with the same energy (*2*). Since observations have indicated that the energy migration and emission processes are the same for all types of excitation, it must be concluded that the resultant decrease in efficiency for heavier particles is related to their interaction with the lattice. It has been suggested (*3*) that the decrease in the heavy-particle efficiency is related to the greater density of excitation centers, causing interactions between the excited molecules which result in a nonradiative loss of energy.

It has long been known that small amounts of naphthalene in anthracene yield fluorescent spectra primarily characteristic of naphthalene (*4*). This phenomenon has also been observed with many other combinations of molecules (*5*), and the conclusion may be drawn from the published data that this migration process occurs in all the organic crystals of the type being considered, even without admixtures, so that the prime excited molecule is not necessarily the molecule that emits the associated energy. Bowen (*6, 7*) and Ganguly (*8*) examined the possibility that the transfer takes place in the anthracene-naphthalene mixtures, for example, by emission of anthracene fluorescence and the subsequent reabsorption of the anthracene emission and fluorescence by the naphthalene molecules. Bowen has shown that this process is inconsistent with the quantum efficiencies found experimentally. A statistical analysis has also been made of the migration problem (*5*), but the nature of the analysis does not permit conclusions as to the physical processes involved.

Franck and Livingston consider three other processes which might be applicable (*9*)—transference of the energy by electrons, excitons, or sensitized fluorescence. There is no appreciable ionization within the crystal even under gamma-ray bombardment (*10*) so that the contribution of electron migrations to the transfer of energy may be neglected. Exciton migration, the movement of energy through a tightly coupled lattice in a time short compared to that for establishing thermal equilibrium (*11, 12*), is also excluded by them as a possibility because absorption spectra of these crystals indicate loose coupling in the lattice. Franck and Livingston also offer the suggestion that the lifetime of the energy transfer is long compared to nuclear vibrations (10^{-13} sec) as evidenced by fluorescence spectra. It would appear more likely, however, to this author, that such information implies thermal equilibrium of the excited molecule before emission rather than long times for energy transfer, since such spectra are indicative of the emitting state.

Sensitized fluorescence, the remaining possibility, is believed by Franck and Livingston to be the mechanism involved in the migration process. It involves the transfer of resonance energy between two atomic systems over distances as great as 100 Å. A well-known example of this is the emission of thallium light from a predominantly mercury gas mixture under stimulation by a light source, the wavelength of which is strongly absorbed by mercury and not by thallium (*13*). Forster's theory of sensitized fluorescence (*14*) is in good agreement with observations on organic scintillators, such as the depolarization of fluorescence, lending further support to the sensitized fluorescence hypothesis.

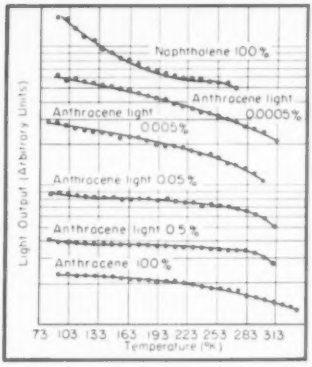

FIG. 3. Temperature effect on light output of organic fluors

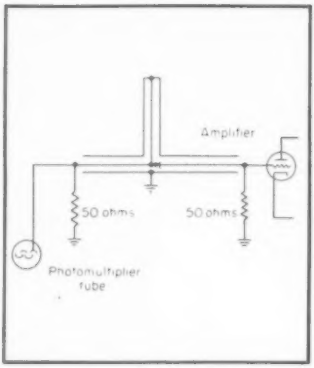

FIG. 4. Circuit employed for scintillation-determination of decay times

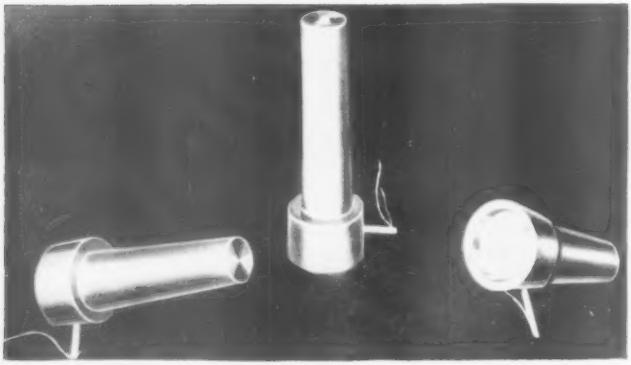

FIG. 2. Brass sample holder with thermocouple mounted on sample face

Sensitized fluorescence would, at first thought, appear to be the least of the three possibilities to be affected by the lattice, although for almost all crystals the transition from solid to liquid at the melting point or in solution is accompanied by a large decrease in the quantum efficiency (*15*). If, however, as may well be the case, the sensitized fluorescence is affected by orientation of the molecules, then it might appear necessary to have a rigid lattice (*5*) for optimum efficiency. Kallman (*1*) observed that all good organic scintillator molecules contain benzene rings and the chain structures within the molecule contain conjugated double bonds. The exact significance of the molecular structure is not as yet understood. However, since the benzene rings are typical of all crystals which have exhibited the type of energy migration under consideration here, it would appear that these rings are a necessity for energy migration.

Light Output vs Temperature

The temperature characteristics of the intensity of light output from organic crystals have been reported by several authors (*16, 17*). The experiments described therein (*17, 18*) were made on anthracene, naphthalene, stilbene, and anthracene-naphthalene mixtures under excitation by a 1 mg radium source. The integrated light output obtained by adding counts in a multichannel discriminator-counter indicated no essential difference from the integrated light output obtained by measuring the current in the output of a photomultiplier observing the scintillations.

Figure 1 shows the apparatus employed. The photomultiplier, cooled by insertion of its socket and base in liquid nitrogen, viewed the crystal scintillations through a long hollow tube which isolated the temperature variation of the crystal from the photomultiplier. The crystals were pressed into brass holders with a thermocouple mounted on the sample face as shown in Fig. 2. This method of preparation was considered adequate since previous measurements indicated little difference between temperature variations of single crystals and samples pressed from small crystals.

The results of measurements on naphthalene and anthracene and mixtures of anthracene in naphthalene are shown in Fig. 3. Measurements on stilbene indicated little variation of light output over the same ranges of temperature. The placement of curves in Fig. 3 does not conform to the relative output luminosity of each sample, but serves to facilitate comparison as the temperature is changed.

The manner in which the absolute anthracene fluorescence varies with percentage composition in a naphthalene matrix has been determined by Bowen (*5*), who has also shown (*6, 7*) that the naphthalene in these mixtures is the major recipient of energy from ultraviolet or gamma-ray excitation. The fluorescence occurs when anthracene is stimulated by this excitation.

As the percentage composition of anthracene is increased, the characteristics become less sensitive to temperature, indicating that the energy is trapped at the anthracene site in times comparable to periods for thermal vibration, and that the thermal loss of energy occurs during the naphthalene transfer process. Under some simplifying assumptions, an order of magnitude for the lifetime (*11, 12*) of a naphthalene excited state may be obtained from this as 10^{-14} sec.

Decay Time of Scintillations

Oscilloscopic observations of individual scintillations due to single gamma rays show a statistical variation of the number of photons emitted during a light flash such that the average shape has a fast rise time and an exponential decay. The decay time of scintillations may be determined by the superposition of a large number of such oscilloscopically observed scintillation pulses, to smooth out the fluctuations of individual pulses (*17*). For this type of observation, amplifiers are required which are capable of faithfully reproducing the pulses, a requirement which is barely satisfied by the best amplifiers available.

An alternative method was devised wherein the time resolution was determined primarily by the frequency response of germanium diodes and coaxial cable (*20*). Figure 4 shows the circuit used for the measurements, and Fig. 5 is a photograph of the equipment. Across the output of the photomultiplier observing the scintillations is a 50-ohm load, the characteristic impedance of the associated coaxial cable. A variable-length cable short-circuited at the far end is connected to the output of the photomultiplier and a germanium diode. The output of the diode is fed into a 50-ohm load to eliminate reflections and thence to an amplifier whose effective time constant is long compared to the decay times to be measured. The output of

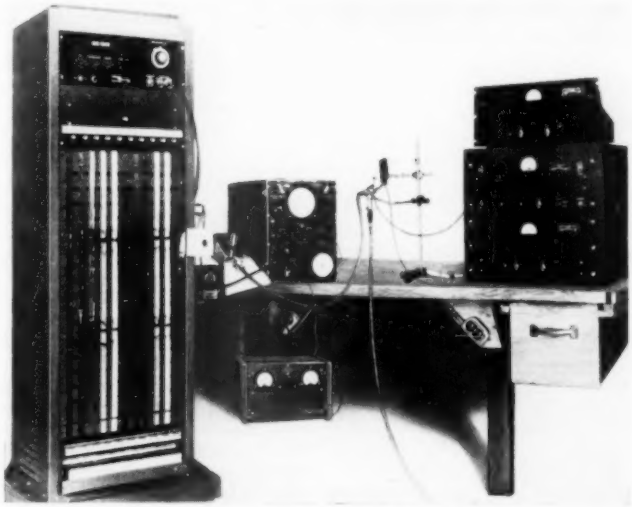

FIG. 5. Apparatus used in the determination of scintillation decay times

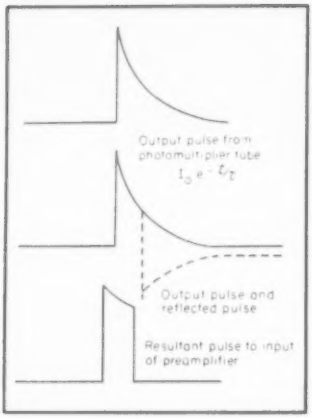
Output pulse from photomultiplier tube
$I_0 e^{-t/\tau}$
Output pulse and reflected pulse
Resultant pulse to input of preamplifier

FIG. 6. Idealized pulse shapes in shorted-line circuit

Decay Times of Fluors

Fluor	*Ultraviolet decay* ($sec \times 10^{-9}$)	*Gamma decay* ($sec \times 10^{-9}$)
Anthracene	1.7	3.0
Anthracene (−195° C)	0.8	1.3
Carbazole	0.7	1.3
Chrysene	2.2	2.6
Diphenyl acetylene	0.25	0.4
1,4-Diphenyl butadiene	0.2	0.6
Fluoranthene	4.6	...
Fluorene	0.88	...
Perylene	1.2	...
Phenanthrene	0.52	...
Quaterphenyl	0.38	0.7
Stilbene	0.31	0.8
Terphenyl	1.1	0.6
½% Anthracene in Benzene	0.20 ± 0.05	...
½% Terphenyl in Toluene	0.25 ± 0.05	0.2

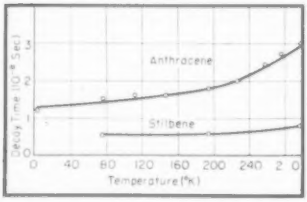

FIG. 7. Temperature variation of decay times

this amplifier goes into a 10-channel discriminator-counter.

As illustrated in Fig. 6, the exponential (average) pulse from the photomultiplier is reflected out of phase at the short circuit cable to provide a self-cancellation of part of the pulse. The diode rectifies this resultant pulse. The output of the amplifier is a pulse whose shape is determined by the amplifier but whose height is proportional to the area under the rectified pulse. The decay time is determined by the equivalent length of short-circuited cable which diminishes the original area under the pulse to $1 - 1/e$.

Since each point for a given discriminator level and shorted arm length is a measurement of thousands of counts, this method automatically averages out the statistical fluctuations of individual pulses.

The shape of the noise pulses had to be postulated since the analysis presupposes a given shape for the input pulse. The results, obtained by assuming a gaussian distribution, gave 6×10^{-9} sec as the width corresponding to twice the standard deviation. The corresponding correction to the measured times of exponential decays would then be approximately -4×10^{-9} sec. Most photomultipliers operated at about 1,500 volts gave this same pulse width, but occasional photomultipliers had noise widths of up to 10^{-8} sec.

Independent measurements made by Dr. R. C. Waddel of this laboratory, with amplifiers and oscilloscopes capable of reproducing the photomultiplier output pulses and dark noise, gave substantial agreement with the results presented herein. The corrected values of decay times are given in the table.

The uncorrected decay time of a ½% mixture of terphenyl in toluene (*21*) was 6.5×10^{-9} seconds. It is interesting to note that the resolution of the system was sufficient to give a corrected value of this decay time, 2.5×10^{-9} sec, which is in good agreement with direct measurements employing pulsed photomultipliers (*22*).

The corrected variation of decay times of anthracene and stilbene with temperature (*23*) are given in Fig. 7. Since the temperature variation of the light output of stilbene and anthracene showed characteristics similar to the type of variations observed in Fig. 3, a simple model was set up to offer a possible explanation of these characteristics. With appropriate degeneracies obtained from Fig. 3, rough agreement was obtained with an idealized energy-level diagram consisting of two states, the lower state giving the radiation transition and the upper state a non-radiation transition. Associated with the non-radiative transition was a lifetime of about 2.5×10^{-8} sec and, with the radiative transition, a lifetime of about 1.6×10^{-8} sec. This is not intended to be an explanation of the phenomena, but does indicate the possibility of coupling between the radiative and non-radiative states of the system in a manner similar to internal conversion.

Decay Time of Fluorescence

Since the measurements based on gamma-ray scintillations did not appear to be in agreement with calculations based on oscillator strengths, a new approach was considered in the form of an ultraviolet fluorometer to measure the decay of fluorescence with ultraviolet excitation.

The fluorometer (*24*), shown in Fig. 8, was a modification of the fluorometer first employed by Gaviola (*25*) and extended by Tumerman (*26*) and is based on the fact that fluorescence excited by a modulated ultraviolet light will contain a fluorescence modulation at the same frequency as that of the incident light, but altered in phase such that $\tan \phi = \omega\tau$, where ϕ is the phase shift, ω is the light modulation angular frequency, and τ is the decay time.

This relation holds when the decay of excited states is of the form of $e^{-t/\tau}$. The incident-modulated ultraviolet light is split into two components, one of which falls directly on the fluorescent material and the other on a photomultiplier. Another photomultiplier observes the light emitted by the crystal through a filter which rejects the ultraviolet light reflected from the crystal surface. The outputs of both photomultipliers are fed into tuned amplifiers operating at 10 Mc, and then to the horizontal and vertical plates of an oscilloscope.

The equipment was balanced by means of a delay box consisting of various lengths of coaxial cable, combinations of which could be inserted in series with a photomultiplier which sees the incident ultraviolet light. To balance the apparatus, ultraviolet light

was made incident on both photomultipliers, and the delay cable was adjusted to degenerate the Lissajous pattern to a 45-degree line. Substitution of a fluorescent crystal in front of one of the photomultipliers caused the observed oscilloscopic pattern to change from a line to an ellipse. The additional inserted time delay necessary to close the pattern determined the phase displacement. This method has the advantage that circuit and photomultiplier time effects are canceled in the measurement.

A check of the apparatus was made by measuring Rhodamine B in water and glycerine, giving times in good agreement with corrected results obtained by Gaviola. The resolution was sufficient with low noise level to observe shifts corresponding to 2×10^{-10} sec.

The data for a series of crystals is given in the table. No appreciable differences were found between mixtures of anthracene in naphthalene and anthracene crystals from the same batch as that used in the mixed crystals, indicating that the migration of energy occurs in times short compared to the resolving time of the apparatus (approximately 5×10^{-10} sec for anthracene).

Since measurements obtained with the ultraviolet fluorometer differed widely from times measured by scintillation methods, an attempt was made to bridge the energy width gap by using X-rays modulated at 10 Mc from an 80-kv grid-controlled X-ray tube. The results obtained by X-ray modulation were identical to those obtained for ultraviolet excitation. This is probably due to the fact that a large component of X-ray energy was comparatively soft.

The decay times of liquid solutions of terphenyl in toluene were, within experimental error, the same for scintillation and ultraviolet measurements. One possibility for the fact that the terphenyl crystal indicated a longer decay for ultraviolet compared to scintillation measurements is that a double decay time may be involved, the total fluorescence depending on two independent lifetimes. The scintillation method would favor the shorter lifetime under these circumstances.

The lifetime under ultraviolet stimulation of a crystal of 0.05% anthracene in naphthalene at room temperature gave the same decay time as the pure anthracene used for the mixture, verifying that the migration of energy does not measurably contribute to the decay time.

Of interest was a single crystal of anthracene whose faces gave decay times varying by as much as 50%. This may have been due to surface impurities, but circumstances did not permit further investigation of this phenomenon.

The comparison of results of time measurements by scintillation and fluorescence decay methods presented herein stimulated recent measurements by Hengst (*27*) who investigated the spectra of anthracene under ultraviolet and high-energy electron excitation. The resultant spectra were considerably different, indicating that, depending on the type of excitation used, different electronic states contribute to the decay time.

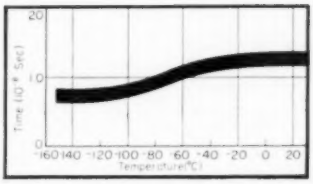

FIG. 9. Temperature effect on ultraviolet-excited decay time of anthracene

Figure 9 shows the results obtained for the temperature variation of fluorescence decay from some anthracene crystals of the same batch.* The black area is the variation of decay times made on several runs with anthracene crystals. Interpretation of these results would depend on a detailed knowledge of the Franck-Condon configurational coordinate diagram of the system, but implies a transition at 200° K.

* * *

This article was presented at the Scintillation Counter Symposium, Washington, D. C., January 29, 1952.

BIBLIOGRAPHY

1. H. Kallmann, *Natur u. Tech.*, July (1947)
2. I. Broser, H. Kallmann, U. M. Martuis, *Z. Naturforsch.* **4A,** 204 (1949)
3. L. Herforth, H. Kallmann, *Ann. Physik* **4,** 231 (1949)
4. A. Winterstein, K. Schön, *Naturwissenschaften* **22,** 237 (1934)
5. E. J. Bowen, E. Mikiewicz, F. W. Smith, *Proc. Phys. Soc. (London)* **A62,** 26 (1949)
6. E. J. Bowen, *J. Chem. Phys.* **13,** 306 (1945)
7. E. J. Bowen, *Nature* **153,** 653 (1944)
8. S. C. Ganguly, *Nature* **153,** 652 (1944)
9. J. Franck, R. Livingston, *Revs. Mod. Phys.* **21,** 505 (1949)
10. N. S. Bayliss, J. C. Riviere, *Nature* **163,** 765 (1949)
11. J. Frenkel, *Phys. Rev.* **37,** 17, 1276 (1931)
12. J. Franck, E. Teller, *J. Chem. Phys.* **6,** 861 (1938)
13. G. Cario, *Z. Physik* **10,** 185 (1922)
14. T. Forster, *Ann. Physik* **2,** 55 (1948)
15. E. J. Bowen, *J. Chem. Phys.* **13,** 306 (1945)
16. J. D. Graves, G. E. Koch, Interim Report ADP-84 (U. S. Naval Radiological Defense Laboratory, San Francisco, Calif., 1949)
17. G. G. Kelley, M. Goodrich, *Phys. Rev.* **77,** 138 (1950)
18. S. H. Liebson, J. W. Keller, *Phys. Rev.* **78,** 305 (1950)
19. S. H. Liebson, R. T. Farrar, *Phys. Rev.* **79,** 733 (1950)
20. J. O. Elliot, S. H. Liebson, R. D. Myers, C. F. Ravilious, *Rev. Sci. Instr.* **21,** 631 (1950)
21. G. T. Reynolds, F. B. Harrison, G. Salvini, *Phys. Rev.* **78,** 488 (1950)
22. R. F. Post, *Phys. Rev.* **79,** 735 (1950)
23. J. O. Elliot, S. H. Liebson, C. F. Ravilious, *Phys. Rev.* **79,** 393 (1950)
24. S. H. Liebson, M. E. Bishop, J. O. Elliot, *Phys. Rev.* **80,** 907 (1950)
25. E. Gaviola, *Z. Physik* **42,** 862 (1927)
26. L. A. Tumerman, *J. Phys. (U. S. S. R.)* **4,** 151 (1941)
27. K. Hengst, *Z. Naturforsch.* **6A,** 540 (1951)

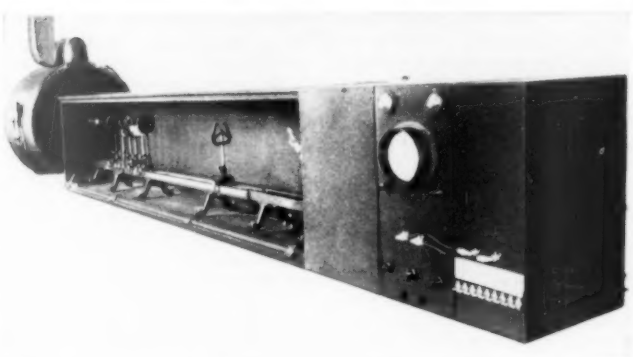

FIG. 8. Fluorometer used for ultraviolet excitation

* Measurements participated in by M. E. Bishop and J. O. Elliot of this laboratory.

Solid and Liquid Scintillation Counters

In this review, emphasis is placed on the energy response of scintillators and on a consideration of the scintillation process. Besides reference data, new material collected at Princeton University is given

By GEORGE T. REYNOLDS
Palmer Physical Laboratory, Princeton University
Princeton, New Jersey

To EXPLOIT the advantages of the scintillation counter, one should not only know the phenomenology, but should also seek an understanding of the observed processes in phosphors. Attention in this article will be restricted to the following approach:

1. Characteristics of scintillation counters and their relation to other types of counters in particle detection.
2. Common scintillation materials, their properties and preparation (solid and liquid; organic and inorganic).
3. Detailed consideration of speed and energy response.
4. Consideration of the scintillation process, including quantum efficiencies, quenching, transport, etc. A good working hypothesis concerning the detailed mechanism of the scintillation process has not appeared in the literature. Some remarks will be made here, but tradition is not likely to be broken.

Characteristics

The major features of scintillation phosphors—energy response, speed, short decay time, high density, flexibility of size and shape—make them very useful as particle detectors. The more important features are discussed in detail later. In this section, brief mention will be made of typical applications.

Generally speaking, the energy response of the crystals leads to their application in beta- and gamma-ray spectroscopy, and their energy response and speed lead to application in certain cosmic ray and lower energy nuclear physics.

The linearity of the response of organic scintillators for electrons with energies greater than 80 kev (*1*) is used in the scintillation-counter beta-ray spectrograph (*2*). Spectra can be determined for weak sources because of the large solid angle the detector can be made to subtend. Energy resolution at the low energies does not compare with conventional spectrographs, but this limitation can be minimized by special geometry.

Weak sources can also be used with the gamma-ray spectrograph (*3*) that makes use of the linear energy response and high stopping power of sodium iodide.

The use of scintillation counters in nuclear physics exploits the fact that they are faster than conventional counters—for example, the use of organic scintillators in determining very short decay times with time resolution of the order of 10^{-8} sec (*4*); that they can be used in small sizes to determine geometry accurately—for example, *p-p* scattering (*5*); that they can be used as very compact proportional counters (*2*)—for electrons > 1 kev, protons > 1 Mev, and alpha particles > 15 Mev in the case of sodium iodide, for electrons > 80 kev and relativistic particles in the case of the common organic scintillators.

The use of scintillation counters in cosmic ray physics is based on their proportional energy response (*6, 7, 8*) (both organic and inorganic scintillators appear linear for relativisitic particles), their fast response (*9, 10*) (meson decay experiments and time-of-flight measurements) and their large areas (*11*) (the use of liquid trays in low flux experiments).

Recently the possibility of using scintillation counters in neutron detection has been developed (*12, 13, 14*). Low-energy (thermal) neutrons can be detected with a LiI(Tl) crystal by the Li^6 reaction, which has a large thermal-neutron cross section. Fast-neutron detection depends for its high efficiency on the large thicknesses and high concentration of hydrogen nuclei

available in liquid organic counters. The detection depends on the observation of recoil protons.

Scintillation Materials

A compilation of data on common scintillation materials has been given by Hofstadter (*15*). Many liquids have been investigated by Kallman (*16, 17*) and by our group at Princeton; in general our results agree with those already published by Kallman.

In a consideration of scintillation materials, the important properties are relative peak height, decay time, emission spectrum, density, and melting point.

1. Relative peak height. The data given in the literature have largely been determined by integral methods such as the output current method. A more satisfactory method has been used with the better scintillators by the Princeton and Illinois (*1*) groups. This method consists of feeding the pulse from a photomultiplier into a fast linear amplifier and then into a differential pulse-height discriminator. In this way relative peak heights can be compared for scintillators exposed to the same monoenergetic particles. Several instrumental and geometric factors influence the shape of the peak and the resolution obtained, but when care is taken, the relative peak heights give a good measure of the performance as a fast particle detector.

This method is evidently more closely related to the performance desired from a fast detector, and freer from possible confusion by a relatively long-time fluorescence (or phosphorescence) than is the integral method, although this latter method must be used for scintillators that are so poor as to make a peak resolution impossible.

Care is needed in the experimental arrangement and in interpreting results to make them meaningful. The response of the photomultiplier may bias the comparison of scintillators that have emission spectra at different wavelengths. With common scintillators, it is customary to neglect this effect when a 5819 photomultiplier is used. It is interesting to note that the special envelopes of the 1P28 do not offer sufficient advantage in the spectral regions of interest to offset their generally inferior performance. The C-7140 tube offers no real advantage over the 5819 when used with common scintillators.

The geometry of the experimental setup—including optical contact between scintillator and photomultiplier, shape and size of scintillator, and reflector—is also important. A useful arrangement that has yielded good reproducibility consists of a truncated conical aluminized-glass-cap reflector that surrounds the scintillator placed on the surface of the photomultiplier. Optical contact is secured by a layer of heavy mineral oil between tube and crystal, or between tube and a thin-walled Pyrex or quartz cup for liquid scintillators. Loose reflective coatings and cement have been avoided because of possible contamination.

As pointed out by Post (*18*), the meaning of "relative pulse height" must be interpreted in terms of the counting speed used. In fast counting, the maximum rate of photon emission from the scintillator is more important than the total, or integrated, photon output. Using electronic circuits with time constants of about 10^{-10} sec, Post has shown that the pulse height from a terphenyl-toluene solution is up to 30% greater than that from a stilbene crystal. Conventional methods involving rise times of about 10^{-8} sec will record integrated photon output and invert the order of performance.

2. Decay time and energy response. The decay time of fluorescence of inorganic scintillators in general is longer than 0.1 μsec; that of organic scintillators is usually shorter than 0.1 μsec. More discussion is given under energy response. In general, the inorganic scintillators have a more nearly linear energy response.

3. Emission spectrum. In general, the spectra of the scintillators fall between 3,300 and 4,800 Å. Using a small quartz spectrograph, we have recorded the spectra of NaI(Tl), anthracene, terphenyl, and of many solutions including terphenyl in benzene, anthracene in xylene, quaterphenyl in xylene, phenanthrene in xylene, and stilbene in xylene (*19*). Samples were irradiated either with 50-kev X-rays or with ultraviolet light (2,537 Å). Results were independent of the method of excitation. This is in agreement with previous results for the fluorescence of condensed systems (*20*).

Dilute solutions would have to be used to obtain good spectral resolution. However, the distortion of the emission curve caused by overlap of the emission and absorption bands in the more concentrated solutions used is more like the situation in actual counters, where the concern is with the light that actually reaches the surface of the scintillator. In general, the effect of greater concentration or distances to be traversed, is to shift the center of the spectrum to longer wavelengths.

Our results showed that, with solutions of terphenyl, the characteristic emission is that of terphenyl and not of the solvent. Shorter wavelengths were observed for terphenyl and anthracene in solution than for the phosphors alone. This should not be taken as evidence that the wavelengths found in crystals are not seen in liquids, but that the shorter wavelengths are relatively much stronger and account for most of the scintillation observed. Results from the plates for terphenyl powder, for example, showed bands at 3,720 and 3,900 Å, whereas those for the solution were found at 3,450, 3,650, and 3,880 Å, the agreement at the two longer wavelengths being within the accuracy of measurement, the appearance of the short wavelengths being due to decreased concentration and thus less absorption.

To check the possibility that the wavelengths observed spectroscopically were the result of phosphorescence or relatively slow fluorescence and therefore of little use in particle detection, use was made of the difference in the spectral response of various photomultipliers. A solution of 4 gm/liter of terphenyl in *p*-xylene was compared to an anthracene crystal. Pulse-height measurements were made with the Cs^{137} electron line, and the ratio of pulse heights from the solution and the crystal was measured for the various photomultipliers. Ratios of 0.4, 0.7, and 0.7 were obtained for 5819, 1P21, and 1P28 photomultipliers respectively.

Using the manufacturer's spectral emission data, and assuming the ratio obtained with the 5819 to be correct, we calculated ratios of 0.67 and 0.70 for 1P21 and 1P28 tubes. The results are consistent, leading to the conclusion that the light emitted in the scintillations is the same as that measured with the spectroscope.

4. Density. Because the scintillators are solid or liquid, they have a far greater stopping power than gas-filled counters of comparable dimensions. Inorganic crystals are best

suited in this respect to detection of gamma rays and relativistic particles.

5. Melting point. This is related to the ease of preparation of crystals and is a most important practical consideration. The common practice is to obtain crystals from the melt in a two-section furnace.

Many crystals can now be obtained commercially, including anthracene, stilbene, dibenzyl, terphenyl, naphthalene, sodium iodide and potassium iodide. Anthracene can be made in clear crystals, but it is difficult to grow or obtain large clear crystals more than a few centimeters in dimension. Stilbene is easier to prepare, and good crystals approximately $\frac{1}{2}'' \times 1'' \times 4''$ have been grown. It is very difficult to obtain clear crystals of phenanthrene, but large clear crystals of dibenzyl, terphenyl, and naphthalene are prepared readily.

The alkali halides with thallium added are relatively easy to prepare in crystal form by adding about a per cent by weight of TlI to the alkali halide prior to furnace treatment (*21*).

Lithium iodide (used as a neutron counter) and sodium iodide are very hygroscopic, so that they must be protected from the air. The technique used with sodium iodide varies with the size of crystal and application, but generally involves cleaving or otherwise preparing fresh crystal surfaces in a dry box. The crystal is then immersed in mineral oil, or sealed in a Lucite container for subsequent use.

Three crystals of NaI each $3'' \times 4'' \times \frac{1}{4}''$ have been successfully sealed and used in parallel for 6 months in a cloud chamber used in cosmic ray experiments (*6*). The crystals were surrounded on five sides by aluminum foil, which also served as a reflector, and on the sixth side by a flat glass plate, to which the foil was cemented with a picein wax preparation.

If the surface of the sodium iodide crystal becomes discolored because of contact with moisture, it can be restored by placing it in a bath of methyl-ethyl-ketone. This procedure must not be overdone, or a sort of inversion of the surface defects will be observed.

Potassium iodide is less hygroscopic, but its relative response is only about one fourth that of sodium iodide. In addition, the natural radioactivity of K^{40} is a disadvantage for low-counting-rate cosmic-ray experiments. Good crystals are available, however. Good small crystals of $CaWO_4$ and $CdWO_4$ can be obtained. ZnS(Ag) is available only as powder or very small crystals.

Liquid scintillators. The ease of preparation is a distinct advantage of the liquid scintillators (*22*). Repeated experience has shown that reproducible counters can be obtained by very simple procedures. If the requirement is only to provide a scintillator of the same approximate efficiency as stilbene, say, then the addition of purified terphenyl to chemically pure toluene in amounts of about 0.5% by weight provides a counter ready to be contained in a small Pyrex cup, an enclosed glass container, or a large metal tank (*11*).

The purifying process for terphenyl obtained commercially consists of boiling it in alcohol in the presence of activated charcoal. The charcoal is then filtered out, and the terphenyl allowed to precipitate out of the alcohol. The process can be repeated several times, although twice is usually sufficient. Comparison with terphenyl purified in this way shows that the commercial material gives solutions about 75% to 90% as efficient.

Absorption of Light by Solvents Used in Scintillation Solutions

Solvent	*Wavelength* (Å)	*Transmission* (%) *Unpurified**	*Purified*†	
Toluene	3600	85.9	97.1	
	3800	90.9	98.4	
	Avg.	88.4	97.7	
m-Xylene	3600	69.6	97.6	
	3800	82.9	101.3	
	Avg.	76.2	99.4	
o-Xylene	3600	77.7	98.0	98.3‡
	3800	89.5	101.2	101.6
	Avg.	83.6	99.6	99.9
p-Xylene	3600	56.1	94.1	
	3800	72.7	100.0	
	Avg.	64.4	97.0	

* Matheson chemicals, as used in cosmic-ray work, were tested before purification.

† The usual purification procedure: two washings in H_2SO_4 followed by distillation in which only the fraction boiling within several degrees of boiling point of pure liquid was collected for tests.

‡ For a check on the effect of further treatment, this sample was washed in H_2O and dried over Na_2SO_4 before distillation; distillation boiling point rise indicated that this procedure removed some impurities.

The particular container device used for the liquid depends upon the application. We have found no completely satisfactory wax or cement that could be counted on to stay liquid tight over extended periods of time and still not poison the solution to an undesirable extent. Some inconsistent results in the literature are very possibly due to the effect of very small impurities added in this way.

An important consideration in the matter of large tanks is the absorption length of the solvent for the radiation of the solvent. Recent measurements indicate an absorption to $1/e$ in toluene in ~25 cm, in benzene in ~30 cm, and in xylene in ~15 cm, for stock solutions.

Transmission values obtained with a Beckman model DU spectrophotometer with some solvents are given in the table on this page. Distilled H_2O was used as the standardizing liquid; 5-cm cells were used. The results are accurate to about ±0.5% with reference to water.

Speed of Response

Only recently have electronic techniques been developed so that short decay times, such as those of interest in scintillation phosphors, could be measured. In general, those phosphors capable of giving nearly linear energy response (inorganic) are the slowest phosphors, so that they cannot be used simultaneously for timing in the millimicrosecond region, and so that in careful energy measurements, the response time of the electronics must be sufficient to allow an integration of the light output. On the other hand, the organic phosphors are fast enough to allow time-interval or coincidence measurements involving the order of several millimicroseconds, but are not linear in their energy response to highly ionizing particles. This gap remains in the versatility of individual scintillation counters.

Decay-time measurements of the common inorganic phosphors have been made by many authors, including Hofstadter (*15*). Similar measurements on organic phosphors require more elaborate techniques and have been made by several investigators including Lundby (*23*), using a delayed coincidence apparatus, Post (*24*) using pulsed photomultipliers, and Hofstadter and co-workers (*25*). In addition, Post has measured rise times in

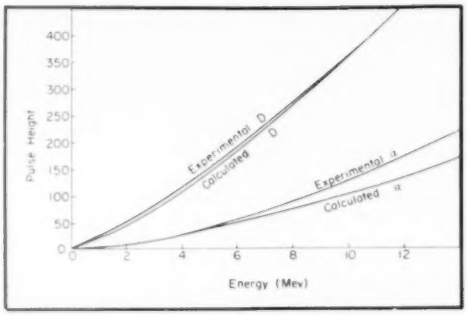

FIG. 1. Comparison between calculated scintillation response and experimental values of anthracene for deuterons and alpha particles (Courtesy W. K. Jentschke)

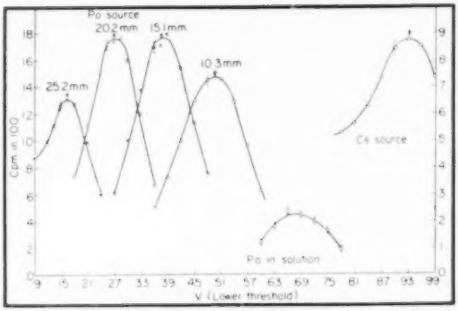

FIG. 2. Pulse heights due to polonium alphas in a solution of terphenyl in toluene as a function of distance from source to solution

terphenyl-toluene solutions and in stilbene to be about 10^{-9} sec, a limitation probably of the electronics involved (*18*).

A statistical analysis has been given by Post and Schiff (*26*) of the limitation on the resolving time due to the performance of the phosphor alone, assuming an emission obeying the Poisson distribution. This analysis indicates an intrinsic rms signal time variation of the order of 10^{-10} sec for the fastest liquids, and considerably longer for slower organic scintillators.

In addition to strictly phosphor effects, several other factors contribute to the spread in time of the pulses. For example, the use of large tanks involves path lengths for photon travel that may differ, due to reflections, by as much as 10 cm. This corresponds to a time spread of 5×10^{-10} sec. Also, the spread in the pulse due to the photomultiplier performance must be considered (*27*). At normal operating voltages, spreads may approach 10^{-9} sec. Experimental observations of time lags encountered in the course of measuring meson capture times to the order of a few millimicroseconds indicate that the impression gained from some of the literature concerning transit-time spread might be overly pessimistic in the sense that the uncertainty in the timing is considerably less than the spread in transit time (*28*).

Energy Response

It has long been recognized that the so-called β/α ratio is not equal to one for all phosphors. This has turned out to be merely indicative of the very complex behavior of phosphors in the matter of their energy response; that is, the number of photons given out in a scintillation caused by an ionizing particle is in general not simply proportional to the energy lost by the particle. There is a qualitative difference between the behavior of inorganic and organic phosphors in this respect. The purpose of the present section is to review, or refer to, very briefly, available literature (*1, 29*) on this very important problem, and to add some further data obtained from study of energy response of liquids.

It is simplest to consider first the case of inorganic crystal phosphors. Generally speaking, the uniformity of their energy response is good, certainly much better than that of the organic scintillators. Sodium iodide can be taken as typical; its linearity was noted earlier. But although for proton energies greater than 1 Mev and for alpha-particle energies greater than about 12 Mev, a plot of pulse height vs energy is a straight line for sodium iodide; nevertheless the pulse obtained from a 12-Mev alpha particle is only about 60% of that obtained for a 12-Mev proton (*1*). Interesting comparisons have been possible using protons, deuterons and alphas of the same rate of energy loss.

A simple formalism describing the process has been offered by Seitz (*1*), assuming the light output to be a function only of the specific energy loss, which has the consequence that the total light output, L, for a given particle of charge, Z, and mass, M, should be related to the energy, E, of the particle in such a way that $L/MZ^2 = h(E/MZ^2)$, where h is a function of E/MZ^2 so that the curves for different particles should reduce to a common curve when L/MZ^2 is plotted against E/MZ^2.

The data of the Illinois group support this approach, but as they point out, the test is somewhat insensitive. If a more sensitive test is applied to these ideas by plotting dL/dE vs $1/(dE/dx)$ in the case of anthracene, reasonably good agreement is found for protons, deuterons and alpha particles, but the electron points are definitely not on the same curve (*1*). Although the possibility of scattering in the electron measurements makes it unwise to accept this disagreement as final evidence of the failure of the ideas, nevertheless it must be considered seriously. It is unlikely that the relationship will be as simple as postulated due to various complications.

Birks (*29*) has combined the idea of dependence upon specific energy loss with the generally accepted qualitative idea that the reason for poor response is due to a local concentration of "damaged" molecules. If the excitation (potentially available for fluorescence) produced per unit path length is proportional to the specific energy loss, $A\,dE/dx$, the number of damaged molecules per unit length of track relative to the number of undamaged molecules is $B\,dE/dx$, and if the energy transfer to a damaged molecule relative to that to an undamaged molecule is k, then the specific luminescence is

$$\frac{dL}{dx} = \frac{A\dfrac{dE}{dx}}{1 + kB\dfrac{dE}{dx}} = \frac{A\dfrac{dE}{dx}}{1 + B'\dfrac{dE}{dx}}$$

The qualitative behavior of the expression for dL/dx is seen to be such that

for large values of dE/dx, dL/dx approaches a constant A/B', whereas for small values of dE/dx (for example, near relativistic velocities, depending on B') the response is linear, $dL/dE = A$. Birks points out the good agreement of the data in the literature with this argument, but the electron data should be investigated further. Recent work of the Illinois group (*30*) indicates disagreement in the case of α-particles above 5 Mev, Fig. 1.

It is interesting to note what investigations of liquids can contribute, due to the possibility of varying concentration. Using Po alpha particles in solution and on a thin source at various distances from the solution, the Princeton group has investigated the energy response for some terphenyl solutions over a very limited alpha-particle energy range from about 2 to 5 Mev. The results were compared with those from the Cs^{137} 624-kev electron with the same solutions. Data for a solution of 5 gm/l of terphenyl in toluene are shown in Fig. 2. It is interesting to note in the subsequent treatment of these data that, within about 3%, the pulse sizes for polonium in solution are consistent with those for the source out of the solution, thus ending any possibility that severe surface effects might account for the poor alpha-particle response. (The 3% variation observed might be due to a slight poisoning of the solution by the Po.) A plot of dL/dE vs dE/dx is shown in Fig. 3. The dependence is very marked. Results consistent with those pointed out by Birks are obtained when L is plotted against residual range, i.e., dL/dx is a constant for high values of dE/dx. This is shown in Fig. 4 for solutions of terphenyl in diphenyl oxide and toluene. The intercept on the range axis can be considered in terms of Birks ideas, since dL/dx can be written as

$$\frac{dL}{dx} = \frac{A}{B' + 1\ (dE/dx)}$$

Thus, as dE/dx increases, the slope should increase. The data of Fig. 4 require a subsequent smaller slope. As E decreases below 1 Mev, dE/dx begins to decrease, thus the behavior is qualitatively reasonable. Although there is a distinct possibility of systematic errors in the experiment as performed, other results (*1*) are similar to these, and the effect is not believed explainable simply on the basis of these errors. More careful considerations on protons (100 kev) and electrons would be necessary to determine the extent of quantitative agreement. The data of Fig. 4 lead to the results that at "saturation," there are 850 photons/cm air equivalent or 140 Å/photon in the solution. The corresponding numbers for anthracene are 1,500 photons/cm air equivalent or about 55 Å/photon. Birks' result gives 1,300 photons/cm air equivalent for anthracene. The agreement is satisfactory in view of the possible differences in crystal quality.

It is instructive to speculate about the source and consequences of the "damaged" molecules held responsible for the observed energy response. Postponing for the moment a consideration of the nature of the damage, a possible consequence can be considered. If a competition exists between transfer of excitation energy to the fluorescent molecules, and self-quenching by solvent molecules, then it is possible that the quenching process might be favored by the high density of excited molecules, i.e., interaction between two excited molecules might result in quenching, rather than transfer of energy. It is interesting to explore the question as to whether the availability of the solute (fluorescent) molecules might not have some influence on the response, i.e., whether, when the density of excited solvent molecules is high, the excitation might not have to travel farther before encountering an unexcited fluorescent molecule and thus have a greater probability of becoming lost by some competitive process. To test this, the ratio of the Cs electron pulse heights to Po alphas was measured as a function of concentration of terphenyl. If the effect mentioned is negligible, then the ratio should be constant. Actually, it varies in the manner shown in Fig. 5, and indicates a dependence on the available fluorescent molecules in the sense expected, but no satisfactory analytical explanation has been formulated.

In terms of Birks' formula, these results can be expressed by saying that decreasing the concentration decreases A but increases B'. This behavior is indicated in Fig. 6 where Kallmann's γ-ray data and Princeton α-particle data have been normalized at 5.5 gm/l. It is seen that the data require more than a simple approach.

Now consider the nature of the "damage" to the molecules that makes them unlikely to give back their energy in the form of luminescence. A possible explanation is that, due to high specific energy loss, perhaps amounting in some cases to tens of volts of energy lost by the ionizing particle per collision, many of the solvent molecules may be dissociated and thus completely altered rather than merely excited. Those that escape this violent damage may still have difficulty in encountering an undisturbed molecule to which to transfer their energy, and thus the energy may be lost through processes other than luminescence. There are several considerations, however, that do not support or require such violent effects as dissociation. In the first place, mass spectrographic analysis (*31*) of the results of allowing low-energy electrons to fall on benzene, toluene, and xylene show that relatively few of the molecules are dissociated and that even in these the dissociation is not violent. Furthermore, as will be pointed out in the following section, even when relativistic particles are considered, with their low specific ionization, for every photon emitted as much as 65–85 volts are lost by the particle in anthracene crystals, and 150 volts in terphenyl-toluene solutions (*32*). Thus, although one does not conclude that these numbers are involved in each collision, nevertheless, the energies involved may be large, even in the region where proportionality of response is found.

Several qualitative mechanisms can be suggested to account for lack of uniform energy response that do not require violent disturbances to individual molecules; their investigation might lead to suggesting better scintillators. In the first place, as will be discussed in more detail later, the transfer of energy in the liquid may well be due to a sort of resonance exchange familiar in discussions of the Frank-Condon principle. It would not take much of a perturbation to shift the levels of the excited states sufficiently to lead to a high probability of nonradiative transitions to the ground state.

A further qualitative suggestion can be made by consideration of the similarity of behavior of liquid and solid organic scintillators. It is possible that the behavior of the liquid

scintillator is not strictly molecular in origin, but depends on groups of molecules, arranged in a sort of "domain" fashion. There is some evidence for this in the regularity of X-ray results for certain liquids (*33*). It would not require a very strong interaction to disturb this domain, upon which the process depends.

Both of these suggestions would indicate that more uniform energy response would be obtained from organic scintillators in which the fluorescence-source was well protected in the structure.

Scintillation Process

In considering possible explanations of the scintillation process, separate discussions must be given to express current ideas concerning the process in inorganic and organic phosphors.

Inorganic phosphors. The luminescence of inorganic phosphors, especially the alkali halides, has been studied for a long time, well before the present concept of the scintillation counter (*21*). These and similar studies involved, among other things, studies of photoconductivity. The conclusions based on these investigations can be summarized for the case of the alkali halides with thallium impurity in the following superficial way, even though the exact details of the process are probably not completely understood at the present time (*34, 35, 37*).

There exist in the cubic lattice of these crystals two main types of irregularities. One, classed as an *F* center, is the result of an irregularity such as the absence of a negative ion. This forms a trap for electrons. The other irregularity is the presence, throughout the lattice, of thallium ions, which form centers having a perturbed potential. When the crystal is illuminated with light of sufficiently high frequency, or experiences the passage of an ionizing particle, electrons are raised into the conduction band of the crystal. The energy that this process represents travels through the crystal until it reaches a perturbation such that the energy is converted into some other form. In the vicinity of the thallium ions this perturbation is such that the energy is transformed into luminescence. Phenomenologically, the absorption and emission bands of such crystals are such that the crystal is almost transparent to its own emission.

Generally speaking, the process of sensitized fluorescence involving the addition of small impurities to a weakly or nonfluorescent crystal, results in increased fluorescence at a wavelength apparently characteristic of the added impurity. This lends support to the idea that the energy wanders through the crystal until trapped at the fluorescent center.

It may be that the relatively better energy response of the inorganic crystals compared to organic crystals is due to the stronger binding forces of the former.

Organic scintillators. The ideas generally presented in a discussion of the scintillation process for organic scintillators have been well summarized by Kallmann (*16*). The approach here differs from his only very slightly, adds a few ideas in the attempt to differentiate among the various processes suggested, and a few numerical results for some of the parameters involved. Although many of the remarks made can be applied to both solid and liquid organic scintillators, the discussion will be pointed particularly to the case of liquids.

It is well to fix in mind certain experimental results, particularly the following: The emission spectra of solutions are characteristic of the solute molecule (the fluorescent molecule) rather than the solvent molecule, even though the fluorescent molecule may be present only to the extent of a few parts in 100,000. This is also true in solid solutions. The second fact is that comparison of the quantity of luminescence of a solution with that to be expected merely on the basis of the very small quantity of fluorescent molecules present shows very forcefully that the energy that ultimately appears as light must originally have been absorbed by the solvent. Thus, a successful explanation of the behavior of these scintillators must account for the fact that energy initially absorbed by the solvent which, were no fluorescent molecules present, would be dissipated due to quenching in a form other than emission, is transported in times the order of 10^{-9} sec or less to the fluorescent molecules, which in turn trap the energy until it is emitted in the form of light.

Postponing any inquiry into the details of the transfer mechanism or quenching processes, one can list the various processes that will influence the over-all efficiency of a scintillator,

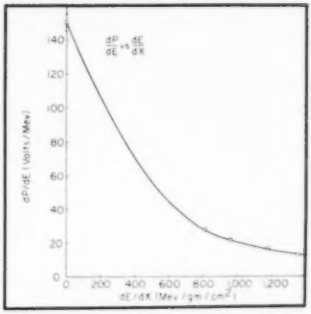

FIG. 3. Dependence of peak height per unit energy loss on density of ionization (data of Fig. 2)

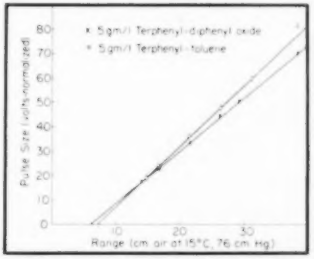

FIG. 4. Dependence of pulse height on residual range of alpha particle (in standard air)

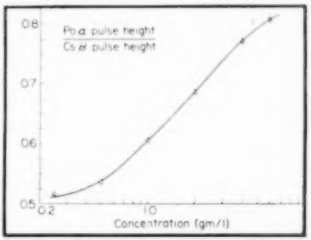

FIG. 5. Ratio of Po alpha to Cs beta pulse heights as a function of concentration for terphenyl-toluene solution

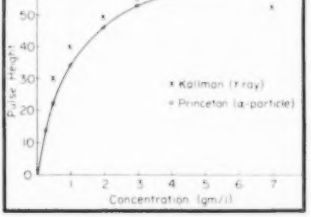

FIG. 6. Comparison of response of terphenyl-xylene solution to gamma rays and alpha particles as a function of concentration (data normalized at 5.5 gm/l)

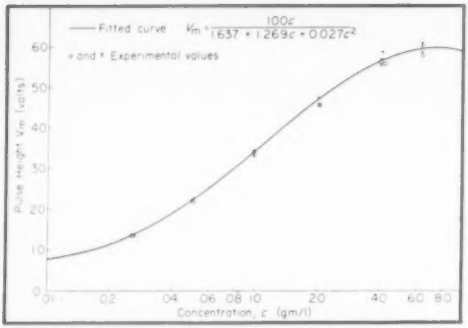

FIG. 7. Response of terphenyl-toluene solution to 5-Mev alpha particles as function of concentration

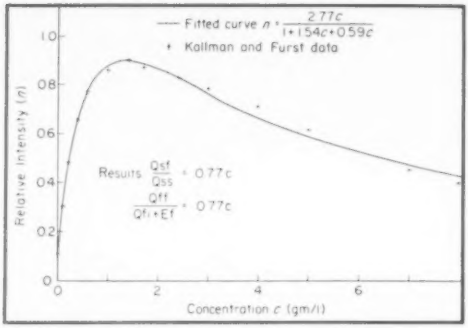

FIG. 8. Data of reference 17 for anthracene in xylene treated according to method described in text

denoting the solvent and fluorescent molecules by S and F respectively: $S + h\nu_1 \rightarrow S^*$, excitation of solvent by electromagnetic field; $S^* \rightarrow S + h\nu_2$, fluorescence of solvent (small); $S^* + S \rightarrow S + S$ or $S^* \rightarrow S$, self quenching of solvent; $S^* + S \rightarrow S + S^*$, energy transfer; $S^* + F \rightarrow S + F^*$, energy transfer to fluorescent substance; $F^* \rightarrow F + h\nu_3$, fluorescence of fluorescent substance; $F^* + F \rightarrow F + F$, self quenching of fluorescent substance, and $F^* + S \rightarrow F + S$ or $F^* \rightarrow F$, internal quenching.

Let $1/\tau_{ss}$ = probability of quenching in the solvent, and $1/\tau_i$ = probability of transfer of excitation energy from the solvent to the fluorescent molecule. Thus if n_s solvent molecules are excited by an initial act, n_f fluorescent molecules will be excited by energy transfer, where

$$n_f = \frac{1/\tau_i}{\frac{1}{\tau_i} + \frac{1}{\tau_{ss}}} n_s = \frac{\tau_{ss}}{\tau_i + \tau_{ss}} n_s$$

Once the energy is trapped in this manner, competition ensues among the various processes listed previously. Thus if $1/\tau_e$ = probability of fluorescent molecule emitting light, $1/\tau_i$ = probability of internal quenching for fluorescent molecule, and $1/\tau_{ff}$ = probability of self quenching for fluorescent molecule, the following intensity of photons emitted by the fluorescent molecule will be observed

$$n_p = \frac{1/\tau_e}{\frac{1}{\tau_e} + \frac{1}{\tau_i} + \frac{1}{\tau_{ff}}} n_f = \frac{n_s}{\left(1 + \frac{\tau_e}{\tau_i} + \frac{\tau_e}{\tau_{ff}}\right)\left(1 + \frac{\tau_i}{\tau_{ss}}\right)}$$

For a solution of concentration c we have

$$\frac{1/\tau_i}{1/\tau_{ss}} = kc = \frac{\tau_{ss}}{\tau_i}$$

and

$$\frac{1/\tau_{ff}}{1/\tau_e + 1/\tau_i} = k'c = \frac{\tau_e\tau_i}{\tau_{ff}(\tau_e + \tau_i)}$$

This differs slightly from Kallman's formulation (17), but there is no disagreement for the concentrations under consideration. Thus

$$n_p = A\left\{\frac{kc}{1 + (k + k')c + kk'c^2}\right\} n_s$$

where

$$A = \frac{1/\tau_e}{1/\tau_e + 1/\tau_i}$$

Experiments have been performed measuring the light output from a solution of varying concentration of terphenyl in toluene, containing Po in solution. The results are shown in Fig. 7. These data give

$$k = 0.75 \pm 0.06 = \frac{1/\tau_i}{1/\tau_{ss}}$$

i.e., ratio of transfer to quenching probabilities, and

$$k' = 0.022 \pm 0.005 = \frac{1/\tau_{ff}}{1/\tau_e + 1/\tau_i}$$

i.e., ratio of self quenching to emission or internal quenching. In terms of Kallmann's constants K, K', K''

$$K = \frac{1}{k} = 1.33$$

$$K'/K'' = k' = 0.022$$

If these numbers now are substituted in the equation relating n_p and n_s

$$n_p/n_s = 0.71A$$

where the data show 0.71 ± 0.03. Thus a quantum yield measurement of the over-all process will give a measure of A and therefore a measure of the relative importance of internal quenching to photon emission. A very preliminary measurement of this nature has been made using a heterochromatic photometer, with light of 2,537 Å. The direct measurement gave a result for $n_p/n_s = 0.9$, which is probably the result of neglecting some direct excitation of the terphenyl component important at this wavelength. Although the result has not been corrected for this effect, it is felt that the evidence is that the importance of internal quenching in terphenyl solutions is small.

Figure 8 shows the result of a similar analysis applied to the results of Kallmann and Furst for the case of anthracene in xylene. Here $k = 0.77$ and $k' = 0.77$, indicating a transfer efficiency about the same as that for the terphenyl solution, but a considerably greater self quenching. It is interesting to note that it would be impossible to explain, on the basis of this first-order approach, a fall off with concentration faster than that observed here. A further saturation effect would have to be invoked for an explanation, or a contamination. In general, we have not observed such rapid fall offs with concentration as reported by Kallmann.

It is now necessary to consider the possible mechanisms responsible for energy transfer. These have been discussed by Kallmann (17); we will review them and suggest how measurements already made may aid in choosing among the various possibilities.

Similar discussions of self-quenching and internal-quenching mechanisms can be based on an extension of the ideas invoked in describing the energy transfer process. It should be noted that all of the mechanisms suggested require that the absorption and emission band of the fluorescent molecule lie on the long-wavelength side of the absorption and emission band of the solvent molecule. All of the sensitized scintillators observed to date meet this condition.

Generally speaking, the passage of an ionizing particle through a solution excites the solvent molecules to high electronic states. These states are strongly coupled through vibrational states, and in a very short time, perhaps $\sim 10^{-12}$ sec, the excited molecule finds itself in the lowest vibrational state of the first excited level. The probability of photon emission from this state is small for the solvents considered, and this excitation energy is kept by the molecule until it is lost by a nonradiative transition to the ground state, or transferred to another molecule. This transfer of energy can be to a solvent molecule or fluorescent molecule. It is easy to calculate that, for the concentrations considered here, the time required for a given solvent molecule to collide with a fluorescent molecule is longer than the observed scintillation rise times already mentioned. However, somehow the energy finds its way quickly to a fluorescent molecule where it is trapped until emitted as a photon (or quenched, as considered above) by virtue of the fact that, since the first excited state of the fluorescent molecule is lower than that of the solvent, the fluorescent molecule cannot return the energy to the solvent. We have already pointed out that the mechanism of transfer cannot be by photon emission by the solvent and subsequent absorption by the fluorescent molecule, since the first stage of this process is known to be weak. Also, the observed times of the scintillation process are too short to allow the energy to be carried about by a particular solvent molecule or dimer (an excited double molecule with lower self-quenching probability).

There remain two possible explanations for the energy transfer. The first was originally suggested by Forster (*36*). It involves a dipole-dipole interaction, leading to a coupling between molecules that varies as $1/R^6$ where R is their distance apart. Whereas this mechanism appears to be successful in explaining the transfer of energy between certain dyes (Trypaflavine to Rhodamine B), a calculation by Harrison (*35*) has shown that the dipole strengths in the case of the scintillators under consideration are so weak that very short distances are required to make the process effective. The distances are so short that it would seem to rule out appreciable transfer between molecules.

The remaining familiar mechanism for energy transfer is that involving the quantum-mechanical phenomenon of energy exchange. The time for energy transfer to a fluorescent molecule in the case of 5 gm terphenyl in 1 liter toluene can be calculated to be 3×10^{-11} sec. (This involves the energy of interaction between molecules as given by the shift of the spectra in the liquid state.) Harrison's work on the dependence of transfer upon concentration shows that the lifetime of the excited state in toluene for quenching is 3×10^{-10} sec. Thus transfer by this mechanism is reasonable in the light of existing measurements.

Other Considerations

Several important considerations remain in addition to those already discussed. These include the question of the relative importance of the primary ionizing particle and the secondary electrons or delta rays it produces in the excitation process. Very little can be said about this at the present time.

It is interesting to ask how much more efficient scintillation counters we may expect to discover in the future. Work by Harrison (*32*) with a photomultiplier specially calibrated at Lancaster by Radio Corporation of America showed that for a solution of terphenyl in toluene, one photon was produced for every 150 volts expended in the solution. The corresponding numbers for anthracene crystals available ranged from 65 to 85 volts. (These are in agreement with other anthracene figures found in the literature.) Since the excitation energy necessary to produce fluorescence is only the order of a few volts, it is important to investigate whether or not we are close to the intrinsic limit of performance due to the detailed nature of the fundamental processes involved, or whether much better scintillators await further investigation.

* * *

This article was presented at the Scintillation Counter Symposium, Washington, D. C., January 29, 1952. The work is sponsored in part by the joint program of the Office of Naval Research and the U. S. Atomic Energy Commission. Much of the new material presented was obtained from work done at Princeton University in connection with the Cosmic Ray Project (ONR supported) during the period Feb. 1, 1950 to August, 1951. Outstanding contributions have been made by F. B. Harrison (Ph. D. thesis, part I, Oct., 1950), and important work has been done by T. N. K. Godfrey, D. A. Hill, (A. B. thesis, 1951), J. W. Keuffel, A. Meyer, and G. N. Whyte. In addition, the author would like to express appreciation for helpful discussions with R. Hofstadter, W. K. Jentschke, P. C. Gugelot, and J. Turkevitch.

BIBLIOGRAPHY

1. C. J. Taylor, W. K. Jentschke, M. E. Remley, F. S. Eby, P. G. Kruger, *Phys. Rev.* **84,** 1034 (1951)
2. W. H. Jordan, P. R. Bell, NUCLEONICS **5,** No. 4, 30 (1949)
3. R. Hofstadter, J. McIntyre, *Phys. Rev.* **80,** 631 (1950)
4. F. K. McGowan, *Phys. Rev.* **80,** 923 (1950)
5. C. L. Oxley, *Phys. Rev.* **76,** 461 (1949)
6. G. Salvini, *Nuovo cimento* **8,** 798 (1951)
7. E. P. Ney, D. M. Thon, *Phys. Rev.* **81,** 1068 (1951)
8. R. Hofstadter, A. M. Hudson, *Bull. Am. Phys. Soc.* **26,** No. 8, 25 (1951)
9. F. B. Harrison, J. W. Keuffel, G. T. Reynolds, *Phys. Rev.* **83,** 60 (1951)
10. J. W. Keuffel, F. B. Harrison, T. N. K. Godfrey, G. T. Reynolds (to be published)
11. F. B. Harrison, NUCLEONICS **10,** No. 6, 40 (1952)
12. J. Schenck, NUCLEONICS (in press)
13. C. E. Falk, H. L. Poss, L. C. L. Yuan, *Phys. Rev.* **83,** 176 (1951)
14. R. Hofstadter, J. A. McIntyre, H. Roderick, H. I. West, Jr., *Phys. Rev.* **82,** 749 (1951)
15. R. Hofstadter, NUCLEONICS **6,** No. 5, 70 (1950)
16. H. Kallman, M. Furst, NUCLEONICS **8,** No. 3, 32 (1951)
17. H. Kallman, M. Furst, *Phys. Rev.* **79,** 857 (1950)
18. R. F. Post, *Phys. Rev.* **79,** 735 (1950)
19. F. B. Harrison, G. T. Reynolds, *Phys. Rev.* **79,** 732 (1950)
20. J. C. D. Milton, R. Hofstadter, *Phys. Rev.* **76,** 1289 (1949)
21. R. Hofstadter, *Phys. Rev.* **75,** 796 (1949)
22. G. T. Reynolds, NUCLEONICS **6,** No. 5, 68 (1950)
23. A. Lundby, *Phys. Rev.* **80,** 477 (1950)
24. R. F. Post, N. S. Shiren, *Phys. Rev.* **78,** 81 (1950)
25. R. Hofstadter, S. H. Liebson, J. O. Elliot, *Phys. Rev.* **78,** 81 (1950)
26. R. F. Post, L. I. Schiff, *Phys. Rev.* **80,** 1113 (1950)
27. G. A. Morton, *R. C. A. Reviews* **10,** 525 (1949)
28. R. F. Post, NUCLEONICS **10,** No. 5, 46 (1952)
29. J. B. Birks, *Proc. Phys. Soc. (London)* **A64,** 874 (1951)
30. W. K. Jentschke, private communication
31. Mass spectral data (American Petroleum Institute, New York, 1951)
32. F. B. Harrison, Ph. D. thesis (Princeton University, Princeton, N. J., 1951)
33. J. T. Randall, "The Diffraction of X-rays by Amorphous Solids, Liquids, and Gases" (John Wiley & Sons, New York, 1934)
34. N. F. Mott, R. W. Gurney, "Electronic Processes in Ionic Crystals" (Clarendon Press, London, 1940)
35. E. Hirschlaff, "Fluorescence and Phosphorescence" (Chemical Publishing Co., Inc., New York, 1938)
36. T. Forster, *Ann. Physik* **2,** 55 (1948)
37. P. Pringsheim, "Fluorescence and Phosphorescence" (Interscience Publishers, New York, 1949)

Gamma-Ray-Diffusion Experiments in Water

The safe, therapeutic use of gamma rays depends in large measure on what we can predict about the radiation field near the source. In the experiments described, radium and radioactive mercury, gold, and cobalt were used to determine the field of small gamma-ray sources in a large water medium

By M. A. VAN DILLA* and G. J. HINE†
Department of Physics and Laboratory for Nuclear Science and Engineering
Massachusetts Institute of Technology
Cambridge, Massachusetts

FIG. 1. Experimental setup

SHIELDING and dosage problems require a knowledge of the penetration of γ-rays through various materials as a function of the nature of the material, the γ-ray energy, and the source-absorber geometry. Although the fundamental interactions of γ-rays with matter (Compton effect, photoelectric effect, and pair production) are well understood, the mathematical difficulties involved when there are multiple interactions are quite formidable. Considerable theoretical work has been done recently on the problem of γ-ray penetration through thick barriers (*1*), but the results of these calculations are not consistent. In contrast with these theoretical efforts, only a little experimental work has been done so far. For a great number of problems, the experimental approach seems to be the simpler one.

The present experimental work is essentially confined to point sources of γ-rays immersed in a large mass of water. Ionization data have been taken with a small liquid-filled ionization chamber at various points between 4–45 cm from the source. Whenever γ-rays are used for therapeutic purposes, the radiation field near the source is of main interest.

In discussing γ-ray attenuation, we shall call the total absorption coefficient μ_0; here we refer to a situation in which the scattered quanta are prevented from reaching the detector. The terms "good geometry" or "narrow beam" are often used in this connection. The total absorption coefficient μ_0 (*2*) is the sum of the effects of photoelectric absorption τ, pair production κ, Compton absorption σ_a, and Compton scattering σ_s:

$$\mu_0 = \tau + \kappa + \sigma_a + \sigma_s$$

In the present experiments, the effective absorption coefficient is always less than μ_0, since a significant fraction of the scattered quanta do reach the detecting instrument. The terms "poor geometry" or "wide beam" are often used to describe this situation.

Experimental Arrangement

A small ionization chamber of about 1-cm³ sensitive volume was used as the γ-ray detector. This ionization chamber was made of Lucite,

* PRESENT ADDRESS: Radiobiology Laboratory, College of Medicine, University of Utah, Salt Lake City, Utah.

† Special Research Fellow of the National Cancer Institute, Bethesda, Md.

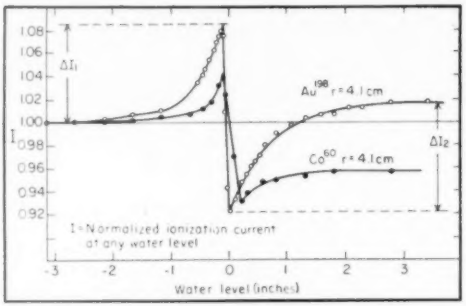

FIG. 2. Normalized ionization current vs water level for a source-chamber separation (r = 4.1 cm)

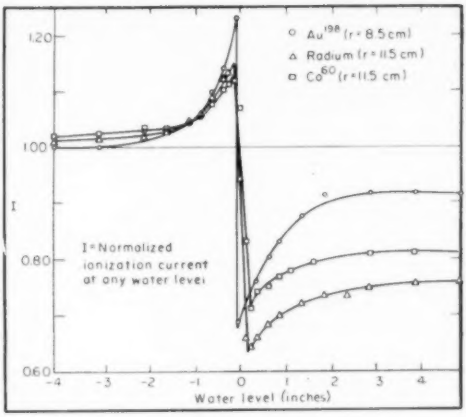

FIG. 3. Normalized ionization current vs water level at constant source-chamber separation (r = 8.5, 11.5 cm)

with Aquadag electrodes. A decane ($C_{10}H_{22}$) filling was used rather than the usual air filling. The chamber sensitivity was about 30 times that of an air-cavity chamber of the same volume.

All experiments were performed in a steel tank $3\frac{1}{2}$ feet high and 3 feet in diameter, as shown in Fig. 1. It could be filled with water to any desired level. The sensitive volume of the ionization chamber was fixed at a point 2 feet from the bottom and 4 inches from the axis of the tank. The ionization chamber was mounted with its coax leads vertical, and was waterproofed with a rubber balloon (not shown in Fig. 1).

The γ-ray sources were contained in a polystyrene tube and were fixed in the same horizontal plane as the chamber sensitive volume. The position of the source relative to the chamber could be reproduced to better than ± 0.25 mm. The absolute source-chamber separation was accurate to ± 0.5 mm.

The γ-ray sources used were mercury-203, gold-198, cobalt-60, and radium. The quantum energies $h\nu_0$ (3) emitted by these sources along with their absorption coefficients in water are given in Table 1. Since, in water, τ and κ are negligible at these energies, $\mu_0 \sim \sigma_a + \sigma_s = \sigma$ in all four cases.

The absorption coefficients were taken from experimental data (4) in the case of Co^{60}, and the others from calculations (5, 6) using the Klein-Nishina formula (taking into account the complex spectrum in the case of radium). In the last column, $1/\mu_0$ corresponds to one mean free path (1 mfp) of the primary γ-rays in cm of water.

The radium source used was contained in a glass tube 2×15 mm which was covered by a thin-walled aluminum tube. The Au^{198} was in the form of thin gold foil, and the Co^{60} was a short piece of metallic cobalt wire. Each of these two sources occupied a volume of less than 10 mm^3. The Hg^{203}, in the form of a mercury salt, occupied a larger volume.

The activity of each of the four sources was ~5–10 millicuries.

Intensity vs Water Level

In the first type of experiment, the radiation intensity was measured as a function of the water level at constant source-chamber separations.

The results are shown in Figs. 2 and 3. Here I, the normalized ionization current (ionization current equals unity for empty tank), is plotted as a function of the water level relative to the source-chamber plane.

The general shape of the experimental curves can be explained as follows: As the water level rises up toward the plane containing source and chamber, the γ-rays scattered from the water into the chamber cause only a small increase in intensity until the water level is within 1 to 2 inches of this plane. Then I increases rather rapidly as the water level approaches this plane. This indicates the importance of small-angle scattering. As soon as the water enters the region between the source and chamber a sharp drop in I is observed; this is caused by γ-ray absorption in the water layer now interposed between source and chamber. Finally, as the water level continues to rise above the source-chamber plane, I increases again due to scattering from the above water, and finally reaches a constant value as soon as the water level is at a point a few inches above this plane.

From Figs. 2 and 3 it is evident that:

1. The softer Au^{198} γ-rays are scattered considerably more than the harder γ-rays from the Co^{60} and radium sources.

2. At the smaller source-chamber separation (r = 4.1 cm), scattering of the Au^{198} γ-rays more than compensates for absorption in the water

TABLE 1—Data on the Four Gamma-ray Sources Used

Isotope	$h\nu_0$ (Mev)	Compton absorption coefficient in cm^{-1} water			1 mfp = $1/\mu_0$ in cm water
		σ_a	σ_s	$\sigma_a + \sigma_s = \sigma$	
Hg^{203}	0.279	0.0316	0.0884	0.120	8.33
Au^{198}	0.411	0.0331	0.0716	0.105	9.55
Co^{60}	1.25 av	0.0299	0.0341	0.0640	15.6
Radium	Complex	0.0302	0.0439	0.0741	13.5

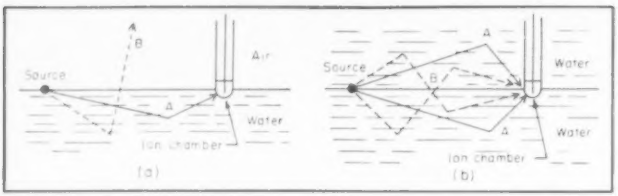

FIG. 4. Single and multiple scattering of gamma-rays

(i.e., the effective absorption coefficient is a negative number); this is not the case for the Co^{60} γ-rays.

3. At the larger source-chamber separations, scattering fails to compensate for absorption for all three sources (i.e., the effective absorption coefficient is a positive number, as is ordinarily the case).

From the Au^{198} curve of Fig. 2, it is seen that ΔI_1, the increase in intensity due to scattering from the mass of water below the source-chamber plane, is not as large as ΔI_2, the increase in ionization due to scattering when an additional large mass of water is introduced above this same plane. This is what one would expect if scattering of an order higher than the first were appreciable, as illustrated in Fig. 4.

In the case of Fig. 4a some of the photons are scattered (either singly or multiply) into the chamber by the water below the source-chamber plane. These photons, represented by A, are responsible for the rise in ionization current given by ΔI_1 in Fig. 2. Of course, some of the scattered photons cross the water-air interface and produce no ionization in the detector; see B in Fig. 4a.

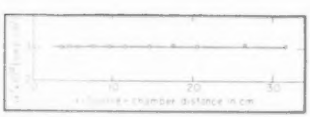

FIG. 5. Dosage rate of radium source in air corrected for inverse-square losses

When the water level has risen such that the source and chamber are in an essentially infinite water medium (Fig. 4b), the resulting rise in ionization current ΔI_2 is caused by two effects: (1) scattering of photons into the chamber from the upper mass of water (this is symmetrical with the scattering just described from the lower mass of water); (2) multiple scattering across the source-chamber plane (represented by the photons B of Fig. 4b). Thus the difference $\Delta I_2 - \Delta I_1$ represents the ionization current produced by those photons that undergo scatterings both above and below this plane.

Examination of the Au^{198} data of Fig. 2 shows that $\Delta I_2 - \Delta I_1 \sim 0.14\ \Delta I_1$; in Fig. 3, $\Delta I_2 - \Delta I_1 \sim 0.20\ \Delta I_1$. Thus it is seen that multiple scattering is already important at source-chamber separations comparable to one mean free path of the primary Au^{198} photons.

For Co^{60} and radium, multiple scattering effects are within the experimental error and do not show up.

If these experiments could be performed under ideal conditions (that is, with an infinitely small source and detector), the absorption coefficients for both good and poor geometry could be obtained from those measurements as shown in Figs. 2 and 3.

In the ideal case, a very small change in the water level would cause the drop of the ionization current from the high to the low peak. By introducing such a small amount of water between source and chamber, the radiation scattered into the chamber is not changed. Therefore, the decrease in intensity must be due to the absorption of the primary γ-rays only. Thus the peak-to-peak distance is a measure of the fractional good-geometry absorption and is given by $(1 - e^{-\mu_0 x})$. The poor-geometry absorption follows from Figs. 2 and 3 by comparison of the ionization currents with the tank empty and full.

Intensity vs Source-Chamber Separation in Air and Water

The γ-ray dosage rates of the four sources described have been measured in air and water for values of r between 4 and 40 cm, where r is the source-chamber distance.

Figure 5 shows the results obtained in air with the radium source; the ionization current (i) times the square of the source-chamber distance (r^2) is plotted as a function of r. These values are independent of $1/r^2$ to an accuracy of ±2%. This indicates that within the range of this experiment scattering of γ-rays from the walls of the tank is negligible.

With the tank filled with water, the data plotted in Fig. 6 to Fig. 9 were obtained. These experimental results are presented in three different ways so as to (1) gain some physical insight into the factors responsible for the γ-ray attenuation curves obtained by us, and (2) make comparisons with the results of previous investigators.

Attenuation curves. The experiments discussed in the preceding section have shown that the water tank can be regarded as an infinite water medium. With the tank filled with water, the variation of ionization current with distance from each of the four sources was measured.

The results are plotted in Figs. 6 and 7 in terms of the ratio of ionization current in water to ionization current in air as a function of r. The division by the air measurements eliminates the inverse square variation; hence any deviation of the experimental curves from horizontal straight lines must be due to scattering and absorption.

For purposes of comparison, Figs. 6 and 7 also show exponential attenuation curves based on the total absorption coefficient, μ_0, and Compton absorption coefficient, σ_a, both coefficients referring to the primary photons (see Table 1). The former attenuation curve would be observed in good geometry, and the latter would be observed in a special case where the scattered photons reach the detector.

From Fig. 6, it is apparent that radium and Co^{60} γ-rays behave quite similarly. The observed attenuation cannot be described by a simple exponential function of the type $e^{-\mu r}$, where the effective absorption coefficient μ is constant. The γ-ray attenuation is considerably less than what one would calculate on the basis of the total absorption coefficient μ_0.

It is significant, however, that the effective absorption coefficient is not very different from σ_a.

To understand this, let us consider the special case of a spherical absorber of low atomic number with a small γ-ray source at its center (*6*). If the radius of this absorber is small compared to one mean free path of the

primary photons, then the energy flux emerging from the sphere is attenuated only by the amount of energy that is transferred to Compton recoil electrons. Hence the attenuation will be given exactly by $e^{-\mu_0 r}$; this is sometimes referred to as "true" absorption.

With this special case in mind, the experimental results of Fig. 6 (and Fig. 9 later) can be better understood. At small absorber thicknesses ($r < 1/\mu_0$), the effective absorption coefficient $\mu(r)$ is observed to be less than σ_a. This is due to the following fact. From the large mass of water beyond the boundaries of the sphere of radius r, secondary photons are scattered backwards into the detector. These backscattered photons are the cause of $\mu(r) < \sigma_a$ at close distances from a γ-ray source in a scattering medium.

The results of Fig. 7 for the softer radiations of Au^{198} and Hg^{203} show this behavior more distinctly than the harder radiations from radium and Co^{60}. In fact, for small r, the presence of a large mass of water actually increases the observed dosage rate over its value in air.

For large distances from the source ($r \sim 2$ mfp), it follows from Figs. 6 and 7 that $\mu(r) > \sigma_a$. With increasing absorber thickness, the probability of multiple scattering and eventual photoelectric absorption increases. The resulting attenuation of the radiation intensity will be greater than the increase caused by the backscattered photons; therefore, $\mu(r) > \sigma_a$ at large r.

Finally, at intermediate values of r ($r \sim 1$ mfp), backscattering tends to cancel the decrease due to multiple scattering, and $\mu(r) \sim \sigma_a$.

The difference between the results obtained with soft and hard radiations (Figs. 6 and 7) can be understood by referring to Table 1. Since σ_a for both the hard and soft radiations is about the same, the main differences in attenuation must be due to σ_s. Because σ_s is considerably larger for the softer radiations, scattering is more pronounced, and at smaller r this increases the observed dosage rate more than for the harder radiations.

Build-up factor. In describing experiments similar to those discussed here, White (*7*) has made use of a build-up factor. This is defined as the ratio of observed dosage rate in water (primary plus secondary radiation) to the primary dosage rate in water. The primary dosage rate can always be calculated exactly since it is based on good-geometry absorption only. The build-up factor BF can be written as:

$$BF = \frac{\text{total dosage rate in water}}{\text{primary dosage rate in water}}$$

or

$$= 1 + \frac{\text{secondary dosage rate in water}}{\text{primary dosage rate in water}}$$

The latter is a concise way of showing the contribution of the scattered photons. Thus, if the scattered photons are prevented from reaching the detector ($BF = 1$), this is the case of good geometry. BF increases in direct proportion to the amount of scattered flux that is allowed to reach the detector; with poor geometry $BF > 1$.

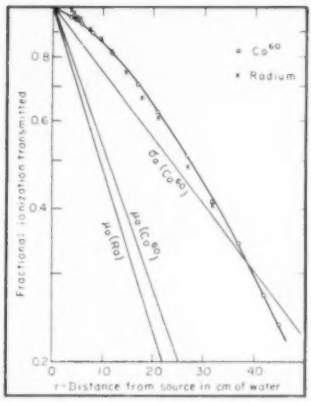

FIG. 6. Radium and Co^{60} point source in water. Fractional ionization transmitted (dosage rate in water divided by dosage rate in air) as a function of r

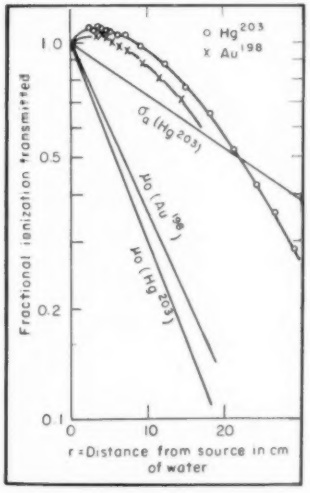

FIG. 7. Hg^{203} and Au^{198} point source in water. Fractional ionization transmitted (dosage rate in water divided by dosage rate in air) as a function of r

White (*7*) has measured the build-up factor for small Co^{60} sources in a large water medium for distances between 30 and 253 cm, and has also compiled the results of earlier experiments of this type. In Fig. 8, White's compilation is shown along with our experimental results recalculated in terms of the build-up factor. Earlier results of Gray (*8*), who used a radon source (with very light filtration) embedded in a large mass of aluminum, are also given in Fig. 8. The build-up factor is plotted against distance in mean free paths of the primary radiation, that is, in terms of $\mu_0 r$.

There is good agreement between our experimental results and those of White on the Co^{60} radiation.* There is also good agreement between our experimental data with the radium γ-radiation and those of Gray (*8*) below 1–2 mfp, but his BF values are considerably smaller at larger distances.

The build-up of the secondary photons with distance seems to be slower as the atomic number of the scattering medium increases. This is due to the increased effectiveness of photoelectric effect in suppressing the softer secondaries in media of higher atomic number. Some recent experimental data (*9*) for the build-up factor for transmission through concrete and lead show this fact clearly.

The soft Au^{198} and Hg^{203} radiation shows a more rapid build-up of the secondaries than is the case for the harder radiations of radium and Co^{60}. This is what one would expect in view of the previous discussion.

The build-up factor increases continuously without reaching equilibrium. The total radiation intensity, however, diminishes rapidly with increasing absorber thickness. The radiation dosage for various points in the absorbing medium cannot be obtained this way; therefore the following presentation of the experimental

* Our experimental values have not been corrected for the wavelength response of the detector used (liquid-filled ionization chamber). This correction is negligible for $\mu_0 r < 1$. In the case of $\mu_0 r = 1$–2, the values of BF shown in Fig. 8 for Co^{60} and radium are 1–2% too low, and those for Au^{198} and Hg^{203} are 5–10% too low.

data appears useful for this kind of problem.

The dosage factor. For radium needles, the γ-ray intensity distribution has been determined in air by various methods. However, very little work has been done so far to investigate the dosage distribution of a needle embedded in a scattering medium (*10*). This is a problem of great interest for interstitial radiation therapy. From the foregoing results, we can determine the dosage distribution around a point source in water. The dosage rates due to extended γ-ray sources can then be obtained by adding the data for a number of point sources.

The attenuation curves given in Figs. 6 and 7 indicate approximately an exponential absorption law with the absorption coefficient σ_w, the Compton absorption coefficient of the primary γ-rays in cm^{-1} of water. With this in mind, a dosage factor *DF* can be defined as

$$DF = \frac{\text{dosage rate in water}}{\text{dosage rate in air} \times e^{-\sigma_w r}}$$

Thus the dosage factor *DF* is a measure for the deviation of the actual dosage rate in water from a simple exponential absorption law.

In Fig. 9, we plot the dosage factor *DF* for the four γ-ray emitters as a function of distance from the source, given in mean free paths of the primary radiation. Out to 2 mfp, *DF* is about the same within 10% for the Co^{60}, radium, and Au^{198} γ-rays. The soft Hg^{203} radiation gives somewhat higher values of *DF*. Above 2–3 mfp, *DF* for all four sources decreases below unity. White's data on Co^{60} include points not plotted in Fig. 9 (i.e., at 6 mfp $DF < 0.4$; at 10 mfp $DF < 0.1$) which show that *DF* approaches zero at very large distances.

The deviation of the dosage factor *DF* from unity as the distance from the source varies can now be explained on the basis of the previous discussion concerning the attenuation curves and the build-up factor. Backscattering tends to make $DF > 1$, while multiple scattering (and also photoelectric absorption) tends to make $DF < 1$. At small values of $\mu_w r$, backscattering is more effective; at large values, multiple scattering and eventually photoelectric absorption predominate. At intermediate values of $\mu_w r$ ($\sim$2.5), these effects cancel, making *DF* equal to unity. The deviations of *DF* from unity increase as the primary quantum energy decreases, as would be expected from the known energy-dependence of Compton and photoelectric effect.

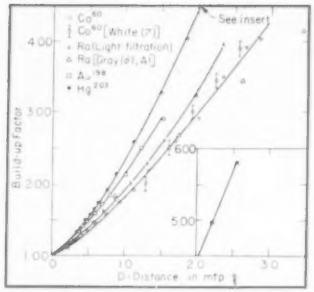

FIG. 8. Experimental values of the build-up factor *BF*

For a γ-ray source of known primary γ-ray energy, the dosage rate $D(r)$ at a distance r from the source in a scattering medium is

$$D(r) = DF \times \text{dosage rate in air} \times e^{-\sigma_w r}$$

where *DF* is given in Fig. 9. For a point source, the dosage rate in air follows the inverse square law; thus

$$D(r) = DF \times (D_1/r^2) \times e^{-\sigma_w r}$$

where D_1 is the γ-ray dosage rate at 1 cm from the source in air (*11*).

For distances up to 2 mfp in Fig. 9, *DF* is greater than one for all primary γ-ray energies. Furthermore, the *DF* curves for the Au^{198}, Co^{60}, and radium γ-rays are not too different from each other and can be regarded as constant for 0.3 to 2 mfp. Therefore, we might replace *DF* by a constant factor $DF = 1.1$ and still have a good approximation for therapeutic dose calculations.

$$D(r) = 1.1(D_1/r^2) \times e^{-\sigma_w r}$$

For small radium and Co^{60} sources, the equation above is a good approximation within about 5%; 2 mfp for the radium and Co^{60} γ-radiation corresponds to 27 and 31 cm of water, respectively. If a γ-ray source is locally implanted for therapeutic purposes for a certain period of time, no points of interest within the human body will be beyond 30 cm from the source. Since only radium and Co^{60} sources are employed for localized radiation therapy, the approximation is satisfactory in this respect.

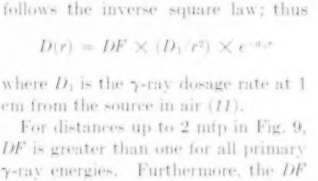

FIG. 9. Experimental values of the dosage factor *DF*

With the present set-up, source and detector size exclude accurate data for a source-chamber separation less than 3–4 cm, which corresponds to about 0.25 mfp for radium. The dosage factor *DF* given in Fig. 9 seems to approach $DF = 1$ for smaller distances. However, the values given for the radium attenuation in Fig. 6 do not exclude the possibility of an intensifying effect of the water close to the source. This has been observed for the softer Au^{198} and Hg^{203} γ-radiation as shown in Fig. 7.

Since radium emits several γ-ray lines of high relative intensity with energies below 0.5 Mev, it might be expected that the soft backscattered γ-radiation overcompensates the absorption of the primary radium γ-rays nearby the source. This is in agreement with earlier observations (*10*).

Therefore, taking $DF = 1.1$ can be regarded as a good approximation even for distances close to a radium source.

* * *

This article is part of a thesis submitted by M. A. Van Dilla in partial fulfillment of the requirements for a Ph.D. degree at the Massachusetts Institute of Technology. The work was supported in part by the joint program of the Office of Naval Research and the Atomic Energy Commission. The authors are indebted to Prof. R. D. Evans for numerous enlightening discussions.

BIBLIOGRAPHY

1. J. O. Hirschfelder, J. L. Magee, M. H. Hull, *Phys. Rev.* **73**, 852 (1948); J. O. Hirschfelder, E. N. Adams, *ibid.* 863; L. V. Spencer, U. Fano, *ibid.* **81**, 464(L) (1951); G. H. Peebles, M. S. Plesset, *ibid.* 430; L. L. Foldy, R. K. Osborn, *ibid.* 400; M. S. Plesset, S. T. Cohen, *J. Applied Phys.* **22**, 350 (1951); J. Corner, F. A. G. Day, R. E. Weir, *Proc. Roy. Soc. (London)* **A204**, 329 (1950)
2. R. G. Flubarty, NUCLEONICS **3**, No. 1, 46 (1948)
3. K. Way, L. Fano, M. R. Scott, K. Thew, "Nuclear Data" (Circular 499, National Bureau of Standards, Washington, D. C., 1950)
4. C. M. Davisson, R. D. Evans, *Phys. Rev.* **81**, 404 (1951)
5. C. M. Davisson, thesis, Massachusetts Institute of Technology (1948)
6. R. D. Evans, R. O. Evans, *Revs. Mod. Phys.* **20**, 305 (1948)
7. G. R. White, *Phys. Rev.* **80**, 154 (1950)
8. L. H. Gray, *Proc. Roy. Soc. (London)* **A159**, 263 (1937)
9. W. R. Dixon, *Phys. Rev.* **85**, 498 (1952)
10. G. J. Hine, M. Friedman, *Am. J. Roentgenol. Radium Therapy* **64**, 989 (1950)
11. L. D. Marinelli, E. H. Quimby, G. J. Hine, *Am. J. Roentgenol. Radium Therapy* **59**, 260 (1948)

AEC WORK . . .

Who's Doing It?

What Does It Cost?

As COLLECTED HERE, the answers to these questions give a picture of the principal work undertaken by industrial contractors for the Atomic Energy Commission. Most of the data presented have not been published previously.

These are the "cost-plus-fixed-fee" contracts that were active as of July 1, 1951, plus subsequent awards through January 31, 1952. Some of the contracts have been completed; others have far-distant completion dates.

Within the limits of security, the work of the contractor is described under one of the four types of service contracts into which the list is divided: (1) construction, (2) architect-engineer, (3) operation, and (4) research and development.

Reference numbers in small type indicate footnotes on page 64.

Construction Contracts

Contractor	Location of work, project description, and responsibilities of contractor	Estimated cost of construction on which fee is based	Fee	Fee as a per cent of estimated cost
Atkinson-Jones Construction Co., San Francisco, Calif.	HANFORD, WASH. Construction of 397 housing units with utilities, construction camp for 11,355 workers, railroad siding, electrical distribution facilities, schools, warehouses, shops, plant telephone system, major production facilities, also miscellaneous construction on a continuing basis. Furnish labor, material, and equipment, install process equipment (special) furnished by others, procure and install equipment, provide maintenance service and plant modification necessarily done by major construction labor.	$289,632,934	$2,697,518	0.931
Girdler Corp., Louisville, Ky.	DANA, IND. Design, procurement, and construction of heavy-water plant and related facilities (operation of pilot plant). Furnish all labor, services, materials, supplies, tools, construction and process equipment.[1]	[2]37,389,000 [3]41,969,000	136,428 669,781	0.365 1.60
Maxon Construction Co., Dayton, Ohio.	OAK RIDGE, TENN. Complete construction of the addition to the K-25 gaseous diffusion plant, including all appurtenant facilities, expansion of electrical supply, temporary construction, and site work.	136,978,465	1,281,487	0.936
Rust Engineering Co., Pittsburgh, Pa.	HUNTINGTON, W. VA. Construction of a reduction pilot plant including process building, compressor building, and miscellaneous facilities and utilities. Furnish all labor, services, materials, necessary tools, and some process and manufacturing equipment.	1,710,000	58,300	3.409

(Continued on next page)

Construction Contracts (continued)

Contractor	Location of work, project description, and responsibilities of contractor	Estimated cost of construction on which fee is based	Fee	Fee as a per cent of estimated cost
F. H. McGraw & Co., Hartford, Conn.	PADUCAH, KY. Construction of process buildings, utility systems, administrative facilities, demolition of ordnance plant. Furnish all labor, services, materials, necessary tools, and equipment not furnished by others.	$322,153,240	$1,592,000	0.492
George A. Fuller Co. New York, N. Y.	FERNALD, OHIO. Construction of feed materials production center. Furnish all labor, services, materials, necessary tools and equipment not furnished by others.	32,563,300	610,000	1.871
Singmaster & Breyer, New York, N. Y.	ST. LOUIS, MO. Design, procurement, engineering, and installation of facilities. Furnish all labor, services, materials, necessary tools, and process equipment.	[2]95,000 [2]240,000	3,270 6,730	3.29 2.80
Wigton-Abbott Corp., Plainfield, N. J.	ST. LOUIS, MO. Design, procurement and installation of equipment for expansion of facilities. Furnish all labor, services, materials, necessary tools, and process equipment.	[2]1,070,000 [2]1,995,614	14,300 47,836	1.34 2.40
Fluor Corp., San Francisco, Calif.	REACTOR TESTING STATION, IDAHO. Construction of materials testing reactor, including miscellaneous related work and services. Furnish all labor, services, materials, necessary tools, and equipment not furnished by others.	11,145,399	213,000	2.00
Bechtel Corp., San Francisco, Calif.	REACTOR TESTING STATION, IDAHO. Construction of chemical processing plant. Furnish all labor, services, materials, necessary tools and construction equipment.	16,413,880	310,000	1.89
California Research & Development Co., San Francisco, Calif.	LIVERMORE, CALIF. Design, development, procurement, construction, and operation of a high-current particle accelerator and auxiliary facilities. Furnish all labor, services, materials, necessary tools, construction and process equipment.	9,400,000	175,000	1.86
Stearns-Roger Manufacturing Co., Denver, Colo.	BOULDER, COLO. Design, procurement, and construction of laboratory facilities at Boulder, to be operated by National Bureau of Standards. Furnish all labor, services, materials, necessary tools, and process equipment.	[2]1,800,000 [2]2,100,000	25,000 55,833	1.39 2.66
The Austin Co., Cleveland, Ohio	ROCKY FLATS, COLO. Design of entire facility, procurement of operating equipment and critical materials and construction of process buildings. Also, on lump-sum basis, a site selection survey. Furnish all labor, services, materials, necessary tools, equipment and operating equipment.	[2][3]30,300,000 [2]21,900,000	225,000 365,000	0.74 1.67
Silas Mason Co., Shreveport, La.	PANTEX, TEX. Design of process buildings, utilities and support facilities, procurement of process equipment and critical materials; construction of process buildings. Furnish all labor, services, materials, necessary tools, and process equipment.	[2]15,800,000 [2]11,100,000	164,000 207,000	1.04 1.86
Holmes & Narver, Los Angeles, Calif.	ENIWETOK TEST SITE. Design, procurement, and construction of scientific structures, circuitry, and other technical facilities plus camp and other support facilities. In addition, provide for camp operation, maintenance and management prior to and during test periods; technical support during test; roll-up services upon completion of test. Furnish all labor, service, materials, necessary tools and equipment.	[2]8,700,000 [2]3,800,000 [2]26,300,000 [2][3]26,300,000	105,000 76,000 516,000 304,000 1,001,000	 1.96 1.15
Holmes & Narver, Los Angeles, Calif.	ENIWETOK TEST SITE. Design, procurement, construction and support for future test activities similar to the services provided under contract above. Furnish all labor, service, materials, necessary tools and equipment.	[2]19,325,000	482,000	2.49
Haddock Engineers, Ltd., Los Angeles, Calif.	NEVADA TEST SITE. Construction of scientific and technical structures, roads, communications and electrical circuitry within the test area. Simple design and detailing of above construction. Furnish all labor, service, materials, necessary tools, and equipment.	[2]3,800,000 [2]3,800,000 [2]1,500,000 [2]1,000,000	38,000 89,300 19,000 13,700 160,000	1.0 2.34
Reynolds Electric Co., El Paso, Tex.	NEVADA TEST SITE. Construction of electric and communications circuitry, hook-ups and instrumentation. Furnish all labor, service, materials, necessary tools and equipment.	[2]1,900,000	44,000	2.32

Architect-Engineer Contracts

Contractor	Location of work, project description, and responsibilities of contractor	Estimated cost of related construction on which fee is based	Fee	Fee as a per cent of estimated cost
Michael Baker, Inc., Rochester, Pa.	Perform all field work necessary to complete a property survey of the community of Oak Ridge, Tenn. including location of all utility lines.	[14]	$30,311	
The Austin Co., Cleveland, Ohio	Design and inspection services for the construction of permanent buildings, utilities and facilities for the administration, research, operation, development and service areas of Oak Ridge National Laboratory.	$21,968,631	187,821	0.855
Giffels & Vallet, Detroit, Mich.	A-E services for gaseous-diffusion plants K-29 and K-31 at Oak Ridge, Tenn.	121,180,669	511,372	0.422
Giffels & Vallet, Detroit, Mich.	A-E services for "C" plant at Paducah, Ky., including: (1) preliminary planning; (2) development of design criteria; (3) site study and planning; (4) design and inspection of construction.	241,761,519	367,000	0.152
Smith, Hichman & Grylls, Inc., Detroit, Mich.	A-E services for water, sewer, steam, air and gas, auxiliary buildings, roads, railroads at Paducah, Ky.	40,794,738	259,000	0.635
Sargent & Lundy, Chicago, Ill.	A-E services in connection with primary power facilities at Oak Ridge, Tenn., and Pacudah, Ky.	42,206,990	182,765	0.433
Vitro Corp. of America, New York, N. Y.	Preliminary investigation of suitable buildings to house a development plant, at Oak Ridge, Tenn.; complete design (excluding process design) of the project. Complete architect engineer supervision.	[15]		
Singmaster & Breyer, New York, N. Y.	A-E services for feed plant (Oak Ridge, Tenn., and Paducah, Ky.)	8,067,271	104,819	1.299
Blaw-Knox, Pittsburgh, Pa.	Complete A-E services for the materials testing reactor including: preliminary surveys, development of design criteria, detailed design drawings, supervision and inspection of construction, as-built drawings (Reactor Testing Station, Idaho)	16,005,874	192,340	1.20
Foster-Wheeler, New York, N. Y.	Complete A-E services for chemical processing plant including assisting Oak Ridge National Laboratory with development, preliminary surveys, development of design criteria, detailed design drawings, supervision of construction (Reactor Testing Station, Idaho)	14,066,380	148,000	1.05
Catalytic Construction Co., Philadelphia, Pa.	A-E services in connection with locating, designing and supervising construction of feed materials production center at Fernald, Ohio.	[8]38,213,000 [9]16,000,000	309,000 86,000	0.809 0.538
Silas Mason Co., Shreveport, La.	Design of scientific structures at Nevada Test Site; roads, electrical and communication circuiting in operational areas; design of additional camp facilities; procurement of critical materials for above work. Management of health and safety engineering program for operation.	[5]5,447,000 [16]1,034,000 [17]	64,074 12,136 2,100 78,310	1.18 1.17
Holmes & Narver, Los Angeles, Calif.	Design of permanent test facilities at Nevada Test Site including control point, Rad-Safe Building, and other permanent structures; roads and basic electrical distribution system; design of camp.	7,300,000	95,525	1.31

Operation Contracts

Contractor	Location of operating facilities, description of work performed, and responsibilities of contractor	Estimated payments, fiscal years 1950–53, inclusive		
		Fee	Overhead allowance	Total payments
The Galigher Co., Salt Lake City, Utah.	Operation of ore-processing facilities at Monticello, Utah.	[18]$153,808		$3,788,893
Walker-Lybarger Construction Co., Grand Junction, Colo.	Maintenance, protection and construction services for activities in Colorado Plateau area.	80,000		3,592,466

(Continued on next page)

Operation Contracts (continued)

Contractor	Location of operating facilities, description of work performed, and responsibilities of contractor	Estimated payments, fiscal years 1950–53, inclusive		
		Fee	Overhead allowance	Total payments
Blockson Chemical Co., Joliet, Ill.	Develop and install process equipment in contractor-owned facility at Joliet, Ill.; operate uranium-processing facility.	$40,000	$24,000	$1,422,751
Brush Beryllium, Cleveland, Ohio.	Perform studies, experimental investigations and other work in connection with the production of pure beryllium and production of zirconium; work to be done in Luckey, Ohio.	396,000	390,320	8,078,740
United Lead Co., New York, N. Y.	Operate and maintain the Middlesex, N. Y., storage and sampling plant.	33,800		685,628
National Lead Co. of Ohio, New York, N. Y.	Operate and maintain the feed materials production center at Fernald, Ohio, now under construction.	[19]200,000		11,779,175
Union Carbide & Carbon Corp., New York, N. Y.	Maintain in stand-by condition the plant at Niagara Falls, N. Y.	30,000	22,746	275,974
Union Carbide & Carbon Corp., New York, N. Y.	Maintain in stand-by condition plant at Tonawanda, N. Y.	7,250	13,237	163,915
Union Carbide & Carbon Corp., New York, N. Y.	Operate and maintain the gaseous diffusion plants including the feed plant and related facilities, the Y-12 area, and Oak Ridge National Laboratory (X-10) at Oak Ridge. Process design, engineering development and procurement of special items of equipment, preoperational inspection and testing and operation and maintenance of the Paducah, Ky., project.	9,788,989		459,972,139
Monsanto Chemical Co., St. Louis, Mo.	Operate and maintain Mound Laboratory at Miamisburg, Ohio.	1,300,900	581,120	22,902,844
American Industrial Transport, Inc., Oak Ridge, Tenn.	Manage, operate, and maintain the Oak Ridge bus system.	93,600		1,193,190
California Research and Development Co., San Francisco, Calif.	Design, construct, and operate particle accelerator located at Livermore, Calif.	279,440		9,844,415
Roane-Anderson Co., Oak Ridge, Tenn.	Perform management services (including management of community services, residential and commercial properties, utilities and related construction, and maintenance services) of Oak Ridge community.	315,500		5,040,376 *Net cost*
E. I. du Pont de Nemours & Co., Wilmington, Del.	Design, construction and operation of production facilities at Savannah River, S. C., and Dana, Ill.		5,900,000	1,086,834,500
General Electric Co., Schenectady, N. Y.	Perform architect-engineer, construction, operation, and process development services at Hanford, Wash., and operation of Knolls Atomic Power Laboratory at Schenectady, N. Y., in conjunction with the G.E. Research Laboratory for fundamental research and development.		3,148,326	400,209,768
Bendix Aviation Corp., (Kansas City Division Kansas City, Mo.)	Engineering, lay-out, preparation, equipping, and operation of facilities for the production and assembly of classified material.	4,882,377	589,169	111,820,000
Dow Chemical Co., Midland, Mich.	Plan and operate the Rocky Flats, Colo., plant in which production, engineering, manufacturing, and assembly of classified critical materials will be undertaken.	[19]932,500		9,345,890
Silas Mason Co., New York, N. Y.	Construction of facilities, movement, personnel training, and facility operation for production of classified material; Burlington, Iowa.	1,271,228		47,114,449
Procter & Gamble, Defense Corp., Cincinnati, Ohio	Technical consultant services, personnel training and operation of the Pantex Ordnance Plant, Amarillo, Tex.	[19]440,000		10,000,000
The Zia Co., Los Alamos, N. Mex.	Operate and maintain all utilities in support of community and technical programs at Los Alamos. Perform technical support for installation of instrumentation, gadgeteering, and maintenance functions within the technical areas. Operate and maintain all housing, concessionaire, and transportation programs and facilities. Perform certain procurement for AEC and contractors.	424,310		26,478,025 *Net cost*

Operation Contracts (continued)

Contractor	Location of operating facilities, description of work performed, and responsibilities of contractor	Estimated payments, fiscal years 1950–53, inclusive		
		Fee	Overhead allowance	Total payments
The Nevada Co., Las Vegas, Nev.	Work at Nevada Test Site. Maintenance of all structures and roads; operation and maintenance of warehouse, transportation, and utility facilities; construction of minor facilities; operation of camp.	$80,000		$5,000,000
Phillips Petroleum Co., Bartlesville, Okla.	Operation of the materials testing reactor at the reactor testing station, Arco, Idaho.	235,250	$314,750	5,475,650
American Cyanamid Co., New York, N. Y.	Operation of a chemical processing plant at the reactor testing station, Arco, Idaho.	130,000	"	6,482,400
Western Equipment Co., Boise, Idaho.	Operation of an equipment repair shop at the reactor testing station, Arco, Idaho.	58,000	"	2,064,864
National Industrial Maintenance Corp., Boise, Ida.	Operation of maintenance and craft shops, services and utility systems at the reactor testing station, Arco, Idaho.	25,000	"	480,000
Lost Rivers Transportation Co., Portland, Oreg.	Operation of transportation system at the reactor testing station, Arco, Idaho.	29,900	"	851,100
Harding-Williams, Chicago, Ill.	Operation of 3 cafeterias at the reactor testing station, Arco, Idaho.	3,983		82,580
Westinghouse Electric Corp., Pittsburgh, Pa.	In Government-owned facilities at Bettis Field, Pittsburgh, Pa., on land leased from the contractor, contractor is responsible for the fabrication, testing, and operation of a nuclear-power plant for propulsion of a submarine and research and developmental work thereon in conjunction with other contractors. The reactor is being constructed at the national reactor testing station, Arco, Idaho.	2,015,182	1,262,263	82,665,405

Research and Development Contracts

Contractor	Location of work, project description, and responsibilities of contractor	Estimated payments, fiscal years 1950–53, inclusive		
		Fee	Overhead allowance	Total payments
The Merrill Co., San Francisco	Study and development of a uranium process at contractor-owned laboratory, San Francisco, Calif.	$3,600	$18,000	$60,000
Sonic Research Corp., Boston	Study and design of certain uranium process equipment at contractor-owned facilities, Boston, Mass.	500		10,500
Vitro Corp. of America, New York, N. Y.	Research and development work with respect to waste residue recovery, scrap recovery, process design, and other related work; Jersey City, N. J.	48,708	194,410	730,949
Sylvania Electric Products, Flushing, N. Y.	Research and development work on preparation of feed materials; Bayside, N. Y.	101,741	710,576	1,809,444
Battelle Memorial Institute, Columbus, Ohio.	Conduct studies and experimental investigations on uranium- and thorium-bearing ores and other specially assigned projects.	26,842	165,345	552,454
New England Lime Co., Canaan, Conn.	Conduct research and development work on the distillation and purification of metal and delivered quantities.	44,306	9,400	923,197
Blaw-Knox Construction Co., Pittsburgh, Pa.	Design and testing of improved denitration equipment.	2,400	6,134	15,992
Radio Corp. of America, New York, N. Y.	Develop and produce quantity of superpower vacuum tubes at Harrison, N. J.	77,815		2,877,800
Edgerton, Germeshausen & Grier, Inc., Boston, Mass.	Work involves (1) research and development and manufacturing incident to installation of scientific test instrumentation at AEC test sites; (2) design, manufacture, test, maintenance of operations systems, weapons systems, (3) participation in weapons test evaluation.	170,232		3,100,000

(Continued on next page)

Research and Development Contracts (continued)

Contractor	Location of work, project description, and responsibilities of contractor	Estimated payments, fiscal years 1950–53, inclusive		
		Fee	Overhead allowance	Total payments
Battelle Memorial Institute, Columbus, Ohio.	Perform work in research, development, and fabrication in the fields of (*a*) metallurgy, (*b*) ceramics, (*c*) concretes and cements, (*d*) the chemistry of substances related to reactors, and (*e*) solid state physics.	$191,135	$1,402,503	$4,306,097
North American Aviation, Inc., Downey, Calif.	Engage in a program of research and development work including the following activities: (*a*) study and development of nuclear reactor materials and components, (*b*) developmental studies on various specific reactor types.	351,409	2,281,797	7,812,676
Corning Glass Works, Corning, N. Y.	Provides for cooperation between the Commission, Argonne National Laboratory, and Corning in studies relating to radiation effects on glass and other transparent materials.	1	0	0
General Electric Co., Schenectady, N. Y.	In non-AEC but Government-owned facilities near Lockland, Ohio, the contractor is responsible for fabrication, testing, and operation of a nuclear power plant for propulsion of aircraft and research and development work thereon in conjunction with other contractors.	[23]	[23]	13,500,000
Stanford Research Institute, Stanford, Calif.	Engage in developing a continuous separation of ions by moving ion-exchange bed and engineering-economic study of the cost and pricing policy of radioisotopes and fission products.	6,500	51,964	142,249
Elgin National Watch Co., Elgin, Ill.	Conduct research on high-speed electromechanical counting registers.	937	8,491	19,190
Armour Research Foundation, Chicago, Ill.	Develop zirconium phase diagrams.	6,338	33,627	99,999
Graham, Crowley & Associates, Inc., Chicago, Ill.	Develop methods for electrowinning of zirconium.	1,300	11,400	23,200
The Rand Corp., Santa Monica, Calif.	Theoretical studies of gamma rays and neutrons through thick media.	6,208	38,689	107,812
Battelle Memorial Institute, Columbus, Ohio.	Development and construction of a pilot plant for zirconium production.	23,505	98,412	412,631
Arthur D. Little, Inc., Cambridge, Mass.	Air-filter research.	7,500	19,309	109,608
Nuclear Development Associates, White Plains, N. Y.	Gamma ray and neutron-shielding research.	11,209	52,777	152,923
H. K. Ferguson Co., New York, N. Y.	Engineering studies related to the development of nuclear reactors.	27,775	135,418	375,000
Vitro Corp. of America, New York, N. Y.	Development of waste treatment systems including equipment development.	50,905	163,547	822,667
North American Aviation, Inc., Downey, Calif.	Analytical engineering studies of a particular type of power plant of interest to the aircraft-nuclear-propulsion program.	16,904	137,491	355,000

[1] Although this is now a subcontract, original negotiations were begun on a prime contract basis and as contract is for general construction, it is included here.
[2] Engineering.
[3] Excluding $5,791 for operation of pilot plant.
[4] Construction.
[5] In addition a lump sum of $17,500 was paid for a site selection survey.
[6] Camp operation, maintenance, and management.
[7] Support and roll-up.
[8] Construction services.
[9] Engineering, design, and inspection.
[10] In addition a lump sum of $20,000 was paid for a preliminary reconnaissance study and report.
[11] Estimated scope.
[12] Operation, maintenance, management of camp and motor pool.
[13] Support and maintenance of test activities.
[14] Engineering survey work only with no related construction. Estimated cost of survey $118,000.
[15] Obligations authorized up to $300,000 only.
[16] Procurement.
[17] Management.
[18] Gallagher Co. fee includes services of full time on-the-job manager and home office supervision and home office overhead; Walker-Lybarger fee includes full time services of 1 partner and part time services of another, and home office overhead.
[19] Intended to cover general and administrative expenses only, with no provision for profit.
[20] The fixed fee is not based specifically on an estimate of the total cost of the work. Rather it represents an estimate (made by the contractor and reviewed by AEC) of the contractor's home-office salaries which can be allocated directly to the Rocky Flats project. The amount of the fee to be paid for subsequent fiscal years will be agreed upon prior to the beginning of each fiscal year. In negotiating for a coming year's fee the AEC audits the prior year's actual home-office salaries.
[21] Costs under these contracts are borne by AEC. Department of Ordnance (Army) negotiated and administers the contract.
[22] Included in fee.
[23] Information not available.

Two New *Berkeley* COUNTING RATE METERS

MODEL 1800—*Laboratory Monitor*

A general-purpose count rate meter with five selectable meter ranges (300, 1000, 3000, 10,000 and 30,000 counts per minute). Visual and aural indication. Built in loudspeaker is regulated by front panel volume control.

BRIEF SPECIFICATIONS

Ranges: 300, 1000, 3000, 10,000 and 30,000 counts per minute.

Accuracy: Approximately ± 5% of full scale. **Power Requirements:** 117 volts ± 10%. 35 watts.

Dimensions: 6½" x 6¼" x 10½". **Front Panel Volume Control** **Net Weight:** Approximately 8 lbs.

Price: $251.00 F.O.B. Factory with Victoreen 1B85 Aluminum Wall G-M Tube, Sliding Shield Probe Assembly & Cable.

BRIEF SPECIFICATIONS

Sensitivity: 0.5 Volt Peak.

Accuracy: ± 5% of full scale.

Ranges: 100; 200; 500; 1000; 2000; 5000; 10,000; 20,000; 50,000; 100,000 counts per minute.

High Voltage: From 0 to + 2500 volts. Regulation 0.05% per % change in line voltage over 105 to 125 volts.

Front Panel Volume Control

Connectors: For Graphic Recorder, and Scintillation Counter.

Power Requirements: 117 Volts ± 10% approximately 150 watts.

Zero Check and Calibrate Switches on Front Panel.

Dimensions: 9¼" x 14¼" x 10⅝"

Net Weight: 25 lbs.

Price: $485.00 F.O.B. Richmond, California.

MODEL 1810—*Count Rate Meter*

This complete laboratory instrument provides panel switch selection of 10 different counting rate ranges from 100 cpm full scale to 100,000 cpm full scale and 7 different response half-times. Results are indicated visually and aurally, and may be fed to a 1 ma graphic recorder for a continuous permanent record. A front panel oscilloscope connector is also provided for observation of input pulses if desired.

A zero meter check and 3600 cpm calibration are also provided. The unit is designed for use with either a G-M tube or scintillation detector.

Berkeley Scientific Corporation

2206 WRIGHT AVENUE • RICHMOND, CALIFORNIA

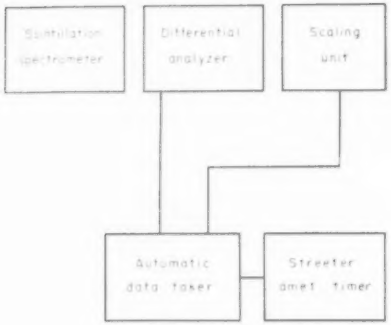

FIG. 1. Block diagram showing position of automatic data taker relative to other components

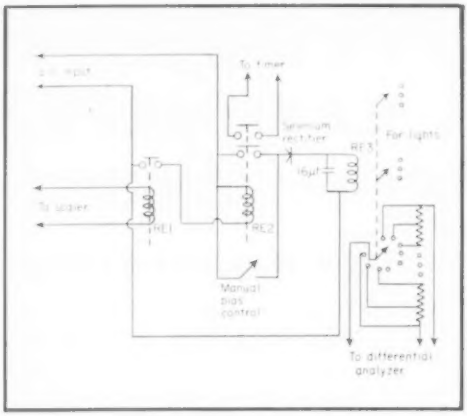

FIG. 2. Schematic of automatic data taker

Automatic Data Recorder for Scintillation Spectrometer

By OTTO H. ZINKE and C. SHARP COOK
*Washington University**
St. Louis, Missouri

For use with a single-channel pulse-height differential analyzer, a device has been constructed which automatically scans and records the spectrum received by the analyzer from a scintillation spectrometer. The device functions over long periods of time in the absence of an operator and may thus serve as an inexpensive substitute for a multichannel analyzer. The over-all system is shown by the block diagram of Fig. 1, and the schematic of the automatic data taker is given by Fig. 2.

The differential analyzer (*1*) selects spectrometer signals whose pulse heights correspond to energies in the range from E_1 to $E_1 + \Delta E$ and feeds them to the automatic data taker through some type of scaling unit, in our case a series of Higinbotham-type scales-of-two. The number of such units depends upon the counting rate of the differential analyzer output and is determined arbitrarily by the operator.

The output pulse activates relay *RE1*, a Western Electric type D-168479 mercury relay. Activation of this relay causes current pulses to flow through the coils of relays *RE2* and *RE3*. *RE2* is any appropriate relay with 110-volt a-c coil; a Clare type SD-71 stepping switch is used for *RE3*. The primary purpose of *RE1* is to produce proper impedance match between the output of the scaling unit and the input of these two coils. If the contacts of *RE1* stick occasionally, a time-delay relay, which de-energizes the whole a-c circuit, should be placed in parallel with *RE2*.

The output of relay *RE2* operates a Streeter-Amet SCI model TIMA-.01M time interval recorder, which records the time since the last pulse through the circuit. This time interval is that required for a fixed number of pulses, N (a function of the number of scaling units), to pass through the differential analyzer. These pulses are, of course, in the energy range E_1 to $E_1 + \Delta E$. After recording the time interval, the Streeter-Amet counter resets itself to zero and begins immediately to record the time interval for the next set of differential-analyzer output signals.

Were it not for the action of relay *RE3*, each successive record would be identical, being that time interval necessary to record N pulses in the energy range E_1 to $E_1 + \Delta E$. However, relay *RE3*, a Clare three-layer, 40-point, spring-driven stepping switch, has an appropriate series of resistors connected to the 40 points on one of its layers. These resistors serve to produce 40 values of feedback voltage

* Assisted by the joint program of the Office of Naval Research and the U. S. Atomic Energy Commission.

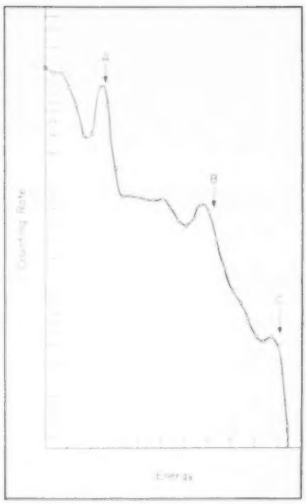

FIG. 3. Secondary electron spectrum from gamma-rays of Na^{22} as plotted on semi-logarithmic scale from data taker. Abscissa is divided according to equal energy steps provided by resistor bank of relay *RE3*. Peak *A* is produced by annihilation radiation photoelectrons, peak *B* by photoelectrons of 1.28-Mev gamma ray; peak C is additive peak explained in reference (2)

to be applied to the differential analyzer. This voltage acts as a bias to control the signal pulse height accepted by the differential analyzer. After the time interval for N counts in the spectral interval E_1 to $E_1 + \Delta E$, the data taker moves on to take N counts in the interval E_2 to $E_2 + \Delta E$, etc., until 40 successive positions, or less, on the spectrum under study have been recorded.

The second and third layers of relay *RE3* serve to operate a series of neon glow tubes placed in the front panel of the automatic data taker, that tell the operator at a glance what part of the spectrum the data taker is recording.

An example of the data which can be obtained in such a manner is illustrated by Fig. 3, which shows the Compton and photoelectric spectrum from the gamma-radiation (*2*) of Na^{22}, using NaI(Tl) crystal and an RCA 5819 photomultiplier tube.

BIBLIOGRAPHY

1. J. Francis, P. R. Bell, and J. Gundlach, *Rev. Sci. Instr.*, **22**, 133 (1951). Our analyzer is not identical but is similar to this.
2. P. Jastram, R. Whalen, and O. H. Zinke, *Phys. Rev.* (in press)

Remote Pipette Control for Radioactive Liquids

By ERVIN J. LILJEGREN and STEWART H. WEBSTER

National Institute of Arthritis and Metabolic Diseases
National Institutes of Heath, U. S. Public Health Service
Bethesda, Maryland

A number of devices for overcoming the danger inherent in pipetting radioactive material by mouth have been described. However, most of these arrangements suffer from one or more limitations, such as small capacity, poor reproducibility, great complexity, high cost or low versatility.

We have devised an arrangement which has met the needs of this laboratory. Essentially it consists of a hypodermic syringe mounted in a holder containing a coarse rack and pinion assembly taken from a microscope, as shown in the illustration. The syringe, connected with a pipette by means of a rubber tube, serves to fill and adjust the liquid level in the pipette, only the latter coming in contact with the radioactive material. By means of adapters and washers the holder can be made to accommodate 30-, 10- or 5-cm^3 syringes, thus providing for the handling of as much as 28 cm^3 or as little as 0.01 cm^3 of liquid. For use with still smaller quantities, adapters to hold a 1-cm^3 syringe can be made.

The arrangement of parts is shown in the exploded view. The plunger holder, *PH*, and the barrel holder, *BH*, are fastened to the rack and pinion assembly, *RP*, which is the coarse adjustment slide assembly from a No. 37 American Optical Co. polarizing microscope. This assembly was selected because of the long travel available (80 mm). The barrel of the syringe, *SB*, fits into the adapter, *A*, which in turn fits into the barrel holder, *BH*, a thin rubber gasket being used to separate the two brass parts and to permit some slight movement when the assembly is tightened. The

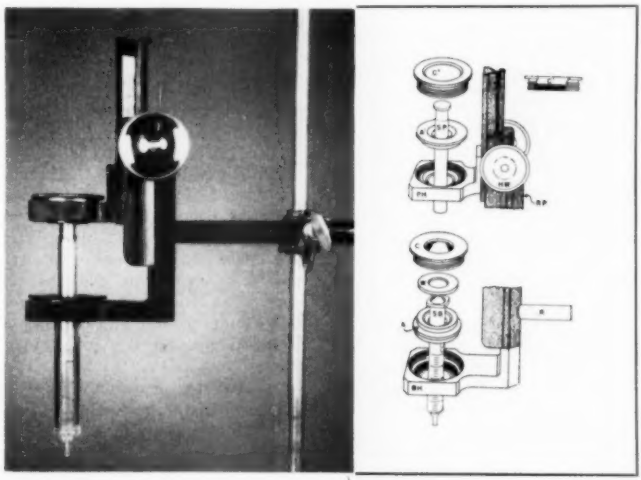

REMOTE PIPETTE CONTROL and exploded view of its components

brass washer, *W*, which serves to keep the barrel in place, is secured by the cap, *C*. By means of this arrangement different sized barrels are accommodated by using different sized adapters and washers. The plunger of the syringe, *SP*, fits into the adapter, *A'*, which in turn fits into the plunger holder, *PH*. The plunger is held in place by the cap, *C'*, on the bottom of which is a rubber plug shown in cross-section detail. This plug cushions the plunger and yet permits a slight movement. Here again the adapter used varies with the size of plunger used.

The whole apparatus is supported at the desired height by means of a clamp attached to the rod, *R*. A flexible rubber tube connecting the tip of the syringe and the pipette lip can be of any convenient length. With fairly heavy-walled tubing, the effects of temperature changes during manipulation are minimized.

To align the barrel and plunger, these two parts are inserted into their holders without tightening the caps. By means of the handwheel, *HW*, the plunger is pushed into the barrel about three-quarters of its length, after which the caps are screwed down firmly. A small amount of vaseline or mineral oil on the plunger will improve the action if there is any tendency toward leakage of air.

With high-activity material, it may be desirable to operate the syringe several feet away from the pipette. The difficulty of accurately reading the small meniscus of the pipette at this distance can easily be overcome by use of a reading telescope conveniently located next to the syringe.

To determine the reproducibility of delivery, ten 1-ml quantities of water were successively measured out using a 1-ml measuring pipette and a 5-cm³ syringe. The meniscus was read with a telescope, and the pipette control was about four feet from the pipette. From the weight of water delivered it was ascertained that the mean deviation in these measurements was 0.0015 ml; the standard deviation was 0.0020 ml. If variations of less than two parts in one thousand are desired, the use of either a smaller syringe or a volumetric pipette is recommended.

* * *

We wish to express our appreciation to Laurence R. Crisp, Head, Instrument Section, National Institutes of Health, for his assistance in the design and construction of this apparatus.

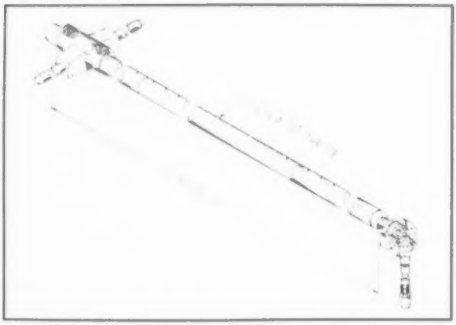

FIG. 1. Wrench that can be extended to 27 ft

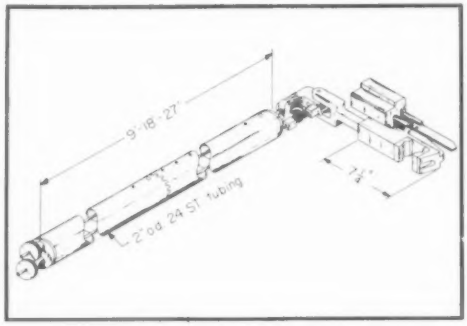

FIG. 2. Remotely operated saw and vise combination

Tools for Dismantling Contaminated Cells

By A. M. TRIPP and FRANK RING, Jr.
Engineering Department
Oak Ridge National Laboratory
Oak Ridge, Tennessee

The task of dismantling piping and chemical process equipment which have become contaminated by radioactive materials requires remotely operated tools. Such tools have been designed for the Chemical Technology Division of ORNL. These tools are used to turn nuts and bolts, and to saw pipe at distances as far as 27 ft below the operator or 15 ft horizontally.

Almost all of the dismantling work is done on equipment set up in deep cells. The use of these tools has materially speeded up this type of work. The complicated piping arrangements inside the cell make it necessary to use a long tubular arm which is constructed to hold either socket wrenches or cutting tools.

This tubular arm consists of one, two or three 9-ft sections of 2-in. O.D. 24ST aluminum tubing, which has a $\frac{1}{16}$-in. wall. The tubing lengths with castellated ends are joined by sliding them over a sleeve. Inverted dog point screws are backed from the sleeve into matching holes in the tubing, thus locking the sections together rigidly.

Wrench arrangement. For the nut and bolt turning, a Piezo Universal Gear Joint is attached to the working end of the tubing handle. See Fig. 1. This universal joint is preset to a desired angle before the wrench is lowered into the cell. The nut or bolt turning is accomplished by turning the long handle. The turning motion is transmitted through the universal joint to the socket wrench. The total

Fast heating and less O_2 with a DPi **high vacuum** furnace

This DPi high vacuum furnace is being used by the Mineral Products Division of the National Bureau of Standards to study phase equilibria of binary and ternary metal-ceramic mixtures.

Operating at pressures of 10^{-4} to 10^{-5} mm Hg, the furnace heats up to 1800 C in ten minutes and is held for one half hour. The absence of thermal conductivity in vacuums of this order helps make such rapid heating possible and temperatures easier to hold.

Moreover, it's usually easier and cheaper to get rid of oxygen by high vacuum rather than to try diluting. With a vacuum of 1×10^{-5} mm Hg, the oxygen content is reduced to 3 parts per billion—a content achieved only with considerable difficulty utilizing an inert atmosphere.

DPi's wealth of experience in high vacuum research and engineering, combined with expert manufacturing experience in metal-heating problems, makes it possible for us to develop trouble-free high vacuum metallurgical furnaces to meet your needs precisely. We can make provisions for addition cups, interchangeable furnace assemblies, sight windows, or whatever you need, and still hold the vacuum.

Whether you are interested in high vacuum metallurgy, a single pump, or any high vacuum application, we will be glad to discuss your problems with you. Just write or phone ***Distillation Products Industries,*** Vacuum Equipment Department, 781 Ridge Road West, Rochester 3, N. Y. (Division of Eastman Kodak Company).

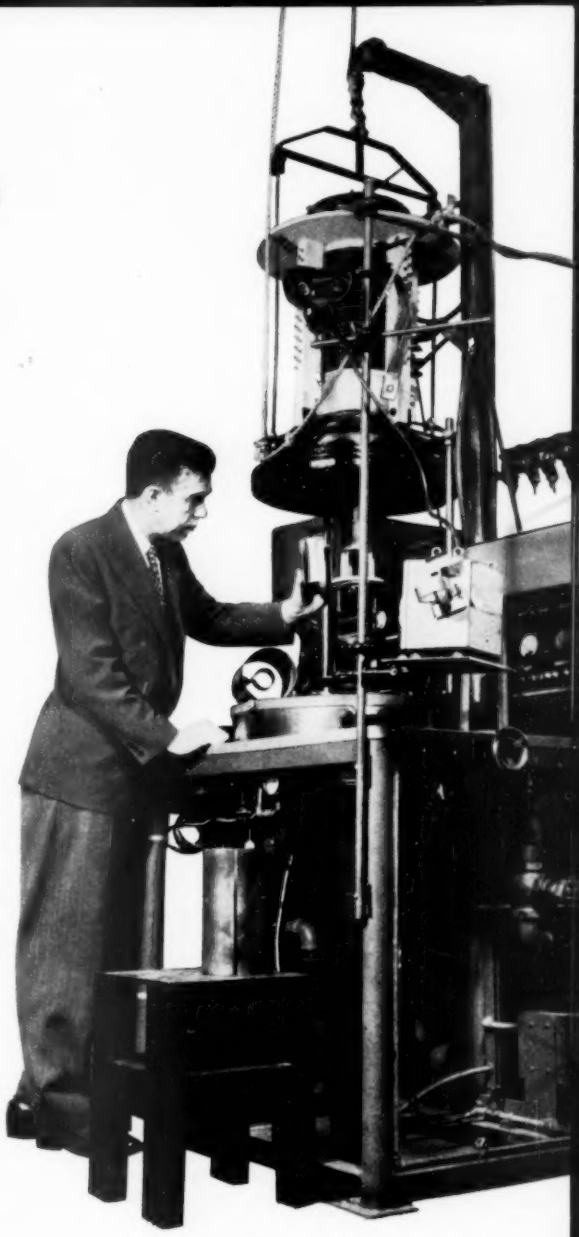

DPi

high vacuum research and engineering

Also . . . vitamins A and E . . . distilled monoglycerides . . . more than 3500 Eastman Organic Chemicals for science and industry

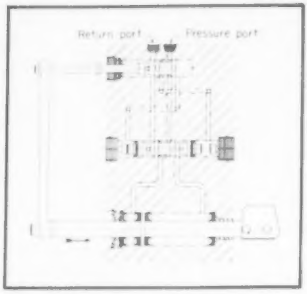

FIG. 3. Hydraulic piston and valve arrangement for saw and vise

weight of the 27-ft handle and wrench is 17 pounds.

Saw and vise combination. The remotely operated hydraulic hacksaw and vise combination is the most important disassembly tool for welded construction or for removing corroded sections. The following design criteria for this saw were set up and successfully complied with:

1. The vise must be able to clamp to the pipe or material to be cut.

2. This type of hacksaw and vise combination must be capable of cutting at least a 1-in. pipe.

3. The sawing action of the cutting blade must be automatic after it has been started by the operator. This is necessary because the saw is sometimes invisible to him.

4. The pressure on the saw blade must be sufficiently heavy for good cutting, but not enough to cause sticking. This is done by balancing cylinder diameter of the vise and the cutting pressure unit.

5. In the event of a pipe binding on the saw blade, it must be possible to free the unit. This is done by making the actuating cylinder large enough to shear the rivets that hold the blade.

As shown in Fig. 2, the hacksaw is essentially a draw-cut keyhole saw mounted on the end of a double-acting hydraulic piston. An arm on the end of this piston actuates a pilot valve which controls a four-way valve which reverses the piston at each end of its stroke. See Fig. 3. The saw is pivoted at the side of a hydraulic vise that clamps to the pipe or member to be cut. The hacksaw blade is a short length of heavy-duty, high-speed steel 0.049-in. thick and 1-in. wide. Only the tooth section is hard.

The vise is a conventionally styled double-acting hydraulic unit with two V-type hardened steel jaws. The same pressure that actuates the vise also actuates a double acting hydraulic cylinder, which being linked to a crank arm, causes the pivoted saw unit to swing the saw against the work and maintain the cutting pressure. This double-acting piston also lifts the blade when the vise jaw is opened.

To dodge intervening pipes and to reach the desired pipe at the proper angle, the hacksaw and vise unit are mounted to the tubular arm with two joints. With the axes at right angles to each other, and about 3 in. apart, each joint can swing 90 degrees either side of center. The blade can be remotely set at any angle with the tubular arm and with any off-set up to the 3 in. By moving the handle and remotely rotating the arm, the hacksaw can be maneuvered through a maze of pipe and supports to the desired point for cutting. Position adjustments are made by turning control shafts operating through the tubular arm via worm gears. Thus the joints are always locked in position. Bevel gears carry the rotational adjustments of one control shaft through the first joint to actuate the second.

For body and structure, 24ST aluminum is used throughout, with RDS used for screws, nuts, pistons, vise jaws, etc., to obtain minimum weight with maximum strength. The total weight of this saw and vise with the 27-ft handle is 23 pounds.

The whole system is designed for 1,000 lb/in² hydraulic pressure. Small diameter high-pressure rubber tubing is used for flexibility. See Figs. 3 and 4. One hydraulic pump is used for both clamping and saw operation. With the saw valved off, an accumulator in the vise is charged to 1,000 lb/in² and then shut off. This maintains the pressure on the vise while the pump is used to operate the saw at any lower pressure required.

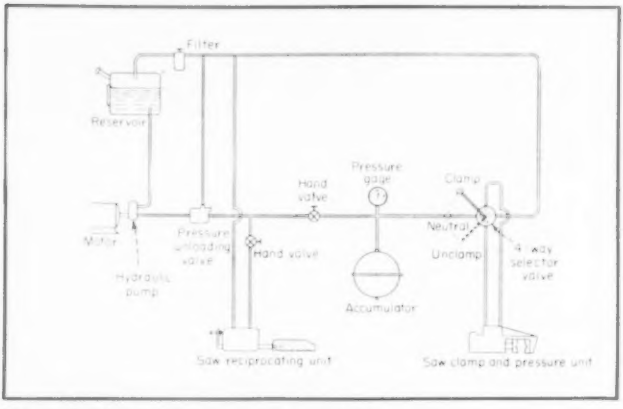

FIG. 4. Complete hydraulic system for saw and vise

TECHNICAL BRIEFS

• **Vacuum coating** with evaporated metallic films is simplified if the glass bell jar is first coated with a thin evaporated film of potassium chloride. This forms a water-soluble film that facilitates removal of the metallic film that usually deposits on the glass. Technique is described by A. E. Cameron in AEC document K-909.

• **Printed circuit** techniques are being applied to special rotary switches for pulse work by the Daven Co., Newark, N. J. Odd-shaped segments and irregular timing intervals are easily obtained with rotary switches.

• **Critical dosage** values specified for personnel dosimeters for civil defense should be revised downward from the present 200-400-600 r range to 100-250-400 r, according to G. V. Taplin in AEC document UCLA-187. A 50-r range would be useful.

• **Boron-free** electrical insulating material made of quartz paper is superior to asbestos. The new paper, developed by the Naval Research Laboratory, Washington, D. C., is made of laboratory-produced fibers by regular paper-making techniques; it will withstand 3,000° F and does not become radioactive when exposed to neutrons.

TWO REVOLUTIONARY MEDICAL INSTRUMENTS

for clinical and research use of radioisotopes.

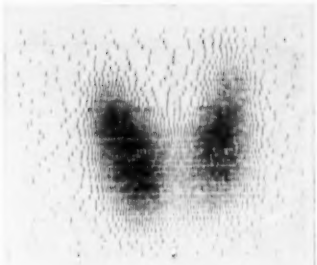

Frontal profile of thyroid gland produced by the Scintiscanner using I-131 radioiodine.

The RAX13A SCINTISCANNER*

. . . automatically prints "pictures" of radioactive sources for immediate study.

The Scintiscanner is a mobile, completely automatic scanning device which produces multiple pictures of in vivo radioactive gamma-emitting sources. Medical papers variously refer to these pictures as "Scintigrams" or "Gammagraphs". An important application of this instrument in medicine has been mapping the frontal profile of the thyroid gland, as shown above. Density of printed lines is determined by the concentration of radioactive iodine in the gland. Doses as low as 100 μc have been used to obtain satisfactory pictures. Innumerable applications of the Scintiscanner are possible and remain to be investigated.

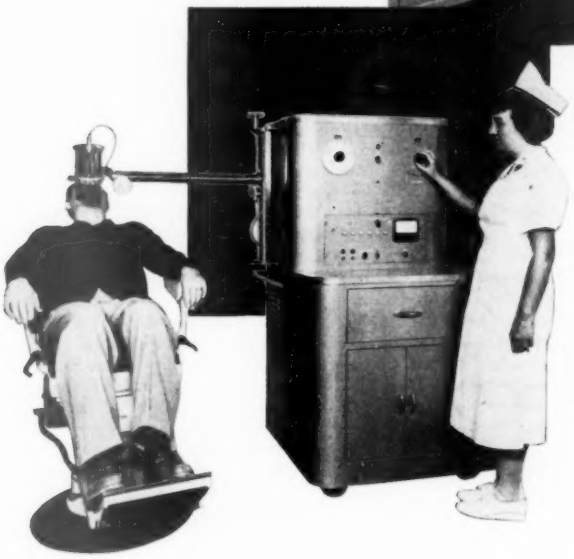

The MAX19TC SCINTIMATIC CONSOLE*

. . . a complete, mobile radiation detection laboratory for performing medical in vivo tracer and radioassay studies.

The Scintimatic is fully automatic, direct reading, and employs the widely used R-C Scientific LAX12 scintillation counter, which permits the use of small tracer doses. It automatically and precisely measures minute in vivo concentrations of I-131, Au-195, Fe-59, or other gamma emitters. Thyroid uptake and urinary excretion studies, for example, can be performed with as little as 1 μc of I-131. Designed especially for medical use in diagnosis and research, the Scintimatic is widely used in thyroid uptake, urinary excretion, blood volume, blood circulation, and other studies where a sensitive, accurate and direct measure of radioactivity from small tracer doses is required.

**These instruments are now being used by hospitals, medical schools, universities, and other research institutions throughout the country.*

For bibliography of medical papers involving use of these instruments or for additional information, please write to:

R-C SCIENTIFIC INSTRUMENT CO., INC.
First in Scintillation Counting Equipment

335 CULVER BOULEVARD,
PLAYA DEL REY, CALIFORNIA

BOOKS

Progress in Cosmic Ray Physics, edited by J. G. Wilson, Interscience Publishers, Inc., New York (or North-Holland Publishing Company, Amsterdam), 1952, xvi + 557 pages, $12.

The celerity with which new developments have emerged during the post-war years, and the broad consequences of the recent significant advances in the state of our knowledge regarding the nature and properties of the cosmic radiation have effectively combined to enhance the value and timeliness of this outstanding volume, which in any event would have merited plaudits in its own right.

Of the 616 individual references cited (in many instances, repeatedly) throughout this book, which depicts the state of affairs in the early months of 1951, approximately 60% are dated 1949 and later. Thus, it is easy to understand why the contemporary specialist in one phase of cosmic radiation may perforce bemoan the fact that he has been unable to remain adequately conversant with all of the other aspects of his field. The active investigator who has craved for authoritative, critical "reviews covering those aspects of the physics of cosmic radiation in which advances of broad significance are now being made" will welcome this book as embodying just what the doctor ordered. There is no doubt that its avowed purpose, as set forth in the preface, has been accomplished admirably.

The book does not purport to constitute a comprehensive text on the subject of cosmic radiation, but consists of eight independent chapters, each entirely self-contained. Owing to the rapidity with which new results are being reported, it would have been impossible for an individual author to prepare a single relatively up-to-date treatise incorporating all of the subject matter covered in this book at an advanced level. The optimum alternative of assembling sections prepared by several contributors has been adopted in this case. This procedure also averts the tendency to overemphasize the specific interests of any single author who might be prone to stress certain favorite topics at the expense of others.

Although all the main lines of cosmic-ray investigations are not surveyed in this single volume, certainly at least from the phenomenological point of view the book actually encompasses a complete account of the life-cycle of cosmic radiation. For indeed, the primary protons, alpha particles and heavier nuclei are followed from their sources far out in our galaxy to the upper regions of our atmosphere (Chapter 4, *The Nature of Primary Cosmic Radiation*, by B. Peters) or from the sun (Chapter 8, *Time Variations of Cosmic-Ray Intensity*, by H. Elliot), taking into account the effect of the earth's magnetic field on charged particles (Chapter 5, *Recent Data on Geomagnetic Effects*, by H. V. Neher).

The progress of the incoming cosmic rays and of their progeny in the form of the N-component consisting of nucleons and π-mesons, μ-mesons, and the photon-electron component, is then traced through the atmosphere (Chapter 6, *The Equilibrium of the Cosmic-Ray Beam in the Atmosphere*, by G. Puppi and N. Dallaporta) down to the greatest depths at which it has been possible to conduct experiments (Chapter 7, *Observations of Cosmic Rays Underground and Their Interpretation*, by E. P. George).

Finally, various individual interactions are examined in detail both from the experimental and theoretical points of view (Chapter 1, *The Analysis of Energetic Nuclear Encounters Occurring in Photographic Emulsions* by U. Camerini, W. O. Lock, and D. H. Perkins; Chapter 2, *Unstable Heavy Cosmic-Ray Particles*, by C. C. Butler; and Chapter 3, *Coupling Properties of Nucleons, Mesons and Leptons*, by L. Michel. Incidentally, if you are tempted to speculate that leptons are new particles discovered by Leprince-Ringuet, read this chapter! You will then learn that, from the viewpoint of the isotopic spin formalism, electrons and neutrinos are the same particle, the lepton.) Of the prolific meson family, only the kappas failed to beat the publisher's deadline.

In lieu of discussing each chapter in detail, it is expedient for the present purposes to venture a few generalizations, merely noting without further elaboration that statistical fluctuations occasionally occur.

Each section comprising approximately 60 pages includes a succinct introduction, a number of extremely well-organized subdivisions, and a summary. The latter usually enumerates outstanding problems, and predicts the lines along which future progress may be expected. The chapters are logically and systematically arranged, lucidly written, and are self-consistent internally. A list of references is appended at the end of each article.

A conscientious effort to present the material objectively and critically has been successful indeed, and each of the authors is clearly competent to prepare an authoritative survey of the state of his subject. In some instances, where discrepancies among the results of different investigators exist, the authors do not hesitate to express doubt regarding the validity of their own earlier conclusions, when this appears warranted.

It would have been desirable to standardize the symbols employed by the various authors, who frequently use different notations for designating a given type of event. However, within any single chapter, there is no ambiguity. There is also some redundancy, which however is not objectionable in view of the desirability of retaining each article as a self-contained unit. The errors which have occasionally slipped by are probably attributable to the speed which was required for quick publication.

The book is profusely illustrated with numerous excellent reproductions of events occurring in photographic emulsions and in cloud chambers. Although experimental and instrumental details are omitted, and the emphasis is upon the fundamentals, whenever the interpretation of the results depends intimately upon the instrumental arrangement, the pertinent details are described. Each author has conscientiously endeavored to portray the most accurate picture possible of his particular subject based upon the best available experimental data, theoretical considerations, and, in some cases, even pure intuition.

Nuclear physicists will especially welcome this book as an ideal source of information regarding the numerous contributions to their field which have arisen from cosmic-ray research and which may be expected in the future. In fact, anyone who desires first-hand information regarding the current trends of cosmic-ray investigations will find this volume of great value.

Active workers in the field of cosmic radiation owe a debt of gratitude to

Every Top Management Man... In Every Industry

SHOULD BE ABLE TO ANSWER THESE QUESTIONS ABOUT A MOST CRITICAL EMERGENCY IN OUR COUNTRY'S AFFAIRS

Q. Why is iron and steel *scrap* a matter of importance to me?

A. Steel for our country's military program and civilian economy is being produced at the annual rate of 107,000,000 tons in 1951 . . . 119,500,000 tons expected in 1952. Steel-making capacity is being increased now to meet those quotas.

What Do I Get For My Scrap?

In addition to being paid for your scrap, you remove nuisance inventory from your plant—saving valuable floor space. Also, you have a better chance of *getting* new steel or steel products. But, *most important*—you help alleviate a dangerous condition threatening our country's capacity to rearm and satisfy civilian requirements at the same time.

Q. How does scrap figure in the production of steel?

A. Steel is composed, generally speaking, 50% of pig iron, 25% of "production" scrap (that is, the scrap which is produced as a by-product of steel-making) and 25% of "purchased" scrap.

Q. Is scrap getting scarce?

A. Yes. The supply of *purchased* scrap is not increasing fast enough to meet the needs of increasing steel production.

Q. What if the needed scrap isn't obtained?

A. Open-hearth furnaces will not be able to operate at capacity. That will mean a loss of steel production . . . and fewer products made of steel.

Q. Why not use pig iron instead of scrap?

A. Every ton of scrap conserves approximately 2 tons of iron ore, 1 ton of coal, nearly ½ ton of limestone and many other vital natural resources—to say nothing of the extra transportation facilities that would be otherwise required.

Q. How can *more* scrap be furnished?

A. By everybody pitching in—as we always do in every emergency—and searching out all possible sources of scrap.

Q. What are these sources?

A. Metal-fabricating plants normally turn over to scrap dealers the scrap left from machining. But there's not enough of this to fill our present enormous need. So everybody—both in and out of the metal-fabricating industries—must sell scrap in the form of *idle metal.*

Every pound of idle metal is needed to keep our steel mills operating at top capacity. Sell your idle metal to a local scrap dealer right away.

What Do I Do *First*?

Write for free booklet. It tells how to set up a Scrap Salvage Program in your plant. Thousands of plants are cooperating. Do your part now! Address Advertising Council, 25 West 45th Street, New York 19, N. Y.

Q. *We* don't *produce* scrap—how can *we* help?

A. Scrap is any kind of iron and steel that's gathering dust—obsolete machines or structures, jigs and fixtures, pulleys and wheels, chains and track, valves and pipe—*anything* with rust on it or dust on it. Non-ferrous scrap is needed, too.

Q. What do we do with it when we find it?

A. Use your normal channels or get in touch with a recognized scrap dealer.

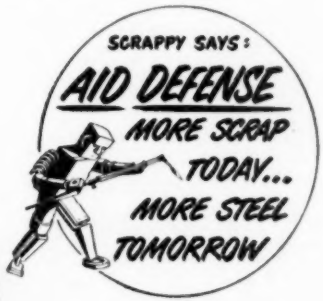

This advertisement is a contribution, in the national interest, by

McGRAW-HILL PUBLISHING COMPANY, INC.

330 WEST 42nd STREET **NEW YORK 36, N. Y.**

A PUBLIC SERVICE PROJECT THE ADVERTISING COUNCIL

Scientifically Tested and Registered for Extreme AIR PURIFICATION

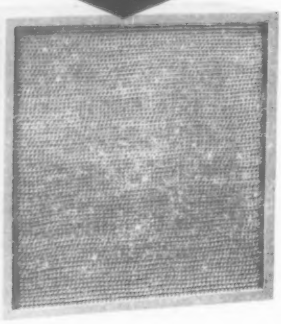

THE M. S. A. ULTRA-AIRE SPACE FILTER

Rigid, controlled testing is a vital part in the manufacture of the M.S.A. Ultra-Aire Space Filter. Before shipment, each filter is examined by modern, accurate instruments for filtering efficiency and resistance. The results are recorded and registered.

Guaranteed at least 99.95% efficient against 0.3 micron diameter chemical smoke (Standard DOP Test) . . . permits maximum air flow with minimum resistance . . . rated capacities are at 1" of water initial resistance . . . available in sizes to meet any need. Write for details today.

Other M.S.A. Equipment

Air Sampling, Beckman Radiation and Gas Detection Instruments—Synthetic and Rubber Clothing—Safety Signs—Respirators—Oxygen Breathing Equipment—First Aid Materials.

MINE SAFETY APPLIANCES CO.

Braddock, Thomas and Meade Sts., Pittsburgh 8, Pa.

At Your Service:

74 Branch Offices in the United States and Canada

Representatives in Principal Cities in Mexico, Central and South America

Cable Address "MINSAF" Pittsburgh

MSA

SAFETY EQUIPMENT HEADQUARTERS

Call the M.S.A. Man on your every safety problem . . . his job is to help you.

Editor Wilson and the contributors for their diligent efforts in producing a very excellent beginning of what it is hoped will develop into a series of volumes maintaining the extremely high standards established here.

—MARTIN A. POMERANTZ
Bartol Research Foundation
Swarthmore, Pennsylvania

BOOKS RECEIVED

Annual Review of Nuclear Science, Vol. 1, Annual Reviews, Inc., Stanford, Calif., 1952, ix + 645 pages, $6. *(To be reviewed.)*

Atomic Power—An Economic and Social Analysis, by Walter Isard and Vincent H. Whitney, The Blakiston Company, New York, 1952, xi + 235 pages, $4.75. A study in industrial location and regional economic development. *(To be reviewed.)*

The Nature of Some of Our Physical Concepts, by P. W. Bridgman, Philosophical Library, New York, 1952, 64 pages, $2.75.

This is a collection of three lectures in which the author tries to analyze reactions between the instrumental and verbal aspects of the physicist's operations. With this in mind, he examines components of the concepts of field and empty space, the fundamental concepts of thermodynamics, and the phenomena of conduction and electricity in massive conductors.

Reports on Progress in Physics, Vol. XV (1952), A. C. Stickland, executive editor, The Physical Society, 1 Lowther Gardens, Prince Consort Road, London S.W. 7, 1952, 338 pages, £2 10s. to non-Fellows, and 27s. 6d. to Fellows.

Contains articles on the hydrogen bond, mass spectrometry, range-energy relations, analysis of high-energy neutron-proton and proton-proton scattering data, turbulent motion, ferrites, band structure of metals, galvanomagnetic effects in conductors, and traveling-wave tubes, together with a cumulative index for Vols. I–XV.

Mechanics and Properties of Matter, by Reginald J. Stephenson, John Wiley & Sons, Inc., New York, 1952, x + 371 pages, $6.

Currently serving as chairman of the faculty of the Oak Ridge School of Reactor Technology on leave from The College of Wooster where he is chairman of the department of physics, the author is well qualified to deal with the subjects he covers. His text is the outcome of a one-semester course given at Wooster and is recommended for the student who has had at least a year in both general college physics and calculus. Using vectors and simple forms of vector analysis throughout to present physical ideas, he covers the subjects of kinematics, force and motion of particles, work and energy of particles, Newton's gravitation law, free and forced harmonic oscillations, translational and rotational motion of rigid bodies, elasticity, statics, hydrostatics and hydrodynamics, and wave motion. A generous selection of problems is offered. There is in the book, if anything, too much material to be fitted into one semester; it may, therefore, serve conveniently in an expanded or selective curriculum.

OTHER LITERATURE

Summaries of Unclassified Basic Research Projects in the Physical Sciences, Atomic Energy Commission (TID-4005). A 190-page index to AEC contracts for research programs in universities and independent research institutions as of January 1, 1952. It should be of assistance in acquainting research investigators in the fields of chemistry, mathematics, metallurgy, and physics with a knowledge of work going on in their own and related fields with a view toward exchange of ideas. *Office of Technical Services, Dept. of Commerce, Washington 25, D. C., $0.60.*

Report of a Conference on the Use of Radioactive Isotopes in Industry. Shortened, illustrated versions of nine papers read at a conference organized by the F.B.I. Industrial Research Committee and the Atomic Energy Research Establishment and held in London, May 1, 1951, are collected in this 55-page pamphlet. Along with suggested applications of radioisotopes with interest to industry in general, specific applications are cited for the chemical, textile, electrical, and metals industries. *Federation of British Industries, 21 Tothill St., London SW1, 2/6d per copy.*

Symposium on Radiation Microbiology and Biochemistry. A 128-page monograph from the *Journal of Cellular and Comparative Physiology* (Vol. 39, Suppl. 1, March, 1952) containing

three abstracted and seven complete papers given at an Atomic Energy Commission research conference, April 11–12, 1949. The conference discussion concerned the effects of radiation at the microbiological level. *Reprint available without cost to scientists in microbiology field; write Biology Division, Oak Ridge National Laboratory, P. O. Box P, Oak Ridge, Tenn.*

X-ray Protection Design, by Harold O. Wyckoff and Lauriston S. Taylor (National Bureau of Standards Handbook 50). Recommended for architects and others responsible for maximum X-ray protection. Data are included on sample design problems and methods of computing barriers for real shielded X-ray installations for fluoroscopy, radiography, or therapy. All information in its 36 pages is based on recommendations of the National Committee on Radiation Protection outlined in NBS Handbook 41. *GPO, Washington 25, D. C.*

Applying Tracer Techniques in the Textile Industry, by William G. Chace. An 8-page bulletin (Series 55, No. 3, Feb., 1952) explaining radioactivity and tracers in simple terms. Uses and choice of isotopes are suggested. *Lowell Textile Institute, Lowell, Mass.*

Atomic Energy Commission Document Price List. No. 20 (issued March, 1952). A listing of all AEC research reports that have been made available for purchase since October, 1951. *Copy of price list free on request from Office of Technical Services, Dept. of Commerce, Washington 25, D. C.*

List of 22 Letters Patents and 2 Applications for Letters Patents Released for Public Use by the AEC (Vol. II, No. 2, April 28, 1952). *Issued by Chief, Patent Branch, Office of the General Counsel, U. S. Atomic Energy Commission, Washington 25, D. C.*

BOOK NEWS

• **Blakiston moves.** The Blakiston Company, medical and scientific publishers in Philadelphia for over a century, will move to New York in the late summer. It will occupy offices at 575 Madison Ave., New York 22, N. Y., with its parent organization, Doubleday and Company, Inc.

Now... a high efficiency

Scintillation Counter

at *Moderate cost!*

1100 COUNTS OVER BACKGROUND... using a ¼" crystal cap with a 1 microcurie source of I^{131} at 15 centimeters.

Large single Sodium Iodide Thallium activated crystal permanently mounted in lucite cap... optically coupled to an RCA 5819 Photomultiplier tube.

SC-1A

NO ADDITIONAL CIRCUITRY NECESSARY... direct connection between 6 foot cable and your scaler or ratemeter!

complete unit only 175^{00}

Write for Bulletin SC-203

Also available with 1" diameter crystal cap to provide 1800 counts over background.

STANDARD EFFICIENCY— UNUSUAL ECONOMY!

Write for data on Voltage Regulator Model No. VS-2A

nuclear research corp.

2563 Grays Ferry Avenue • Philadelphia 46, Pa.

NUCLEONIC EVENTS

Senate OK's House Cut of $174-million in AEC Budget; Reactor Development and Physical Research Hit Hard

No effort was made in the Senate, when it passed the Independent Offices Appropriation bill, to restore any of the $174,272,500 that was cut from the AEC budget for fiscal 1953 by the House. When it approved the budget figure of $1,137,727,500, the Senate Appropriations Subcommittee noted that a supplemental bill for atomic energy plant expansion would soon be submitted to Congress. Although the budget is still subject to House-Senate conference, the amount passed by the Senate will probably be the final figure since there was no difference in the amounts passed by each house.

On May 29, President Truman made a request for $3.1-billion as supplementary funds for atomic energy plant expansion for a five-year period. No breakdown was given for the expenditure of these funds, but speculation is that a good part of it would be for preparations for an H-bomb test. It is said that funds for a new diffusion plant in the Ohio Valley are also included.

On June 27, the House approved only $1.45-billion of the President's request for supplementary funds. The House also passed a proviso banning commencement of AEC projects not yet fully funded by Congress.

The cuts in the budget for this year hit hard at some of the research and development items. Reactor development was cut 24%, and reactor development facilities 54%. Physical research was cut 23%, and physical research facilities 83%. Special reactor materials and other special materials were each cut 50%. Weapons facilities received a major cut, 50%.

Other items that received large cuts are community operations and community facilities, 36% and 73%, respectively. Stores and inventories was cut 94%.

The only items not cut appreciably, aside from weapons operations and source and fissionable materials operations and facilities, were biology and medicine operations and facilities.

The table shows a detailed breakdown of the funds allowed, and the amount by which the original request was decreased.

Detailed Breakdown of AEC Budget for Fiscal 1953

Project or item	*Amount allowed*	*Decrease*
Operations		
Source and fissionable materials	$315,900,000	$25,600,000
Weapons	208,000,000	20,000,000
Reactor development	70,000,000	22,400,000
Physical research	33,100,000	10,000,000
Biology and medicine	23,285,500	1,314,500
Community operations	1,800,000	1,000,000
Program direction and administration	30,000,000	5,400,000
Stores and inventories	202,000	3,000,000
Special reactor materials	2,780,500	2,780,500
Other special materials	1,018,500	1,018,500
Working capital	700,000	—
Unliquidated obligations	22,200,000	—
Total operating obligations	708,986,500	92,513,500
Plant and Equipment		
Source and fissionable materials	300,826,000	10,574,000
Weapons	27,500,000	27,500,000
Reactor development	20,400,000	23,700,000
Physical research	1,000,000	4,985,000
Biology and medicine	515,000	—
Community facilities	1,500,000	4,000,000
Equipment not included in construction projects	20,000,000	11,000,000
Total plant and equipment obligations	371,741,000	81,759,000
Cash to liquidate prior contract authority	57,000,000	
Grand total obligations	1,137,727,500	174,272,500

Isotopes for Cancer Use No Longer Free

Radioisotopes for use in cancer research, therapy, and diagnosis are now subject to a charge of 20% of the production cost (effective July 1, 1952). In making this announcement, the Atomic Energy Commission said that it was in agreement with its Advisory Committees on Isotope Distribution and Biology and Medicine that "the stimulus of completely free distribution no longer is necessary to encourage the use of radioisotopes in the field of cancer."

Heretofore users have only paid transportation and handling costs, but AEC has borne the production cost. Now, those using radioisotopes for cancer will also pay part of the production cost in accordance with the following table. These prices are compared with those for noncancer use.

Isotope	*Cancer use*	*Noncancer use*
I^{131}	$0.15/mc	$0.75/mc
P^{32}	0.22	1.10
Au^{198}	0.05	0.24
C^{14}	7.20	36.00

This change in policy affects the price only, and not the availability of isotopes; production will continue to meet all demands.

For the purposes of the program, cancer research is interpreted to mean: investigations of the basic aspects of normal and abnormal cellular growth; and development and evaluation of therapeutic and diagnostic procedures for cancer and allied diseases.

Radioactive materials for fixed

sources such as Co^{60} and Cs^{137} are not included in this arrangement.

Materials for use in synthesis of radioisotope-labeled compounds in the applicant's laboratory can be obtained at the reduced price if the labeled compound is for cancer research, diagnosis, or therapy.

Persons or firms who furnish radioisotopes on authorization from the Commission to persons authorized to receive radioisotopes at the reduced price for cancer use may have the delivered activity replaced at the reduced price, provided the original activity was obtained from the AEC or an AEC distributor.

According to both Dr. Sergei Feitelberg of the Mt. Sinai Hospital and Dr. C. P. Rhoads of the Sloan-Kettering Institute, both in New York City, the new policy will pose a financial problem. The cost of the radioisotopes for therapy and diagnosis will have to be passed on to patients. In the case of patients who cannot afford to pay, this cost will have to be borne by the institutions, since the patients will not be turned away.

It is to be expected that the additional cost of the isotopes will add $10–20 to the bills of private patients, and that this will partially offset the cost of treating the free patients.

Both Dr. Rhoads and Dr. Feitelberg said that new funds for support of research will have to be found. If sufficient funds are not found, research will have to be cut back.

However, in acknowledging AEC support, Dr. Feitelberg said: "The clinical worker has no more reason to complain about the charges for isotopes than about costs of antibiotic drugs or new hormonal extracts. During the past years, the free supply of radioisotopes has been in effect a direct support of clinical and research work. It is probable that the scope of clinical and research use of radioisotopes, and their relatively wide acceptance as a medical and biological tool is due to the program of free distribution. The establishment of charges, at a fraction of the production cost, should not let us forget our debt of gratitude to AEC."

The distribution of radioisotopes is only a part of the AEC's support of cancer research, both within and outside its facilities. For fiscal 1953 total support will reach an all-time high of $2,750,000, which includes $450,000 for the cancer isotopes program.

Atomic Weapons Organization

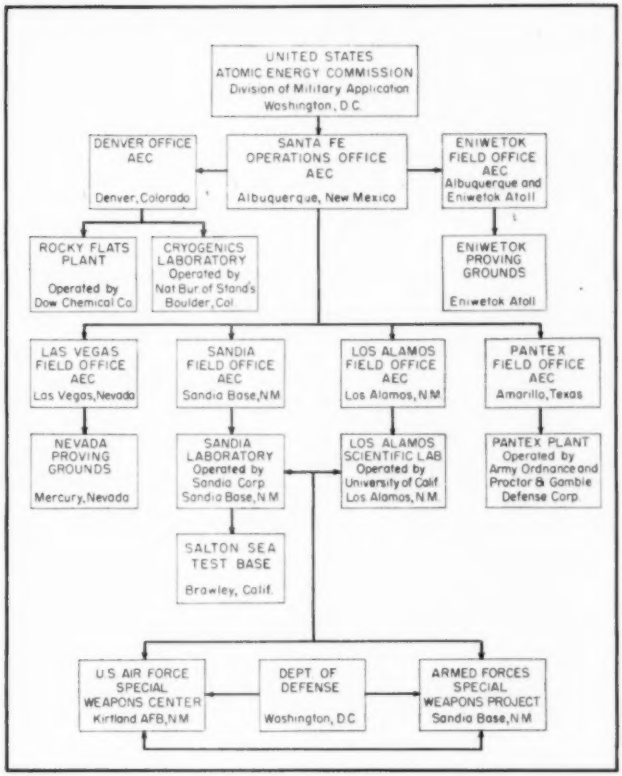

This chart shows exactly how each operation fits into the over-all test program

Technical Need for Weapons Tests and Instrumentation Involved are Explained by Test Director

The complex atomic weapons organization, whose various divisions and their interrelations are shown in the chart, is set up to test "experimental nuclear devices" rather than "atomic weapons or bombs." This fine distinction was made recently by Dr. Alvin C. Graves of the Los Alamos Scientific Laboratory and Test Director at Nevada Proving Ground.

The distinction is a real one. The devices when tested are simplified as much as possible so that they will give the answer to a single question. To minimize consumption of fissionable material, as little as possible is used in the devices, and consequently they would not usually be useful as weapons.

Field tests are held to reduce delays in the development of different designs. Although weapons are not usually tested, the tests of the devices affect weapon design. The design problem is set when strategic or technical considerations determine the necessary method of delivery, the attendant size and weight limitations, and the required yield.

Two basic types of questions are asked of the experiments performed at the detonation of the devices. The first is how the device operates, and the second is what the effects on materials are. To answer the first question, the experiments must determine yield

and efficiency, and prove that the measured yield is not a fluke of some sort. The second category of experiments must determine neutron energies as functions of time and distance, as well as the protection afforded by structures, shelters, and the like. At the tests at Yucca Flat, Nevada, in April (NU, May '52, pp. 9, 10) experiments were designed to answer questions in both categories.

At the heart of the instrumentation for a test setup is the sequence timer, which refers the operation of all the equipment to the zero time of detonation. For a tower shot, the zero time can be preset, but for an air drop, the time can only be set roughly, and then must be checked against a signal from the plane.

Large underground bunkers to shield recording instruments against blast and radiation are located near ground zero in several firing areas. These bunkers, which vary considerably in design, are used to record blast, heat, neutron or gamma radiation, or for taking photographs.

The detecting instruments located above ground, some of them within the detonation itself, may be vaporized at the instant of detonation. For this reason the resolving time of the equipment must be very short.

Coaxial cables carry the signals to the recording instruments inside the bunker. Since the time of the event is so short, photographic records of oscilloscope traces can be made only if the light is very intense. So as not to fog the film before the recording instant, the electron beam is reduced in intensity and deflected off screen. A tap off the cable gives the signal to turn on the intensifier. The main signal travels through a greater length of cable and arrives at the screen a microsecond or so later.

203 Receive Renewals of AEC-Sponsored Fellowships

The last major renewal of AEC-sponsored fellowships was made on May 26 by the fellowship board at the Oak Ridge Institute of Nuclear Studies. The AEC fellowship program is being closed out because of the establishment of the National Science Foundation's fellowship program covering the same fields of study.

More than 200 fellows received extensions for all or part of the 1952–53 school year. Of this group, 139 are in the physical sciences, of which 8 are postdoctoral; 62 are in the biological sciences, of which 9 are postdoctoral; and 2 are postdoctoral fellows in the medical sciences.

The extensions were made to give assistance in the completion of research and study programs. Three of the postdoctoral fellows are working abroad, one in Germany, one in Denmark, and one in Bermuda.

Uranium Deposits

• Uranium in Nigeria. One of the world's largest uranium deposits has been discovered in the British colony of Nigeria. Each ton of ore is estimated to contain $14 worth of uranium and niobium. The field covers 200 acres with 700,000 tons of ore to the vertical foot. The depth of the deposit is unknown. Mining rights to the land belong to the British Crown.

• Uranium in Germany. Substantial deposits of uranium are reported to be in the mountains of the Black Forest of West Germany. Size of the fields and the amount discovered were not revealed. The amount is said to be sufficient for the needs of West German atomic research.

AEC Contracts for Yearly Zr Supply of 150,000 lb.

The Atomic Energy Commission has contracted with the Carborundum Metals Co., Inc., a subsidiary of the Carborundum Co. of Niagara Falls, N. Y., for the supply of 150,000 pounds of zirconium and hafnium sponge metal a year for a period of five years, at a unit price of less than $15 per pound. The company will design, build, and operate its own production facilities.

Zirconium metal is needed in the construction of reactors where one use is as casing for fuel elements. It has a low neutron-absorption cross section, and good high-temperature properties. Other desirable properties are its corrosion resistance and ductility.

Present requirements for zirconium and hafnium are being met by pilot plant production in government-owned facilities. A year ago, the U. S. Bureau of Mines, Northwest Electro-developmental Laboratory, Albany, Oregon, was producing 7,000 pounds of zirconium metal a month, and was shooting for a production figure of 10,000 pounds a month.

The raw material is converted to pure zirconium oxide at Oak Ridge, Tenn., and the metal produced from the oxide at the Oregon plant. Before the government began these pilot plant operations two years ago, zirconium had not been produced on a large scale.

ORINS and Medical Schools Plan Teletherapy Units

Twenty-five representatives of sixteen Southern medical schools met in Oak Ridge on May 15–16 and unanimously endorsed a plan for the co-operative design, construction, and clinical evaluation of a teletherapy unit. The unit will make use of either Cs^{137}, Co^{60}, or Eu. The concensus of opinion was that cesium would be the most suitable source, although the other two possibilities were left open in case reactor time became available for their production. The cesium isotope is a fission product and its availability doesn't depend on reactor time.

The proposal calls for the Medical Division of the Oak Ridge Institute of Nuclear Studies to build a prototype unit for testing physical and biological characteristics of the beam, as well as limited clinical application. When this phase is complete, a number of the medical schools will procure units and take part in a coordinated clinical testing program under the direction of a teletherapy evaluation board.

The first phase of the project will take about three years. It will be finished at about the time when sufficient materials should be available for simultaneous use of several multicurie units.

Under the plan, the medical schools would appoint a member to serve on the evaluation board, contribute $2,500 over the next three years towards the operating costs of the research program, make every effort to procure a teletherapy unit of the approved design, and permit the board to make use of the unit in the joint evaluation program.

The medical schools and hospitals represented at the meeting were Bowman Gray School of Medicine, Winston-Salem, N. C.; Georgia School of Medicine, Augusta; Medical College of Virginia, Richmond; Duke University School of Medicine, Durham, N. C.; University of Maryland Hos-

pital, Baltimore; M. D. Anderson Hospital for Cancer Research of the University of Texas, Houston; Tulane University Medical School, New Orleans, La.

Also Baylor University School of Medicine, Houston, Texas; Vanderbilt University Medical School, Nashville, Tenn.; University of Arkansas School of Medicine, Little Rock; Medical College of Alabama, Birmingham; University of Tennessee Medical School, Memphis; Emory University School of Medicine, Atlanta, Ga.; University of Louisville School of Medicine, Louisville, Ky.; and Baptist Hospital, Winston-Salem, N. C.

Instrument Society Will Conduct Two Clinics

A clinic on complex analytical instruments will be held in conjunction with the Seventh National Instrument Conference which will be run by the Instrument Society of America at Cleveland, Ohio, September 8–12, 1952.

The clinic will consist of a lecture and demonstration course, in which nine instrument manufacturing companies will participate. Among the instruments to be demonstrated are spectrophotometers, a mass-spectrometer leak detector, radioactivity instrumentation, gas analyzers, and some X-ray devices.

The schedule will be so arranged that each participant will be able to attend six different lectures and demonstrations.

During September 5–7, the three days preceding the conference, the ISA will conduct another clinic, devoted to instrument maintenance. The subjects to be covered are: thermal elements, electrical measuring circuits, pressure elements and primary flow elements, electrical deflection and indicators, total quantity meters, electronic positioning devices, pneumatic positioning devices, and final control elements.

ACS Exposition Will Feature Atomic Energy in Industry

The American Chemical Society's Seventh Annual Chemical Exposition, to be run by the Chicago Section will devote the entire day of September 11 to the industrial uses of atomic energy.

For the morning session, the proposed program lists three papers:

Thermal Shock
can't harm parts made of *Stupalith*

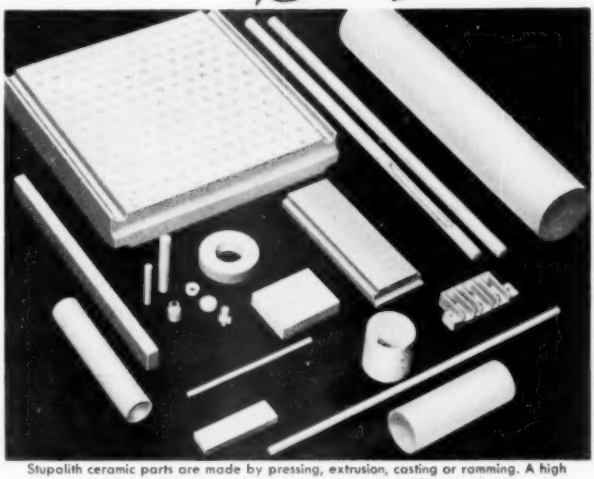

Stupalith ceramic parts are made by pressing, extrusion, casting or ramming. A high degree of uniformity and close tolerances are readily maintained.

Low-Expansivity Ceramic Material

Where thermal shock conditions prevail, parts made of STUPALITH will withstand extremely severe service. Stupakoff makes parts ranging from a fraction of an ounce to several pounds in weight, in simple or intricate shapes.

Two principal compositions are ordinarily employed: "zero" expansivity compositions, and non-porous compositions having near-zero expansivities. By varying the ingredients and processing of these compositions, parts having desired expansivity characteristics (negative or low positive) are obtained. For parts requiring a high degree of dimensional accuracy, our production process includes machining or grinding to precision tolerances. Safely used at temperatures up to 2400° F.

Stupakoff will be glad to design and produce in STUPALITH, parts having the resistance to thermal shock or the expansivity your application demands.

Send for descriptive Bulletin 1051

Stupakoff
CERAMIC & MANUFACTURING CO.
LATROBE, PENNSYLVANIA

THIS NEW BOOKLET TELLS WHY

You can't beat the system

WHEN IT'S A

Sanborn Recording System

By means of pert illustrations and pertinent text, this 16-page booklet tells why so many engineers in research and in industry are choosing **SANBORN** Recording Systems for immediate, permanent, and *accurate* recording of a wide variety of electrical and mechanical phenomena.

Whatever your recording problem, you will find it worth your while to know more about **SANBORN** via this new booklet.

For your copy, simply fill in and mail the convenient coupon below.

Please send me a copy of "7 Advantages of Sanborn Recorders for Industrial Users."

NAME_____

TITLE_____

COMPANY_____

ADDRESS_____

SANBORN CO.

CAMBRIDGE 39 MASSACHUSETTS

Production, Availability, and Costs of Fission Products; Facilities Required for Conducting an Industrial Atomic Energy Research Program; and Design of Tracer Experiments.

In the afternoon, three more papers will be given. The topics are: Survey of Industrial Applications of Atomic Energy; Case Histories of Industrial Applications in Radiography, Gaging, Liquid Flow Through Pipes, Friction Wear Measurements, Metallurgy, Studying Detergency, Mineral Flotation, and Studying Catalysis; and A Look into the Future of Atomic Energy in Industry.

In the evening, a talk will be given on the economic, political, and sociological aspects of the uses of atomic energy in industry.

In addition to the talks and speeches, there will be a large special exhibit on the uses of atomic energy in industry. The AEC will assist with the organization of this display.

IN BRIEF

• **Maniac finished.** The new electronic digital computer, called the Maniac, has been successfully operated at the University of California's Los Alamos Scientific Laboratory where it was designed and constructed. The Maniac, whose name is not the initials of some longer phrase, is more compact, simpler, and capable of handling more complex problems than its forerunners. Three years and $330,000 were expended in construction of the computer.

• **AEC films.** *The commission has made available about 100,000 feet of unedited, assembled, 35-mm film (without sound track). The footage covers unclassified AEC and contractor activities. It is available through the government at standard government rates.*

• **10-ton windows.** Workers at the AEC's Savannah River plant will be protected from high-level gamma radiation by windows weighing more than ten tons each. They will be made of Pittsburgh Plate Glass Company's specially formulated non-browning glass by E. I. du Pont de Nemours & Co., contractor for the project. About 25,000 square feet of the glass will be used at a cost of $1,000,000.

• **Measurements conference.** *A symposium on methods of measurement in nuclear physics and radioactivity will be one of the principal features of the "Third Instruments and Measurements*

Why you can depend on proportional counters by

nuclear measurements corp.

NMC MODEL PC-3

PRECISION IS HIGHER — Total instrumental error is less than 0.5%: the character of the "Candid Decade" scaling circuit guarantees that scaling errors will not participate. No geometry or window error exists. Resolution loss 1% per 100,000 c/m.

YIELD IS HIGHER — The yield runs typically 5 to 50 times higher than an end-window G-M counter.

BACKGROUND IS LOWER — Beta background runs less than 2 c/m per cm² of counting area; Alpha background is less than 0.1 c/m.

VERSATILITY EXCEPTIONAL — Built-in automatic features reduce the operating cycle to 4 rapid operations.

DECONTAMINATION IS EASIER — Less than 10 minutes is required to decontaminate, clean and reassemble the counting chamber.

OPERATION MORE RAPID — Designed specifically for Proportional Counting with the least possible compromise.

DESIGN INTEGRATED — The instrument counts Alphas, Betas and Gammas. Alphas are counted with complete discrimination from high intensity Beta activity. Betas are counted in the presence of Alpha activity.

You can depend on Instruments by Nuclear Measurements when you need Instruments for

RADIOCHEMISTRY — MINERAL ASSAY
RADIOBIOLOGY — WATER & SEWAGE ASSAY
RADIOTHERAPY — NUCLEAR PHYSICS
HEALTH PHYSICS — MINERAL SEARCH

NMC — *Contact NMC First . . . For The Finest*

nuclear measurements corp.

2450 W. ARLINGTON • CH. 2415 • INDIANAPOLIS, IND.

Conference" to be held in Stockholm, September 22–25, 1952. Sponsors are the Royal Swedish Academy of Engineering Sciences and the Association of Technical Physicists; the secretary is Mr. Yngve Axner, Kungl. Tekniska, Högskolan, Stockholm 70, Sweden.

NUCLEAR NEWSMAKERS

Karl R. Van Tassel has been appointed general manager of the operating department of the Knolls Atomic Power Laboratory. He replaces **William H. Milton, Jr.,** who is resigning as of August 1.

Arthur F. Abt, Chicago pediatrician, has been appointed director of the Radioisotope Unit of the Veterans Administration Hospital in Durham, N. C., and professor of pediatrics at Duke University.

Glenn T. Seaborg, 1951 Nobel Laureate in Chemistry and member of the staff of the Radiation Laboratory of the University of California, is completing two months of special research work at Argonne National Laboratory.

Marion T. Clark is serving as acting chairman of the University Relations Division of the Oak Ridge Institute of Nuclear Studies during the absence-on-leave of **Russell S. Poor.**

L. R. Phillips, former associate professor of chemistry at the University of Florida, has joined the staff of the materials chemistry division of the Oak Ridge National Laboratory.

MEETINGS

Photographic Society of America (Symposium on Photography in Medicine and Biology)—Hotel New Yorker, New York, Aug. 12

8th International Congress of Applied Mechanics—Istanbul, Turkey, Aug. 15–Sept. 15

International Union of Theoretical and Applied Mechanics, 2d General Assembly—Istanbul, Turkey, Aug. 25–Sept. 2

4th Annual Oak Ridge Summer Symposium (The Role of Atomic Energy in Agricultural Research)—Oak Ridge, Tenn., Aug. 25–29

International Conference on Beta and Gamma Radioactivity—Amsterdam, The Netherlands, Sept. 1–6

American Mathematical Society, Summer Meeting—East Lansing, Mich., Sept. 3–6

American Physical Society (Division of Electron Physics)—Princeton University, Princeton, N. J., Sept. 4–6

2d International Congress on Analytical Chemistry—Oxford, England, Sept. 4–9

Instrument Society of America, Annual Meeting—Cleveland, O., Sept. 8–12

ENGINEERING OPPORTUNITIES

CONSOLIDATED VULTEE

NOW AVAILABLE IN...

DESIGN AND DRAFTING
STRUCTURAL AIRFRAME
APPLIED MECHANICS
EQUIPMENT DESIGN
NUCLEAR PHYSICS
THERMODYNAMICS
AERODYNAMICS
ELECTRONICS
DYNAMICS

A straight line to success

STRUCTURES
ELECTRICAL
MECHANICAL
PROPULSION
AEROPHYSICS
WEIGHTS CONTROL
SERVO MECHANICS

YOUR ADVANTAGES AT CONVAIR

- Travel and moving expenses paid for engineers who qualify
- Currently working 45-hour, 5-day work week
- 6 paid holidays yearly
- Paid vacation
- Liberal retirement plan
- Group insurance including hospitalization for employees and families
- 28 recreational activities for employees and families
- Opportunity for "in plant" graduate and undergraduate study
- Excellent climate and living conditions
- Ideal working conditions in air-conditioned plant
- Excellent advancement opportunities in world's largest aircraft factory

CONVAIR

CONSOLIDATED VULTEE AIRCRAFT CORP.
Attn. M. L. TAYLOR, ENG. PERSONNEL DEPT. 6Y
FORT WORTH, TEXAS

As an engineer available for employment now or in the near future, I'm interested in the opportunities at Convair. Send me additional information.

My line of engineering is_____

MY NAME_____

MY ADDRESS_____

MY CITY_____ STATE_____

PRODUCTS AND MATERIALS

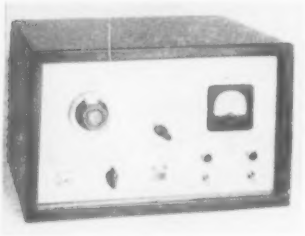

Scintillation Convertor

Nuclear Research and Development, Inc., 1094 Sutter Ave., St. Louis 5, Mo. The model A-200 scintillation convertor unit, which contains a high-gain linear response amplifier, a pulse-height discriminator, and a regulated high-voltage power supply, allows a scintillation counter to be used with an ordinary scaler. The amplifier has a rise time of 0.25 μsec and a variable gain up to 2,000; the instrument is sensitive to 0.75-mv pulses. The discriminator is adjustable for 0 to −100 volts. The voltage regulation gives better than 0.005% change in output voltage for a 1-volt change in input between 95 and 130 volts.

Gammometer Cell

Ohmart Corp., 2347 Ferguson Rd., Cincinnati 38, Ohio. The model RT gammometer operates on the same principle as the models AH-1 and AH-2 described in the May issue of NUCLEONICS (the latter models are calibrated in microcuries, and not, as erroneously reported, in millicuries). The model RT is specifically designed for use with a high-impedance millivolt recorder for the measurement of gamma radiation. It can be used for recording ambient radiation, for following chemical processes, and, by equipping the recorder with a controller, for controlling the chemical processes. The cell can also be used directly with sensitive galvanometers for detecting radioactivity in excess of 10 mc. When exposed to 1 mr/hr from a Co^{60} source, the cell generates a current of 1×10^{-12} amperes. A tube, projecting inside the cell, permits measurement of radioactivity by insertion of a sample within the cell, and facilitates calibration checking. Longtime precision is said to be ±1% of full scale when used with a self-balancing potentiometer type of recorder.

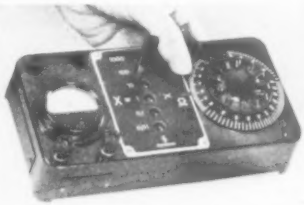

Measuring Bridge

Herman H. Sticht Co., 27 Park Place, New York 7, N. Y. The type Z measuring bridge has a range of 0.05–50,000 ohms over six ranges. The bridge, with a flashlight battery as supply source, is claimed to have an accuracy of ±1%. It may be used for d-c measurements with galvanometer and battery, or for d-c and a-c with an auxiliary plug-in buzzer and headphone.

Galvanometer

Shallcross Mfg. Co., 10 Jackson Ave., Collingdale, Pa. The coil and its mechanism are mounted on rod supports, and protected by a removable aluminum cover, in the type 1951 d-c galvanometer system. Panel mounting holes are standard. Four different types are available, having sensitivities of 4, 2, 1, and 0.5μ a per mm. The pointer reads on a scale calibrated in 15 1-mm divisions, either side of center.

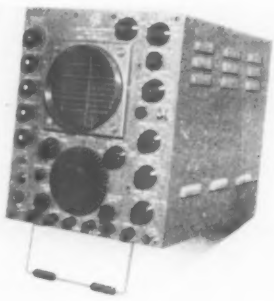

Oscilloscope

Laboratory for Electronics, Inc., 75 Pitts St., Boston 14, Mass. The model 401 oscilloscope is suited for examination of pulse waveforms and transient phenoma, in addition to customary applications. The Y-axis characteristics are: deflection sensitivity, 15 mv/cm peak-to-peak; frequency response, 0 to 10 Mc; transient response rise time, 0.035 μsec; and signal delay, 0.25 μsec. The X-axis characteristics are: sweep range, 0.01 sec/cm to 0.1 μsec/cm; continuously adjustable delayed sweep range; 0–5,000 μsec in three ranges; and positive or negative internal or external triggers, 60 cycles (delayed trigger outputs are available). The unit is supplied with a low-capacity probe.

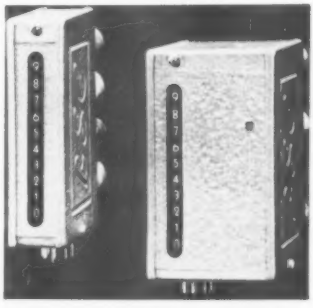

Counting Units

Berkeley Scientific Corp., 2200 Wright Ave., Richmond, Calif. These direct-reading, scale-of-ten decimal counting units present an illuminated numerical reading; no interpolation is necessary. The plug-in units may be connected in cascade to create a counter or scaler

having any desired number of decimal places. Models 700A and 705A have maximum counting rates of 40,000 and 100,000 cps with a resolution of paired pulses of 5 μsec. Models 706A and 707A provide maximum counting rates of 350,000 and 1,000,000 cps with resolutions of 1 μsec and 0.8 μsec.

G-M Tube

Tracerlab, Inc., 130 High St., Boston 10, Mass. The TGC-8 is a stainless-steel end-window G-M tube designed for gamma counting. Multiple baffles are used inside the metal sleeve to provide high efficiency. Operating voltage is 1,100 volts; minimum plateau length is 150 volts, and slope is 2% per 100 volts. The useful life is said to be 10^8 counts. The fill gas is helium with an organic quench; recovery time is 200 μsec.

Servo Amplifier

Automatic Temperature Control Co., Inc., 5200 Pulaski Ave., Philadelphia 44, Pa. This high-gain amplifier is designed for driving servo mechanisms from small a-c input potentials. The full voltage-gain setting is 150,000, with settings for 110,000, 65,000, and 12,000. With a 53-rpm servo motor, there are 5,000 motor-driven positions. Output is a combination of d-c and a-c; the d-c component is approximately 0.024 ampere with a 5,000-ohm resistance load, and the maximum a-c power output into a 5,000-ohm resistance load is 3 watts.

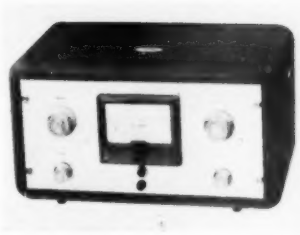

Micromicroammeter

Beckman Instruments, Inc., South Pasadena 5, Calif. The model V Micromicroammeter measures direct currents from 0.3 $\mu\mu$amp to 0.3 $\mu\mu$amp, full scale, with an accuracy claimed of better than 5%, and detects currents as low as 10^{-15} amperes. Zero-drift is reportedly less than 0.0005 volt in a 24-hr period; the reproducibility of +1% is unaffected by ambient temperature or line voltage variations. Terminals are provided on the chassis for current and voltage input, regulated polarizing voltage, connection of a 50-mv potentiometer recorder and an oscilloscope, and 120-cycle a-c amplifier output.

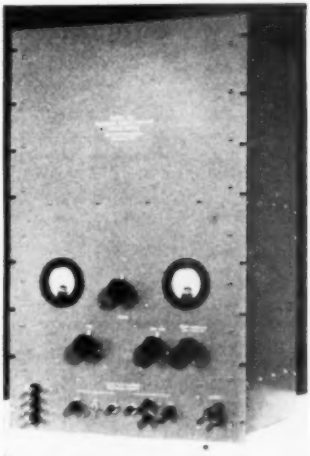

Power Supply

John Fluke Engineering Co., P. O. Box 755, Springdale, Conn. The model 301A power supply has an output adjustable from 7.5 to 750 volts at 0–500 ma. Regulation from zero to full load is within 40 ppm. Regulation against line voltage changes of $\pm 10\%$ (105–130 volts) is ± 20 ppm. For any output voltage setting, stability is within 100 ppm per day under usual conditions. Auxiliary negative voltages of 350 and 700 volts, d-c, at $\frac{1}{2}\%$ regulation at 10 ma, and 6.3 volts, a-c, at 10 amperes are provided.

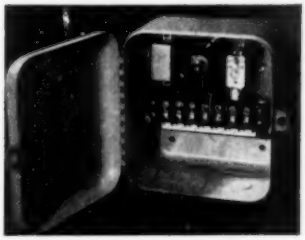

Pilot Relay

Haledy Electronics Co., 57 William St., New York, N. Y. Large values of current and power may be controlled with a current flow of 2 μa by this electronic relay. A cold-cathode triode is employed in the device, and no warm-up is necessary. Current amplification is said to be 2.5×10^6. The relay will operate over any input resistance from dead short to 10 megohms. The instrument works on 115 volts, 60 cycle, and uses 2 watts.

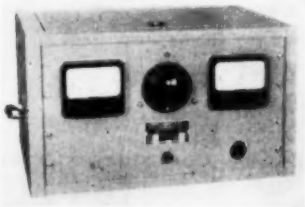

Power Supply

Perkin Engineering Corp., 345 Kansas St., El Segundo, Calif. The model MS168B power supply is rated at 0–30 volts and 15 amperes with a ripple of less than 1% and a voltage regulation of $\pm \frac{1}{2}$ volt from no load to full load. The unit utilizes selenium rectifiers, a magnetic amplifier circuit for voltage regulation, and a continuously variable transformer.

Exhaust Systems

American Agile Corp., P. O. Box 168, Bedford, Ohio. Exhaust systems for corrosive vapors and fumes made of polyethylene can be made to cus-

In nucleonics — for insulation against heat, flame, moisture and grounding — use REFRASIL. A refined fibrous silica product, REFRASIL applications are virtually unlimited: An ideal insulation for power equipment ... electric muffle furnaces ... soldering iron heating elements ... electric heating mantles, rheostats ... and for thermocouple lead wire covering. If insulation is your problem — specify REFRASIL—the most versatile product of its kind in use today in many industries.

IMPORTANT FEATURES

- ★ Chemical resistance of pure silica
- ★ Resists temperatures up to 1800° F.
- ★ Low thermal conductivity
- ★ Fiber diameter .00020-.00040 in.
- ★ Specific heat .19
- ★ Thickness .14-.15 in.
- ★ Surface density .05 lb./sq. ft.

Light and versatile, REFRASIL is supplied in many forms, as illustrated, to meet virtually any insulation need.

CONSULTATION SERVICE

Mail this ad with your letterhead to nearest Refrasil Representative for consultation service — at no charge.

WRITE OR CALL YOUR NEAREST REPRESENTATIVE:

EASTERN: Fred W. Muhlenfeld, 6650 Loch Hill Rd., Baltimore 12, Md., Valley 3135

TEXAS, OKLA. & KANSAS: Thomson Engineering Service, 708 Hemphill St., Fort Worth 4, Texas, Fortune 5340

MIDWEST: Burnie L. Weddle, 3219 West 29th St., Indianapolis 22, Ind., Hickory 8085

HILCO

THE H. I. THOMPSON COMPANY
1741 CORDOVA STREET
LOS ANGELES 7, CALIF.

tomer's specifications. The material is said to be resistant to most acid fumes; it should be used in the temperature range from −20° to 170° F.

Dehumidifier

Abbeon Supply Co., 179-15 Jamaica Ave., Jamaica 32, N. Y. The model WA-5 dehumidifier can be obtained with or without automatic control. The unit, $13 \times 13 \times 29\frac{1}{2}$ in., will dehumidify about 13,500 ft³ of air. A fixture is provided in the bottom of the unit for drainage.

Telepipette

Apis Engineering and Research, Ltd., 136 Pinner Rd., Northwood, Middlesex, England. The model 3 telepipette, for the remote handling of radioactive liquids, holds the pipette more than 3 ft from the operator, and the calibration can be read from a greater distance. The end of the pipette can be moved to any position inside an 8-in. square moving round a 2-ft radius. Exchangeable pipettes are supplied in sizes of 25, 10, 5, 2, or 1 ml. The 10-ml pump is fitted with

HOW TO
SOLUBILIZE
RADIOACTIVE PARTICLES

There are few effective ways to remove radioactive contamination. One is to solubilize the offending material and rinse it away with large quantities of water. Another is to remove the soil by detergent action. Neither method is entirely satisfactory.

However, Versene (the sodium salt of ethylene diamine tetra acetic acid) is a particularly efficient decontaminating agent. It dissolves and chelates (complexes) the salts of practically every metal, including radioactive particles. At the same time it substantially increases the cleansing power of synthetic detergents.

By forming extremely stable, water-soluble complex compounds, the Versenes give you exacting chemical control over cations in solution. Try these exciting new "tools" of research. They are "industry's most modern chemicals."

Write Dept. I for Technical Bulletin No. 2. Samples on request. ®Trade Mark

BERSWORTH CHEMICAL CO.
FRAMINGHAM, MASS.

RECORDERS
RECORD TIME COUNT QUANTITY AND WEIGHT

Actuated by an electrical impulse ... operates on the output of a scaler, photo tube, limit switch or any similar device. Records counts with relation to time and quantity on a roll of tape . . . automatically resets to zero.

In Radioactive Research, it saves precious man hours and results in greater economy and efficiency.

In Industry, it maintains a permanent record automatically, recording production and time each hour.

Whatever your counting problems, our Engineering Department can adapt these Recorders to meet your particular need.

Write for interesting Booklet SC24

WEIGHT RECORDERS
SCALES
HI-SPEED COUNTERS

STREETER-AMET COMPANY
4101 RAVENSWOOD AVENUE
CHICAGO 13, ILLINOIS

a tap; a plastic screen can be fitted for beta protection. The apparatus is easily dismantled.

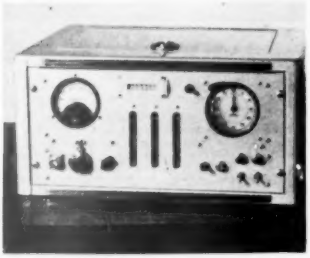

Decimal Scaler

Radiation Instrument Development Laboratory, 2337 W. 67th St., Chicago 36, Ill. The model 1200 direct-reading decimal scaler is designed for all types of counting. It incorporates a linear amplifier and a high-voltage supply continuously variable from 500–5,000 volts with regulation of 0.01% per 1% change in line voltage. Input sensitivity is continuously variable from 3 mv to 10 volts. The resolving time is less than 5 μsec to the pulse pair, and register speed is 17 cps for evenly-spaced pulses. The unit possesses an automatic high-voltage delay relay.

Porous Metal Filters

Micro Metallic Corp., 30 Sea Cliff Ave., Glen Cove, N. Y. These filters are made of a high-temperature alloy composed of 50% cobalt, 20% chromium, 15% tungsten, and 10% nickel. The filters can be used at temperatures as high as 1,200° F. The material has high tensile strength and good ductility; porous sheets can be rolled and welded to form cylinders and other forms. It is also said to have high resistance to corrosion.

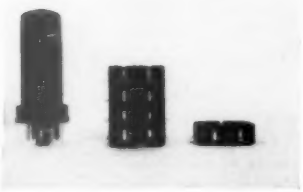

Multiple Scaler

Wang Laboratories, 296 Columbus Ave., Boston 16, Mass. The types 220 binary scaler and 020 decade scaler use magnetic cores as memory elements,

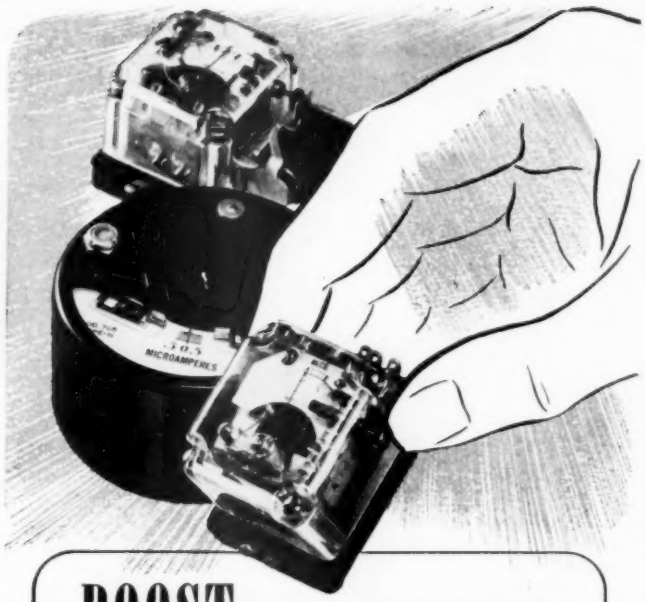

BOOST feeble input signals with SENSITROL® ultra-sensitive relays

How many devices do *you* know of that use an amplifier to boost a feeble input signal up to where it will operate a relay? Most of them would be more reliable . . . more compact . . . more economical—if the amplifier could be omitted.

It can be omitted! For rugged Weston Sensitrol Relays operate reliably on input signals as slight as *1 millivolt* or *½ microampere*, handle substantial wattage *at 110 volts!* They require no power for excitation.

Engineering assistance is freely offered to help you adapt these Sensitrol Relays to present products, or any new problems you may have in mind. Simply consult your nearest Weston Representative, or write Weston Electrical Instrument Corporation, 617 Frelinghuysen Avenue, Newark 5, New Jersey . . . manufacturers of Weston and TAGliabue instruments.

A Type for Every Need

So sensitive that they operate direct on the output of a photo-electric cell or thermocouple, Sensitrol relays enable the instrument engineer to dispense with amplifiers, vacuum tubes and auxiliary power supplies. Single or double contacts, fixed or adjustable, manual or solenoid reset. Be sure you have a copy of Bulletin B-25-B, which gives detailed data on Sensitrol and other Weston relays.

WESTON *Instruments*

high efficiency
PORTABLE
SCINTILLATION SURVEY
METER

FEATURES:

Range (full scale): .01, .05, .25, 1.0, 5.0 and 25 mR hr.
Linearity: ± 5%, 0-5 mR hr.
Waterproof Gun Section
Long Battery Life
Ruggedized and Compact
Light and Balanced Gun
Illuminated Dial
5819 Photomultiplier
Permanently Sealed Na I (Tl)

LA ROE INSTRUMENTS, Inc.
743 Investment Bldg.
Washington 5, D. C.

Radiac-wash

REMOVES RADIOACTIVE CONTAMINATION

contains *Versene**

RADIACWASH is a concentrated liquid radioactivity decontaminant. It acts with amazing rapidity and effectiveness in removing radioactive contamination. For ordinary use, it should be diluted with 5 to 8 parts of water.
RADIACWASH, containing *Versene* acts in two ways. It solubilizes radioactive metallic particles and increases detergency. Thus "RW" makes it possible to easily *rinse away contamination* from laboratory instruments, glassware, furniture, floors, walls, etc. *RADIACWASH is safe for use on the hands or other body surfaces.* It is also superior to soaps and detergents in the laundry and is far more effective.
BE PREPARED FOR ANY TYPE OF EMERGENCY!!!
One gallon of "RW" costs $4.98. Discounts are available for larger quantities. Send today for descriptive leaflet with price schedule.

*T. M. Bersworth Chemical Co.

ATOMLAB INC.
489 FIFTH AVENUE
NEW YORK 17, NEW YORK

and require low power consumption. A triode supplies the triggering action. The maximum operating frequency is 110 kc. Input is 15 volts, 20 ma with a 4–7-μsec positive pulse; output is 15 volts, 20 ma, and 5 μsec (outputs can drive directly the next binary stage).

Organic Tracers

Radioactive Products, Inc., 443 W. Congress St., Detroit 26, Mich. Carbon-14 ring-labeled cholestenone, cholesterol, and testosterone are available in minimum quantities of 1 mg with specific activities of 5 mc/mg. Also available are methyl iodide and methyl alcohol in minimum quantities of 1 mc, with specific activities of 2 mc/millimole.

Dosage Calculator

"Radiation Calculator," P. O. Box 27, Storrs, Conn. This plastic dosage calculator, designed for civil-defense work, solves the problems of dosage rate and dose which arise with the rapidly changing radiation level in a contaminated area after an explosion. The calculator is recommended as a training aid in making clear the importance of the decay rate of fission products during the early stages of radiological monitoring after a contaminating explosion.

INDUSTRY NOTES

▶**Hagan Corp.,** 323 Fourth Ave., Pittsburgh, Pa., has organized an aeronautical and special products division under the managership of William F. Waina. Included in its initial work will be development of controls for atomic power plants, aeronautical engine and guided-missile testing, and force-measuring systems.

▶**Consolidated Engineering Corp.,** 300 N. Sierra Madre Villa, Pasadena 8, Calif., has formed Consolidated Engineering Corp. Instruments, Inc., as a sales and service subsidiary. Factory-trained sales, application, and service engineers will be stationed across the country. Offices are already in operation in New York City, Philadelphia, Dayton, Chicago, and Washington, D. C.

▶**Technical Operations, Inc.,** 6 Schouler Court, Arlington 74, Mass., engaged in contract research and development in the nuclear field, operations research, and the production of radioactive

SEARCHLIGHT SECTION
(Classified Advertising)
EMPLOYMENT — EQUIPMENT — USED OR BUSINESS — RESALE
OPPORTUNITIES

UNDISPLAYED RATE
$1.50 a line. Minimum 3 lines.
DISPLAYED RATE
$15.00 per inch.
ADVERTISING INCH: ½" on one column, 2 columns—14 inches—to a page.
NEW ADVERTISEMENTS
Address: 330 W. 42nd St., New York 36, N. Y., for August issue closing July 21st.

Bendix

AVIATION CORPORATION

has the following openings for experienced men:

- Mechanical Engineers
- Electronic Engineers
- Electronic Technicians
- Radio-Chemists
- Physicists

These permanent positions will involve work in all phases of nuclear technology. Special emphasis will be on the design and development of instruments, equipment and components for measurement of radiation and radioactivity, as well as the synthesis and application of radio-compounds.

Excellent opportunity for advancement with new, expanding division of one of the country's most progressive corporations.

Please forward resume of educational background and experience.

to Personnel Manager
BENDIX AVIATION CORP.
203 W. Third Street
Cincinnati 2, Ohio

PHYSICIST
METALLURGY

SYLVANIA needs for its new metallurgy laboratory, now being completed at Bayside, L.I. an applied physicist to operate Radio-activity laboratory. Work involves making radio-activity measurements in connection with metallurgical & chemical research problems. Supervision over small group of technicians. B.S. in applied Physics or Metallurgy & laboratory experience in handling Radio Isotopes essential. Some experience in selection & operation of radio activity measuring instruments highly desirable. Unusual opportunity to head up & develop well-equipped radio activity laboratory, working on a wide variety of research programs. Send complete resume:

MANAGER OF PERSONNEL
SYLVANIA
Electric Products, Inc.
40-22 Lawrence St., Flushing, N.Y.

sources and auxiliary equipment, has recently moved from 16 Court St., Boston.

▶**Tracerlab, Inc.,** 130 High St., Boston 10, Mass., now has 11 directors. S. Sydney Minault and Robert G. Millar are the two new members.

▶**Pi-Square Engineering Co.,** 400 Western Union Bldg., Boston 10, Mass., has been formed as a consulting partnership by Henry M. Paynter and George A. Philbrick. The company will advise on computing aids to dynamic and transient performance analysis.

LITERATURE AVAILABLE

Potentiometer. Bulletin 101-N describes line of external phasing potentiometers. *DeJur-Amsco Corp., Industrial Sales Division, 45-01 Northern Blvd., Long Island City 1, N. Y.*

Therapy sources. Bulletins describe Co^{60} and eye-therapy sources. *Technical Operations, Inc., 6 Schouler Court, Arlington 74, Mass.*

Resistors. Brochure describes wirewound, hermetically sealed, and miniature resistors. *Daven Co., Dept. RB, 191 Central Ave., Newark 4, N. J.*

Connectors. Catalog Supplement No. 1 describes rack and panel connectors, and watertight and universal binding posts. *Hugh H. Eby, Inc., 4700 Stenton Ave., Philadelphia, Pa.*

Capacitor. Catalog 1117 gives data on the Stabelex "D" capacitor. *Industrial Condenser Corp., 3243 N. California Ave., Chicago 18, Ill.*

Thermal controls. Catalog 400 gives data and uses of temperature control devices. *Fenwal Inc., 218 Pleasant St., Ashland, Mass.*

Radioisotope uses. Brochure discusses industrial uses of radioisotopes. *Nuclear Research and Development, Inc., 1094 Sutter Ave., St. Louis 5, Mo.*

Insulators. Booklets give properties of natural steatite insulators. *M. Kirchberger and Co., Inc., 1425 37th St., Brooklyn, N. Y.*

Power supply. Bulletin V1051 describes regulated d-c power supply. *Superior Electric Co., Bristol, Conn.*

Counter tubes. Catalog gives technical data on line of G-M tubes. *Amperex Electronic Corp., 25 Washington St., Brooklyn 1, N. Y.*

fused quartz

- ¾ JOINTS
- SPHERICAL JOINTS
- SEMI-BALL JOINTS
- GRADED SEALS
- SPECIAL APPARATUS
- LABORATORY WARE
- GENERAL TUBING, RODS, PIPES AND FLATS
- POLISHED PLATES AND WINDOWS

Cooper Hewitt fused quartz possesses numerous characteristics which make it highly desirable for industrial and laboratory use.

Outstanding amongst these are high melting point, low coefficient of expansion and ability to withstand large and rapid temperature changes, superior electrical insulation qualities, chemical inertness and transparency.

COOPER HEWITT ELECTRIC COMPANY
Est. 1902
Dept. G, 721 Grand Street
Hoboken, N. J.

Cooper Hewitt

METALLIC SINGLE CRYSTALS

Single Crystals of the following high-purity metals and alloys are now available:

Copper	Tin	Bronzes
Zinc	Bismuth	Nickel
Lead	Aluminum	Permalloy
Cadmium	Brasses	Cobalt

Iron-Nickel Alloys

Available in rod form ¼" to 1¼" diameter up to 10" long.
Special shapes provided upon request.
We will be glad to answer your request for information on prices, specifications, and special problems in this field.

HORIZONS INCORPORATED
2891 E. 79TH STREET CLEVELAND, OHIO

Moving?

If you are moving (or have moved), tell us about it, won't you? Your copies of NUCLEONICS will not follow you unless we have your new address immediately. Make sure you don't miss a single important issue . . . and help us make the correction as speedily as possible by giving us your old address, to

NUCLEONICS
Circulation Dept.
330 W. 42nd St. New York 36, N. Y.

CHEMELEC ELECTRONIC PARTS

MADE OF TEFLON*

Chemelec Teflon*-insulated electronic components include a complete line of 7 and 9 pin miniature tube sockets, crystal sockets, feed-through insulators and terminals.

All provide the same high performance which this superior insulating material assures. Surface resistivity 3.5 x 10^{13} ohms. Loss factor less than 0.0005. Dielectric constant 2.0 (60 cycles to 30,000 megacycles). Serviceable at −110°F. to 500°F. Won't carbonize under arcing. Zero water absorption by ASTM Test. Unaffected by extreme humidity. Won't DC plate. Chemically inert, non-gassing, immune to corrosive atmospheres, fungus, oil, solvents. Non-flammable, tough, resilient, withstands and absorbs mechanical shock and vibration.

TEFLON and KEL-F STOCK and Custom-Fabricated Parts

Fabricating "Know-how", the result of years of specialized experience—and the most modern facilities for rapid, low-cost, close-tolerance production are at your command when you specify Teflon or Kel-F†, fabricated by the United States Gasket Company. Ours is the most complete line in the country—sheets, tape, rods, cylinders, tubing, bars, and custom-machined or molded parts to manufacturers' specifications.

*duPont's trademark for its tetrafluoroethylene resin.

†Trademark M. W. Kellogg Co.

UNITED STATES GASKET COMPANY

FLUOROCARBON PRODUCTS DIVISION

FABRICATORS OF "TEFLON", KEL-F AND OTHER FLUOROCARBON PLASTICS

CAMDEN 1, NEW JERSEY

INDEX TO ADVERTISERS

July, 1952

Advertising Council, The . . 73
Atomlab, Inc. 86
Berkeley Scientific Corporation 65
Bersworth Chemical Co. . . 84
Cole Ltd., E. K. 4
Consolidated Vultee Aircraft Corp. 81
Cooper Hewitt Electric Company 87
Distillation Products Industries 69
General Electric Co. 6
High Voltage Engineering Corp. 5
Horizons, Incorporated . . 87
Kinney Manufacturing Co. . . 3
LaRoe Instruments, Inc. . . . 86
Mine Safety Appliances Co. 74
Nuclear Instrument & Chemical Corp. Fourth Cover
Nuclear Measurements Corp. 80
Nuclear Research Corporation 75
Radiation Counter Laboratories, Inc. . . . . Third Cover
R-C Scientific Instrument Co., Inc. 71
Sanborn Co. 80
Searchlight Section 86
Streeter-Amet Company . . 84
Stupakoff Ceramic & Manufacturing Co. 79
Thompson Company, H. I. 84
Tracerlab, Inc. 2
United States Gasket Co. . 88
Victoreen Instrument Co. Second Cover
Weston Electrical Instrument Corp. 85

•

SEARCHLIGHT SECTION
(Classified Advertising)
H. E. Hilty, Mgr.

EMPLOYMENT 86

This index is published as a convenience to the readers. Every care is taken to make it accurate, but NUCLEONICS assumes no responsibility for errors or omissions.

It Takes Many Skills

TO MAKE RADIATION COUNTERS AND
RADIATION COUNTER LABORATORIES HAS THOSE SKILLS

Side arm being fused onto flow meter used in monitoring city water supply for radioactive contamination. Geiger counter shell previously was delicately sealed within glass outer jacket.

Radiation counters being sealed onto a vacuum system in preparation for filling with a special mixture of gases developed to achieve the right kind of ionization, quenching in tube. Often research is needed to find best mix for new type counter.

Research-born bismuth coated cathode screen being fitted to glass shell of special-purpose radiation counter. Other parts: tungsten-nickel cathode leads, tungsten anode, mica base.

Sealing special cathode within glass counter shell requires rapid precise melting and manipulating since bismuth coating melts at 400 F.

Below: RCL's Special Glass Instrument Division, originally developed to fabricate glass components of radiation counting devices, now offers its scientific services to other fields.

Below: Research director Bernd Ross connects gas-filled and sealed counter tube to voltmeter and scaler for testing. Bismuth Cathode Counter, developed after 2½ years, is five times as efficient in measuring rays from radioactive iodine, hence is being used in the treatment of hyperthroidism.

CREATORS OF ALL TYPES OF RADIATION COUNTING DEVICES

Send in your order today

RADIATION COUNTER LABORATORIES, INC.

5122 West Grove St. *Nucleonic Park* Skokie (Chicago), Illinois

FOR YOUR CARBON^{14} COUNTING:

COMPLETE
nuclear
PACKAGED LABORATORIES

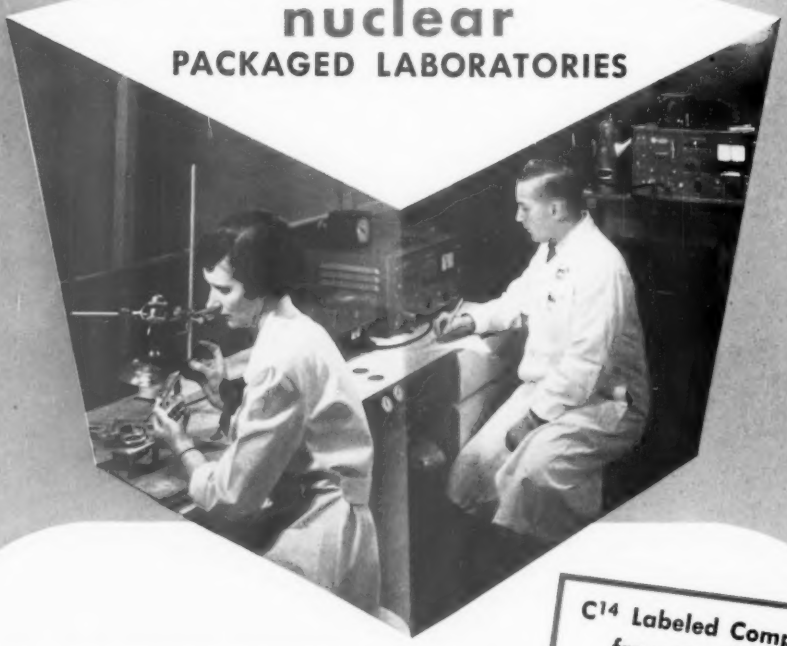

● Here is the *easy* way to select reliable equipment for radiocarbon work. Complete NUCLEAR Packaged Laboratories contain *everything* you need . . . And at prices as low as $475.00!

These Packaged Laboratories save you the time and trouble of picking out equipment, piece by piece, from several sources. Let us do the work. Just tell us what you want to do. We'll send you our list of Packaged Laboratories and recommend the best one for *you*.

All NUCLEAR equipment is built to high standards of quality, and backed by our exclusive ONE YEAR GUARANTEE. Manual and automatic NUCLEAR Instruments are available for measuring, analyzing, and tracing in virtually every field of radioactivity use.

Write today for details on the NUCLEAR Packaged Laboratory which best meets your needs.

C^{14} Labeled Compounds from nuclear's "Isotope Farm"

Uniformly labeled C^{14} compounds immediately available from NUCLEAR . . . produced biosynthetically to highest purity standards:

Introductory Package: 40 mg. of d-glucose (50,000 disintegration/min./mg.). Without AEC Authorization . . . Only $17.50

sucrose — d-fructose
d-glucose — algae (chlorella)

Also Available:

Fructose Phosphates*
Glucose Phosphates*
Glycosides
Amino Acids
Fatty Acids
Chlorophyll
Carotene
Ergosterol
Digitalis
Digitoxin
Acetate
Carbon Black
Sodium Phosphate
Urea
Other compounds from biological or organic synthesis.

*Either C^{14} or P^{32} labeled

nuclear INSTRUMENT & CHEMICAL CORPORATION

235 West Erie Street • Chicago 10, Illinois
Branch Offices: 1063 Colorado Blvd., Los Angeles 41, California
10407 Georgia Avenue, Silver Spring, Maryland
Export Department: 13 E. 40th St., New York 16, New York
Cable Address: Arlab, New York

- Scaling Units for Every Type of Radiation Counting
- Complete "Packaged" Counting Systems
- Health Monitoring Instruments for Personnel Protection
- Glass Wall, Mica Window, and Windowless Counters
- Portable Count Rate Meters
- Radioactive Chemicals
- Complete Line of Accessories for the Nuclear Laboratory

nuclear "PRECISION INSTRUMENTATION FOR NUCLEAR MEASUREMENTS"